To the Graduate Council·

I am submitting herewith a thesis written by Catherine C Large entitled "Excited-state properties of deoxyguanosine, and the electrostatic interactions in DNA." I have examined the final copy of this thesis for form and content and recommend that it be accepted in partial fulfillment of the requirements for the degree of Master of Science, with a major in Physics.

Solon Georghiou, Major Professor

We have read this thesis
and recommend its acceptance

Accepted for the Council.

Associate Vice Chancellor and
Dean of The Graduate School

EXCITED STATE PROPERTIES OF DEOXYGUANOSINE,

AND

THE ELECTROSTATIC INTERACTIONS IN DNA

A Thesis

Presented for the

Master of Science

Degree

The University of Tennessee, Knoxville

Catherine C Large

May, 2000

Copyright © Solon Georghiou and Catherine C. Large, 2000

All rights reserved

ACKNOWLEDGMENTS

I would very much like to thank Dr. Solon Georghiou, my research advisor, for the profound knowledge of Biophysics which I have acquired under his supervision. I greatly appreciate his encouragement. The guidance and wisdom given to me by him are immeasurable. I also very much appreciate having had the opportunity to know him as a friend

In addition, I would like to thank the other members of my committee: Dr. Engin H. Serpersu, Dr. Chia C. Shih, and Dr. Henry C. Simpson The comments they made during my presentations helped in the development of this thesis In addition, I would like to thank Dr Serpersu and Dr. Shih for being very helpful in the planning and interpretation of specific experiments. I would also like to acknowledge the members of my research group, Stacy Taylor-Gerke and Anas Ababneh. Stacy spent many hours teaching me specific laboratory procedures, and Anas has worked diligently in helping me tie up loose ends. Also, I would like to express my appreciation to Dr. Lee L Riedinger and Dr. William M. Bugg, the present and former Head of the Physics Department, respectively, for the award of a teaching assistantship while I pursued this degree.

ABSTRACT

The photophysical properties of deoxyguanosine, dG, have been studied in aqueous solution as well as in organic solvents of varying polarity. The fluorescence quantum yield, q, is found to increase as the solvent polarity is decreased: in diethyl ether, the solvent of lowest polarity used in the present study, q has been found to increase by a factor of 35 relative to the value of q in aqueous buffer. This suggests that hydrophobic interactions reduce considerably the rate constant of the radiationless process of internal conversion. On the other hand, upon increasing the viscosity, η (through addition of sucrose), q has been found to increase by a factor of 1.7 for $\eta = 14$ cP and by a factor of 7.4 for $\eta = 149$ cP. These results suggest that the increase in the rigidity of dG and of the hydrophobic nature of its environment, which occur when dG becomes part of DNA, are not responsible for the very small value of q in DNA· 0.8×10^{-5} as compared to that of 0.8×10^{-4} for free dG in water. An attractive alternative is provided by differences in the hydration network between free dG and dG in DNA. Support for this proposal was obtained from an experiment with an 8% water/butanol mixture which suggested that the hydration network affects profoundly the photophysical properties of free dG. Measurements in this water/butanol mixture were pursued further Surprisingly, it was found that the results depended on the sequence of the steps used in preparing the solution. This is consistent with the reported very large, about - 20 kcal/mol, solvation free energy of guanine We measured the fluorescence of dG at room temperature after the solution was incubated for 10 minutes at a number of temperatures ranging from 23 to 40 °C. An Arrhenius plot yielded $\Delta H \approx -6$ kcal/mol and $\Delta S \approx 48$ cal/mol K. A potential implication of these findings is that intermolecular

hydrogen bonds in DNA, once broken by thermal fluctuations, would tend to remain broken; consequently, the helix would appear to contain a number of GC open or "unzipped" base pairs. Because of the known coupling between base pair opening and bending, it would take relatively little energy for the DNA to bend at GC open sites

We have also employed the theoretical analysis of Jarque and Buckingham, for two ions of the same charge embedded in a polarizable medium, to calculate the contribution which is made by the polarization effects to the electrostatic interaction between the negatively-charged phosphate groups in DNA It is found that many-body, non-additive polarization interactions greatly diminish the effect of the repulsive Coulomb interactions between phosphates both across the DNA minor groove (but not across the major groove) and along the same DNA strand. This reduction is found to be dramatic for groove widths in the range of about 3.5-5 Å for a nearest neighbor distance β of about 3.5 Å. This value of β appears to be realistic for DNA Thus, variations in the minor groove width caused by sequence effects or by thermal fluctuations induce local anisotropic interactions with concomitant local DNA bending toward the groove with the smaller width. Other values of β ranging from 3 2 to 5 Å have also been used From the derivative of the effective potential with respect to the groove width, the overall force F was calculated and its magnitude and direction were found to be strongly dependent on the value of β for small groove widths F is negative, *i e* attractive for $\beta \leq 4$ Å, and positive for larger β values. Thus, the conformation of DNA exerts a profound effect on the ability of DNA to control its dynamics. Based on the fact that the A-tracts have a narrow groove width of about 3.5 Å, the present findings suggest that they would tend to bend toward that groove This prediction is in agreement with the results of

electrophoresis studies. Because of the known coupling between DNA bending and opening of its base pairs, the present findings suggest that base pair opening is a process that does not appear to be very infrequent and is driven by both sequence effects (of static origin) and by thermal fluctuations (of dynamic origin). Such a process may contribute to the creation of the intercalation cavity during drug-DNA interaction. This analysis also offers an explanation for the wrapping of DNA around the histone octamer in nucleosomes: because the A-tracts in DNA are known to bind with their minor grooves facing in toward the histone octamer, the DNA in those regions would bend toward those tracts. Because of the known gradual decrease of the width of the grooves of these tracts from 5' to 3' and the large increase of the strength of the polarization interaction that occurs with this groove width decrease, the DNA wrapping would be done with considerable force. The present analysis brings into question the validity of the continuum dielectric screening model currently being used in the literature to calculate electrostatic interactions.

TABLE OF CONTENTS

PART I. EXCITED STATE PROPERTIES OF DEOXYGUANOSINE

1. INTRODUCTION 2
2. MATERIALS AND METHODS 6
3 RESULTS 15
    Solvents 15
    Hydrogen bonding 34
    Viscosity 43
4. DISCUSSION 61
    Solvents 61
    Fluorescence Spectrum Tail 70
    Hydrogen Bonding 71
    Affinity of Deoxyguanosine for Water 79
5. REFERENCES 87

PART II: ELECTROSTATIC INTERACTIONS IN DNA

1. INTRODUCTION 90
2. THEORY 91
    DNA 91
    Protein-DNA Complexes 109
3. REFERENCES 112

VITA 117

LISTS OF TABLES

TABLE PAGE

PART I. EXCITED STATE PROPERTIES OF DEOXYGUANOSINE

1. Comparison of the quantum yields, full-widths-two-thirds maxima of the fluorescence and absorption spectra, tail-to-peak fluorescence spectral ratios γ, and absorption and fluorescence spectral peak locations of deoxyguanosine in the solvents used in the present study. 17

2 Values of the polarizability, dielectric constant, and solvent polarity empirical parameter E_N^T for the organic solvents used in the present study. 36

3 Comparison of the viscosities, fluorescence quantum yields, and fluorescence spectral peak locations for deoxyguanosine in the sucrose solutions used in the present study. 52

LIST OF FIGURES

FIGURE PAGE

PART I: EXCITED-STATE PROPERTIES OF DEOXYGUANOSINE

1 The chemical structure of deoxyguanosine (Saenger, 1984); here, deoxyguanosine is shown on the right as it forms Watson-Crick hydrogen bonds with cytosine. 3

2. Comparison of the fluorescence spectra of deoxyguanosine in various solvents used in this study. 9

3. Comparison of the fluorescence spectra of deoxyguanosine in various solvents used in this study. The spectra have been normalized at the peak 10

4 Comparison of the fluorescence spectrum of deoxyguanosine in water to that of deoxyguanosine in buffer consisting of 0.1 M NaCl, 0.05 M sodium cacodylate, pH 7.0 in triply distilled water. 11

5. Comparison of the absorption spectrum of deoxyguanosine in water to that of deoxyguanosine in buffer; the spectra have been normalized at the peak. 12

6. Comparison of the fluorescence spectrum of deoxyguanosine in butanol at room temperature to that of deoxyguanosine in butanol at room temperature after a 10 minute incubation at 40 °C. 13

7. Comparison of the fluorescence spectrum of deoxyguanosine in acetonitrile to that of deoxyguanosine in buffer. The bar indicates the error associated with the fluorescence spectra presented in this study. 16

8 Comparison of the fluorescence spectrum of deoxyguanosine in acetonitrile to that of deoxyguanosine in buffer, the spectra have been normalized at the peak. The bar indicates the of error associated with the fluorescence spectral tail presented in this study. 18

9 Comparison of the fluorescence spectrum of deoxyguanosine in poly (dG-dC)•poly (dG-dC) to that of deoxyguanosine in buffer; the spectra have been normalized at the peak (data taken from Huang and Georghiou, 1992). 19

10. Comparison of the absorption spectrum of deoxyguanosine in acetonitrile to that of deoxyguanosine in buffer; the spectra have been normalized at the peak. The bar indicates the error associated with the absorption spectra presented in this study. 20

11 Comparison of the absolute fluorescence spectrum of deoxyguanosine in methanol to that of deoxyguanosine in buffer. 21

12. Comparison of the fluorescence spectrum of deoxyguanosine in methanol to that of deoxyguanosine in buffer; the spectra have been normalized at the peak. 22

13. Comparison of the absorption spectrum of deoxyguanosine in methanol to that of deoxyguanosine in buffer; the spectra have been normalized at the peak. 24

14. Comparison of the fluorescence spectrum of deoxyguanosine in 2-propanol to that of deoxyguanosine in buffer. 25

15. Comparison of the fluorescence spectrum of deoxyguanosine in 2-propanol to that of deoxyguanosine in buffer; the spectra have been normalized at the peak. 26

16. Comparison of the absorption spectrum of deoxyguanosine in 2-propanol to that of deoxyguanosine in buffer; the spectra have been normalized at the peak. 27

17. Comparison of the fluorescence spectrum of deoxyguanosine in ethyl acetate to that of deoxyguanosine in buffer. 28

18 Comparison of the fluorescence spectrum of deoxyguanosine in ethyl acetate to that of deoxyguanosine in buffer; the spectra have been normalized at the peak. 29

19 Comparison of the absorption spectrum of deoxyguanosine in ethyl acetate to that of deoxyguanosine in buffer; the spectra have been normalized at the peak. 30

20. Comparison of the fluorescence spectrum of deoxyguanosine in diethyl ether to that of deoxyguanosine in buffer. 31

21. Comparison of the fluorescence spectrum of deoxyguanosine in diethyl ether to that of deoxyguanosine in buffer; the spectra have been normalized at the peak. 32

22. Comparison of the fluorescence spectrum of deoxyguanosine in methylene chloride to that of deoxyguanosine in buffer. 33

23. Comparison of the fluorescence spectrum of deoxyguanosine in methylene chloride to that of deoxyguanosine in buffer; the spectra have been normalized at the peak. 35

24. A plot of the polarizability *vs* the solvent polarity according to the E_N^T values for the solvents used in this study. 37

25. A plot of the dielectric constant *vs* the solvent polarity according to the E_N^T values for the solvents used in this study. 38

26 A plot of the polarizability *vs* the dielectric constant for the solvents used in this study. 39

27. Comparison of the fluorescence spectrum of deoxyguanosine in pH 11 to that of deoxyguanosine in buffer. 40

28 Comparison of the fluorescence spectrum of deoxyguanosine in pH 11 to that of deoxyguanosine in buffer; the spectra have been normalized at the peak. 41

29. Comparison of the absorption spectrum of deoxyguanosine in pH 11 to that of deoxyguanosine in buffer; the spectra have been normalized at the peak. 42

30 Comparison of the fluorescence spectrum of deoxyguanosine in pH 0.5 to that of deoxyguanosine in buffer. 44

31. Comparison of the fluorescence spectrum of deoxyguanosine in pH 0.5 to that of deoxyguanosine in buffer; the spectra have been normalized at the peak. 45

32 Comparison of the absorption spectrum of deoxyguanosine in pH 0 5 to that of deoxyguanosine in buffer; the spectra have been normalized at the peak. 46

33. Comparison of the fluorescence spectrum of deoxyguanosine in 60% sucrose solution, with a viscosity of 14 cP, to that of deoxyguanosine in buffer at room temperature. 47

34. Comparison of the fluorescence spectrum of deoxyguanosine in 60% sucrose solution at 5 °C, with a viscosity of 29 cP, to that of deoxyguanosine in buffer at room temperature 48

35. Comparison of the fluorescence spectrum of deoxyguanosine in 77% sucrose solution, with a viscosity of 58 cP, to that of deoxyguanosine in buffer at room temperature. 49

36 Comparison of the fluorescence spectrum of deoxyguanosine in 77% sucrose solution at 5 °C, with a viscosity of 149 cP, to that of deoxyguanosine in buffer at room temperature. 50

37. Comparison of the absorption spectrum of deoxyguanosine in 60% sucrose solution to that of deoxyguanosine in buffer at room temperature; the spectra have been normalized at the peak. 53

38. Comparison of the absorption spectrum of deoxyguanosine in 77% sucrose solution to that of deoxyguanosine in buffer at room temperature; the spectra have been normalized at the peak. 54

39. Comparison of the absorption spectrum of deoxyguanosine in 77% sucrose solution at 5 °C to that of deoxyguanosine in buffer at room temperature. 55

40. Comparison of the absorption spectrum of deoxyguanosine in buffer at room temperature to that at 5 °C 56

41. Comparison of the fluorescence spectrum of deoxyguanosine in buffer at room temperature to that of deoxyguanosine in buffer at 5°C. 58

42. Comparison of the fluorescence spectra of deoxyguanosine in 0% sucrose solution at 5 °C, 60% sucrose solution at room temperature, 60% sucrose solution at 5°C, 77% sucrose solution at room temperature, and 77% sucrose solution at 5 °C, to that of deoxyguanosine in buffer at room temperature. 59

43. A plot of the fluorescence quantum yield of deoxyguanosine as a function of viscosity of the various sucrose solutions used in the present study 60

44. Plot of the fluorescence quantum yield of deoxyguanosine as a function of solvent dielectric constant. 62

45. Plot of the difference between the wavenumbers of the maxima of the absorption and fluorescence spectra (ν_a - ν_f) of deoxyguanosine as a function of solvent polarity according to Lippert's function; the open symbol pertains to methylene chloride. 63

46. Plot of the fluorescence quantum yield of deoxyguanosine as a function of solvent polarity according to Lippert's function. 64

47. Plot of the fluorescence quantum yield of deoxyguanosine as a function of the empirical measure of solvent polarity according to E_N^T values 66

48 Plot of the fluorescence quantum yield of deoxyguanosine as a function of solvent polarizability 67

49. Plot of the fluorescence quantum yield of deoxyguanosine as a function of the solvent viscosity. 68

50 Plot of the fluorescence tail-to-peak ratio of deoxyguanosine as a function of the solvent dielectric constant. 72

51 Plot of the fluorescence tail-to-peak ratio of deoxyguanosine as a function of the solvent polarity according to the values of the E_N^T scale 73

52 Plot of the fluorescence tail-to-peak ratio of deoxyguanosine as a function of the solvent polarizability. 74

53. Plot of the fluorescence tail-to-peak ratio of deoxyguanosine as a function of the fluorescence quantum yield. 75

54. Plot of the fluorescence tail-to-peak ratio of deoxyguanosine as a function of the solvent viscosity. 76

55. Comparison of the fluorescence spectrum of deoxyguanosine in 8% water/butanol mixtures in which the water was added using three different methods: "carried its own water," where deoxyguanosine was dissolved in water and then added to butanol, "injected," where water was added to butanol that already contained deoxyguanosine, and "premixed" where water and butanol were mixed, and then deoxyguanosine was dissolved in the mixture. The error bar pertains to the measurement for the "premixed" solution; this is a rather large error which may have its origin in the sensitivity of the fluorescence signal to relatively small variations in the hydration pattern of water around deoxyguanosine. 80

56. Comparison of the fluorescence spectrum of deoxyguanosine in an 8% water/butanol solution in which water and butanol were mixed before dissolving the dG in it The deoxyguanosine solutions were then heated to 27 °C, 31 °C,

35 °C, and 40 °C, and the fluorescence spectra were measured after the solutions reached room temperature. 82

57 A plot of the natural logarithm of the intensity I of the fluorescence spectra of deoxyguanosine *vs.* 1/absolute temperature for the measurements described in the caption to Fig. 56 83

PART II: ELECTROSTATIC INTERACTIONS IN DNA

58. A plot of the relative polarization potential for electrostatic interactions as a function of $\delta = s/\beta$, where s is the distance between two ions of the same sign and β is the nearest neighbor distance, for the reduced polarizability α^* values of 0.05, 0.1, and 0.5. α^* is defined as α/β^3, where α is the polarizability of the medium. The open circles are data obtained by using an interpolation computer program based on Lagrange's method to obtain data for $\alpha^* = 0.18$. These values of the potential must be multiplied by $2.3 \times 10^{-18}/\beta$, with β in Å, for converting their units to Joules. 93

59. A plot of the Coulomb potential, V_{coul}, the polarization potential, V_{pol}, and the effective potential, $V_{eff} = V_{coul} + V_{pol}$, for a nearest neighbor distance of $\beta = 3.5$ Å and a reduced polarizability $\alpha^* = 0.18$, as a function of groove width s. 95

60. A plot of the effective interaction potential $V_{eff} = V_{coul} + V_{pol}$ as a function of groove width for different odd nearest neighbor values β as indicated on the curves. 96

61. A plot of the effective interaction potential $V_{eff} = V_{coul} + V_{pol}$ as a function of groove width for different even nearest neighbor values β as indicated on the curves. 97

62. A plot of the effective electrostatic force F as a function of groove width for the following values of the nearest neighbor distance β: 3.2, 3.5, 3.7, 3.9, 4.1, 4.5, and 5 0 Å. The force was calculated from the negative derivative of the V_{eff} with respect to the groove width s. The error bar shown for $\beta = 3.2$ Å indicates the uncertainty in the calculation of the force. 100

63. A comparison of the effective polarization potentials for electrostatic interactions across the grooves of DNA in the absence and in the presence of protein. 110

LIST OF ABBREVIATIONS

Full-width at Two-Thirds Maximum..... .....FWTTM

Deoxyguanosine..... . .. .dG

Thymidine ....T

PART I
EXCITED-STATE PROPERTIES OF DEOXYGUANOSINE

I. INTRODUCTION

This work has been done in order to investigate the photophysical properties of the internal environment of the DNA double helix. The bases are connected to the sugar and are situated in the interior of the helix; however, they have some access to their external aqueous environment through the major and minor grooves. The excited-state properties of nucleic acids yield a great deal of information with regard to their environment. Although free deoxyguanosine, dG, has a fluorescence quantum yield comparable to that of free thymidine, T, (in buffer), 0.8×10^{-4} and 1×10^{-4}, respectively (Vigny and Ballini, 1997), T remains the major emitter in DNA, with guanine fluorescing minimally (Huang and Georghiou, 1992). We would like to gain an insight into the internal environment of DNA to determine why this is so regarding dG. Our study uses free dG in a variety of organic solvents The structure of dG is shown in Fig. 1.

An interesting property of guanine is its affinity for water. It has a high free energy of solvation ΔG, approximately - 20 kcal/mol (Bash *et al* , 1987, Mohan *et al.*, 1992; Elcock and Richards, 1993). The ability of guanine to remain solvated may explain several important processes, properties, and conformations of DNA. We will test this possibility in this study. There is also an interesting property of the polynucleotide poly(dG-dC)•poly(dG-dC), for which dG is the only fluorophore (Georghiou and Saim, 1986)· the intensity of the fluorescence spectrum drops rather slowly at long wavelengths, and this results in the formation of a tail. Studies regarding the internal environment of DNA may explain this formation.

The aims of this study are to investigate (i) the quenching of the fluorescence of dG in native DNA, (ii) the extent to which dG is exposed to the aqueous environment,

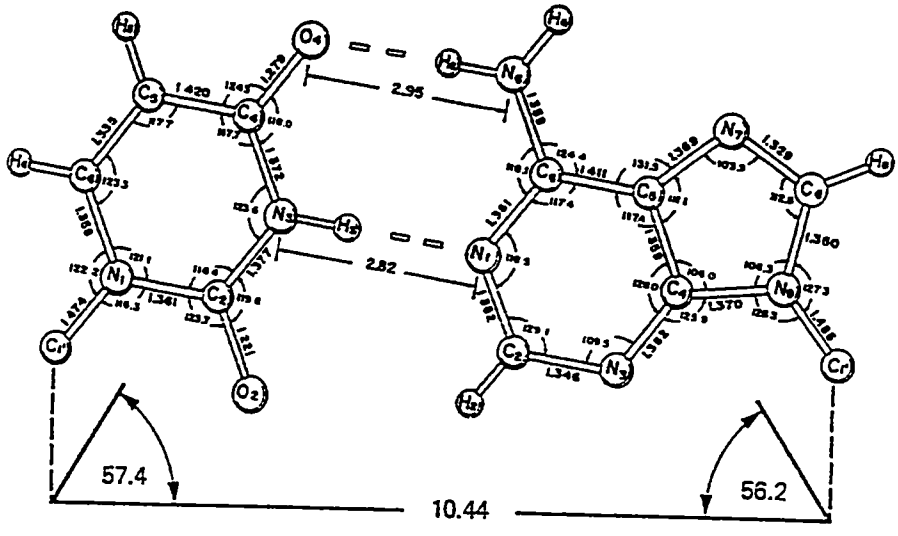


Figure 1
The chemical structure of deoxyguanosine (Saenger, 1984); here, deoxyguanosine is shown on the right as it forms Watson-Crick hydrogen bonds with cytosine

(iii) the extent of hydrogen bonding effects on the photophysical properties of dG, (iv) the affinity of dG for water, (v) the formation of the tail in the fluorescence spectrum of poly(dG-dC)•poly(dG-dC), and (vi) the effect of the rigid structure of DNA on the photophysical properties of dG by allowing the bases less freedom to move.

The first five aims are investigated by using organic solvents, selected according to their purity and absorption in the UV region, that have varying dielectric constants and polarizabilities As a result of the fact that the internal environment of DNA is less polar than its external environment, exposing free dG to different polarities should provide information about the environment of dG in DNA. A comparison has been made of the shifts in the peak wavelengths of the fluorescence and absorption spectra, of changes in the fluorescence quantum yield relative to that in buffer, and finally of changes in the tail-to-peak fluorescence ratios.

The third aim of this study utilizes the above approach but, in addition, investigates effects of hydrogen bonding. First, pH solutions of 0.5 and 11 are used to study whether adding or removing a proton from specific binding sites of dG makes any significant difference in the absorption or fluorescence spectra. The sites involved are at N7 and N1, respectively. The second method has utilized a small percentage a water that has been added to butanol, and the observed changes in the peak wavelength, in the quantum yield, and in the tail-to-peak ratio were quantified. Methylation of the N7 position has already been studied by previous work done in our laboratory. Other sites of interest, N3 and N2, cannot be studied due to lack of product availability.

The fourth aim arose as a result of the aforementioned experiments that employed a mixture of a small percentage of water with butanol. The water was added by using

three different methods: (i) injecting water into a solution that contained dG and butanol, (ii) dissolving dG in neat water, then adding this to butanol, and (iii) mixing the water and the butanol together, then adding the dG. The photophysical properties of dG are found to depend on the sequence of the steps which are used to add the water. The results have implications regarding the solvation of dG in DNA and the extent to which dG regions in DNA are "unzipped."

The final aim, to imitate the rigid structure of DNA by allowing the bases less freedom to move, was addressed by varying the viscosity of the environment while retaining the aqueous polar environment This was accomplished by studying the changes in the fluorescence spectra through a set of five experiments: (i) dG in buffer at 5°C for which the viscosity is 1.5 cP compared to that of 1 cP at room temperature (Lide, 1992-1993), (ii) dG in a 60% w/v sucrose solution, viscosity of 14 cP (Barber, 1966), (iii) dG in a 60% sucrose solution at 5°C, viscosity of 29 cP, (iv) dG in a 77% w/v sucrose solution, viscosity of 58 cP (Barber, 1966), and (v) dG in a 77% sucrose solution at 5°C, viscosity of 149 cP.

II. MATERIALS AND METHODS

Deoxyguanosine was obtained from Sigma (St. Louis, MO). Optima grade methanol, optima grade 2-propanol, and nonstabilized HPLC grade methylene chloride were all obtained from Fisher Scientific (Pittsburgh, PA). HPLC grade acetonitrile manufactured by Mallinckrodt and high purity grade n-butanol manufactured by Burdick and Jackson were obtained from VWR (Suwanee, GA). Carbonyl free, high purity ethyl acetate and nonstabilized HPLC grade diethyl ether were obtained from Burdick and Jackson (Fisher, Pittsburgh). Ultrapure sucrose was obtained from Boehringer Mannheim (Indianapolis, IN) and further purified in our laboratory using activated charcoal (Sigma, St. Louis). All absorption measurements were made with a Shimadzu UV-254 spectrophotometer (Columbia, MD). Fluorescence measurements were made with a spectrofluorometer employing a 1 kW Xe-Hg lamp (Spectral Energy Corp, Hillsdale, NJ) for excitation and a 0.32 m focal length HR-320 Instruments SA monochromator (Metuchen, NJ) for emission, a Stanford Research Systems SR440 preamplifier and a SR400 photon counter (Sunnyvale, CA), and a thermoelectrically cooled 9558 QB EMI photomultiplier (Fairfield, NJ) (Ge and Georghiou, 1991). Unless noted otherwise, all absorption and fluorescence measurements were made at room temperature, 23 °C. All measurements in this study were made with an excitation wavelength of 265 nm with emission and excitation bandwidths of 5 nm and 1.7 nm, respectively. The excitation entrance/exit slit widths of the monochromator were 4 mm/3 mm, whereas those for the emission slit width were 2 mm/2 mm, respectively. For the aqueous measurements, a 0.1 M NaCl (Fisher, Pittsburgh), 0.05 M sodium cacodylate (Fluka, Ronkonkana, NY), pH 7 buffer prepared in triply distilled water (Carolina Biological Supply, Burlington,

NC) was used. Sample absorbance was kept between 0.05 and 0.06 to insure proportionality between the fluorescence signal and the sample concentration. In diethyl ether and methlyene chloride lower absorbances were used because of the low solubility of dG in these solvents All organic solvents used were selected by previous work done in our laboratory (Taylor-Gerke, 1996), and all solutions were formed by using glassware that had been washed in chromic acid. The full-width at two-thirds maximum (FWTTM) $\Delta\bar{\nu}$ (cm^{-1}) of the fluorescence and absorption spectrum were calculated using the following formula:

$$\Delta\bar{\nu}=(\Delta\lambda)\frac{10^7}{<\lambda>^2}$$

where $\Delta\lambda$ is the two-thirds widths in terms of wavelength and $<\lambda>$ is the average wavelength of the spectral band. We chose to use the two-thirds maximum, instead of the half-maximum, in order to avoid any contribution to $\Delta\bar{\nu}$ from the fluorescence spectral tail. The estimated uncertainty in the fluorescence spectral peak wavelength was ± 2 nm, and that for the absorption spectral peak wavelength was ± 0.25 nm The tail-to-peak calculation was made by using the following formula:

$$\gamma=\frac{flu_{460}}{flu_{peak}}$$

where flu_{peak} is the fluorescence intensity at the peak and flu_{460} is the fluorescence intensity at λ = 460 nm Quantum yields were determined relative to that in buffer. A

plot of the fluorescence spectra of dG in various solvents is shown in Fig. 2. Figure 3 shows the spectra normalized at their peaks.

Solutions in organic solvents were prepared in Kimax culture tubes that had been washed in chromic acid. The solvent was added to the tube followed by a very small amount of dG. The solution was then stirred until dG dissolved. The absorbance was then checked and adjusted. Diethyl ether and methylene chloride were the only exceptions to this procedure. Because these solvents are highly unstable and sensitive to the formation of photoproducts upon exposure to light, solutions in them were prepared in a fume hood in the absence of light. Due to the volatile nature of diethyl ether, it could not be stirred. Consequently, the solution prepared in this solvent was kept overnight covered with aluminum foil to protect it from light.

The butanol/water mixtures were made as outlined above. It should be noted here that water was used in these mixtures instead of buffer because buffer is not miscible with butanol. In this regard, there is no change in the fluorescence spectrum of dG in water *vs* that in buffer (Fig 4) Also, after incubating the butanol/water mixture at 40 °C, it was observed that upon cooling to room temperature the absorption spectrum of dG did not change. We should note that that was also the case for the absorption as well as the fluorescence spectrum of dG in pure butanol (Figs. 5 and 6). Therefore, no chemical reaction occurred between butanol and dG upon heating. We should also note that the two peaks appearing in the absorption spectra stem from the two excited states of dG (Ge *et al.*, 1990). At an excitation wavelength of 265 nm, 85% of the absorption is due to the second excited state (Ge *et al.*, 1990). Within the range of interest, this is the best place to excite because the absorption of the first excited state is at its minimum, and our

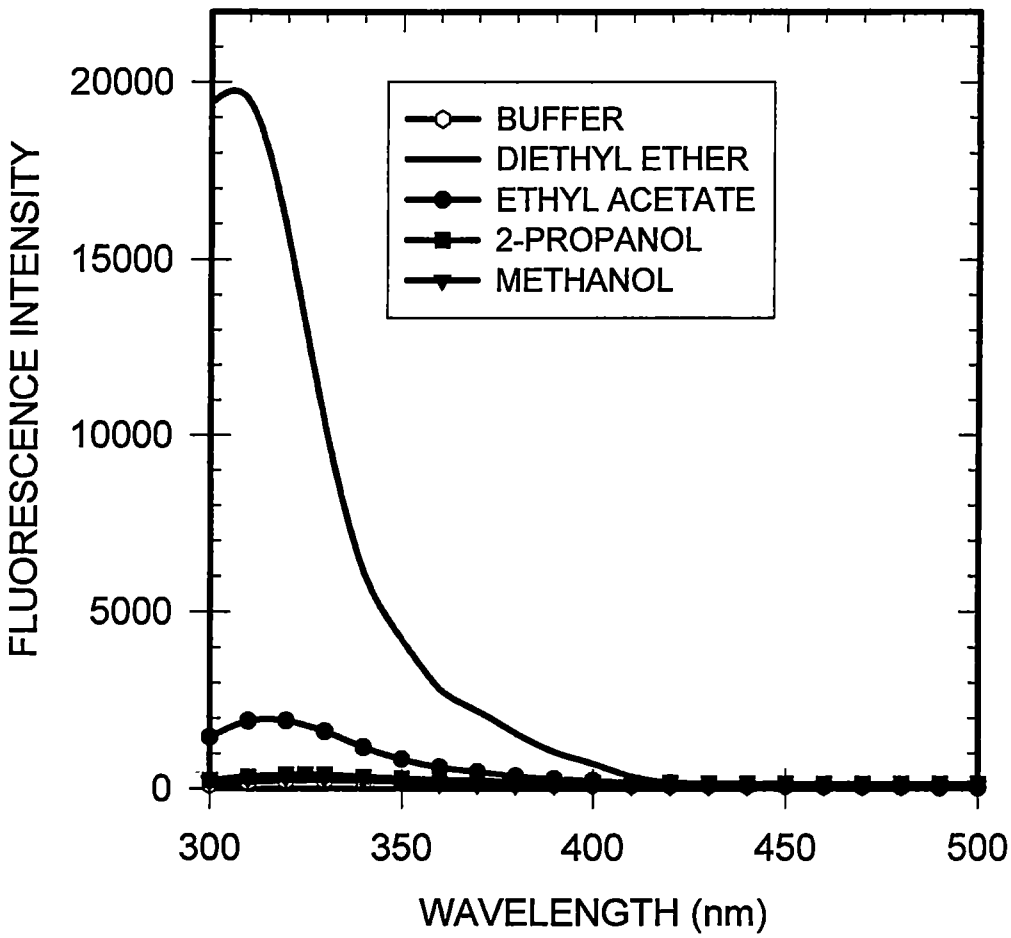


Figure 2
Comparison of the fluorescence spectra of deoxyguanosine in various solvents used in this study.

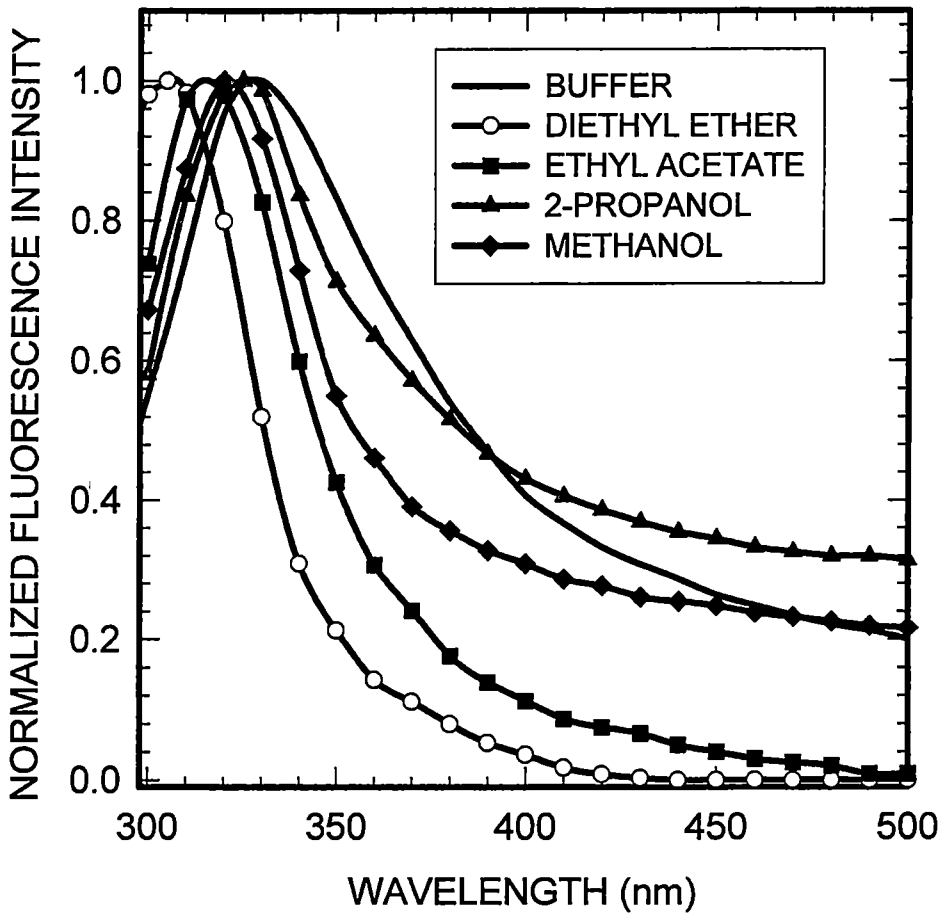


Figure 3
Comparison of the fluorescence spectra of deoxyguanosine in various solvents used in this study. The spectra have been normalized at the peak.

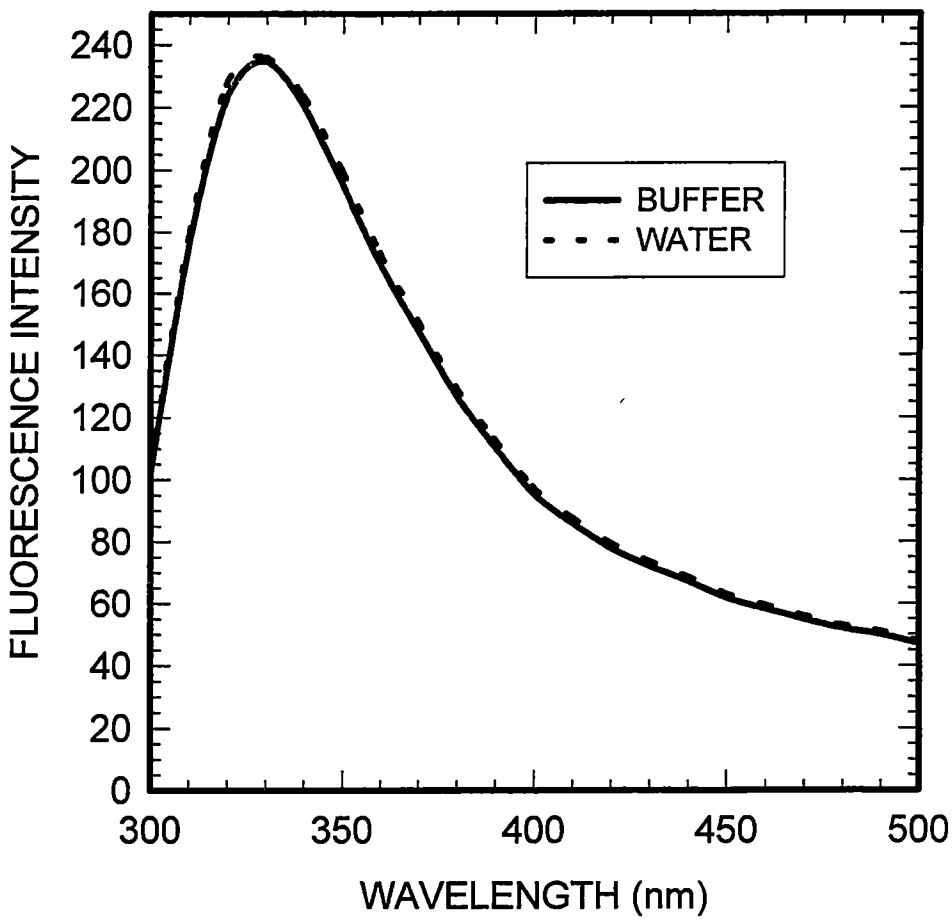


Figure 4
Comparison of the fluorescence spectrum of deoxyguanosine in water to that of deoxyguanosine in buffer consisting of 0.1 M NaCl, 0.05 M sodium cacodylate, pH 7.0 in triply distilled water.

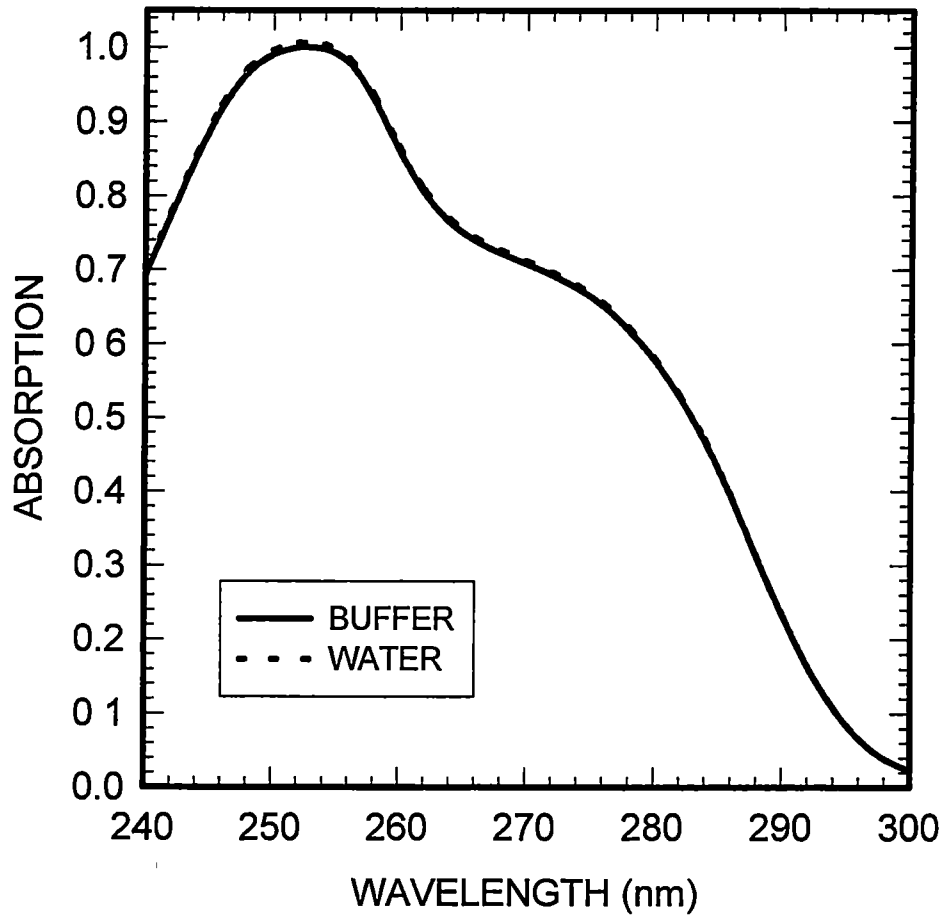


Figure 5
Comparison of the absorption spectrum of deoxyguanosine in water to that of deoxyguanosine in buffer, the spectra have been normalized at the peak.

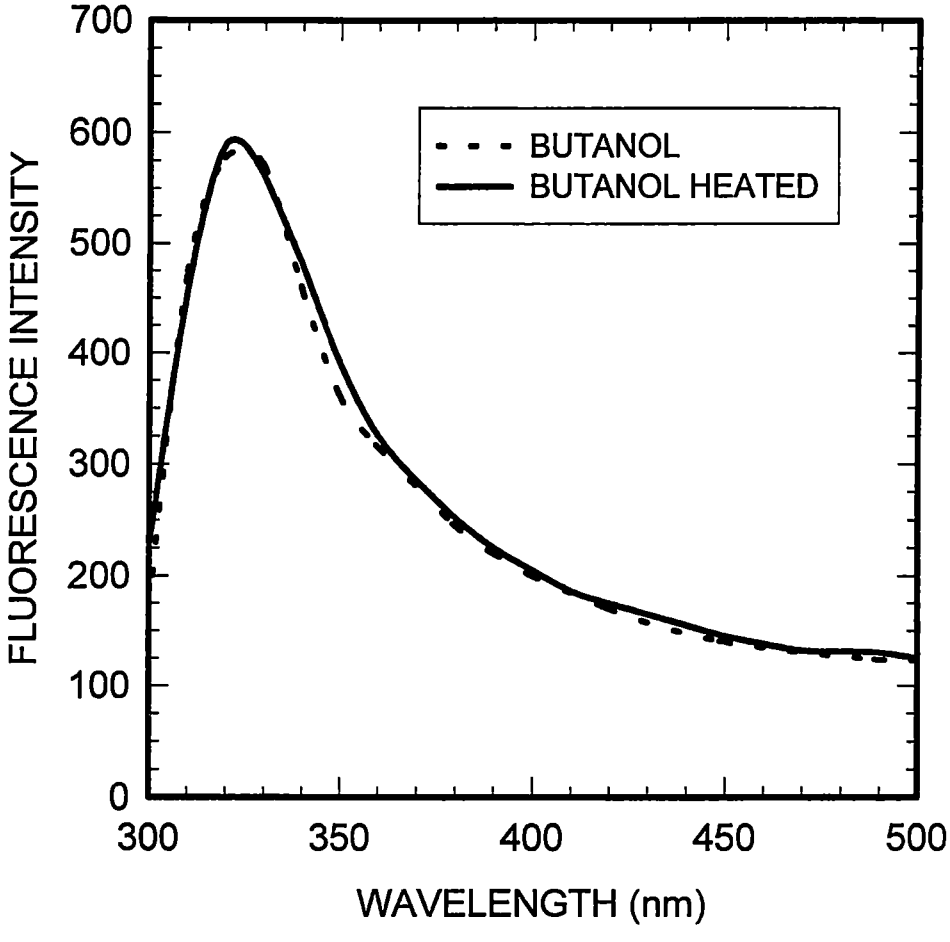


Figure 6
Comparison of the fluorescence spectrum of deoxyguanosine in butanol at room temperature to that of deoxyguanosine in butanol at room temperature after a 10 minute incubation at 40 °C.

Hg- Xenon lamp has a strong intensity line at this wavelength

The pH 0.5 solution was also prepared in acid washed glassware, and the base solution was prepared in a 250 ml acid-washed flask. Both were diluted to the requisite pH and then formed as outlined above.

Sucrose solutions were made by mixing the appropriate amount of sucrose and buffer in acid-washed vials. These solutions were hand shaken, and then allowed to sit overnight. For the 77% sucrose solution, some vortexing was also done. Low temperature measurements were made by pumping a 50% v/v deionized water and ethylene glycol mixture through the cuvette holder. During the cooling period and during the measurements, the cuvettes were kept free of water condensation by allowing a gentle stream of purified nitrogen to pass through the cuvette chamber.

III. RESULTS

SOLVENTS

The solvents used in this study were selected according to their purity, absorption in the UV region, physical and chemical properties, and ability to sufficiently dissolve deoxyguanosine, dG. Listed in order of decreasing dielectric constant, the solvents were: buffer (80), acetonitrile (38), methanol (33), 2-propanol (18), methylene chloride (9), ethyl acetate (6), and diethyl ether (4) (Dean, 1992). All calculations for fluorescence quantum yields were made relative to that in buffer.

The relative quantum yield in acetonitrile was found to be 1.2 (Fig. 7, Table 1). The appearance of the fluorescence spectrum is quite narrower than that in buffer with a full width at two thirds maximum, FWTTM, of 3048 ± 183 cm^{-1} as compared to 4432 ± 267 cm^{-1} in buffer. The peak has shifted slightly to shorter wavelengths, to 320 nm compared to that of 330 nm in buffer (Fig. 8). The value of the tail-to-peak ratio γ of 0.19 in acetonitrile is the same as that for poly(dG-dC)•poly(dG-dC) (Huang and Georghiou, 1992) (Fig. 9). The absorption spectrum in acetonitrile peaks at 255 nm, whereas that in buffer peaks at 252 nm. The FWTTM for the absorption spectrum in acetonitrile is slightly narrower being 4883 ± 293 cm^{-1}, while that in buffer is 5419 ± 325 cm^{-1} (Fig 10). The quantum yield in methanol is equal to 1.6 (Fig 11, Table 1); the fluorescence spectrum is narrower than that in buffer, but the difference is not as dramatic as that of the spectrum in acetonitrile: its FWTTM value is 3602 ± 216 cm^{-1} In methanol, like in acetonitrile, the peak wavelength is 320 nm (Fig. 12). The γ ratio for dG in methanol is 0.24. The absorption spectrum of dG in methanol is very similar to that in acetonitrile, having a peak wavelength of 255 nm and

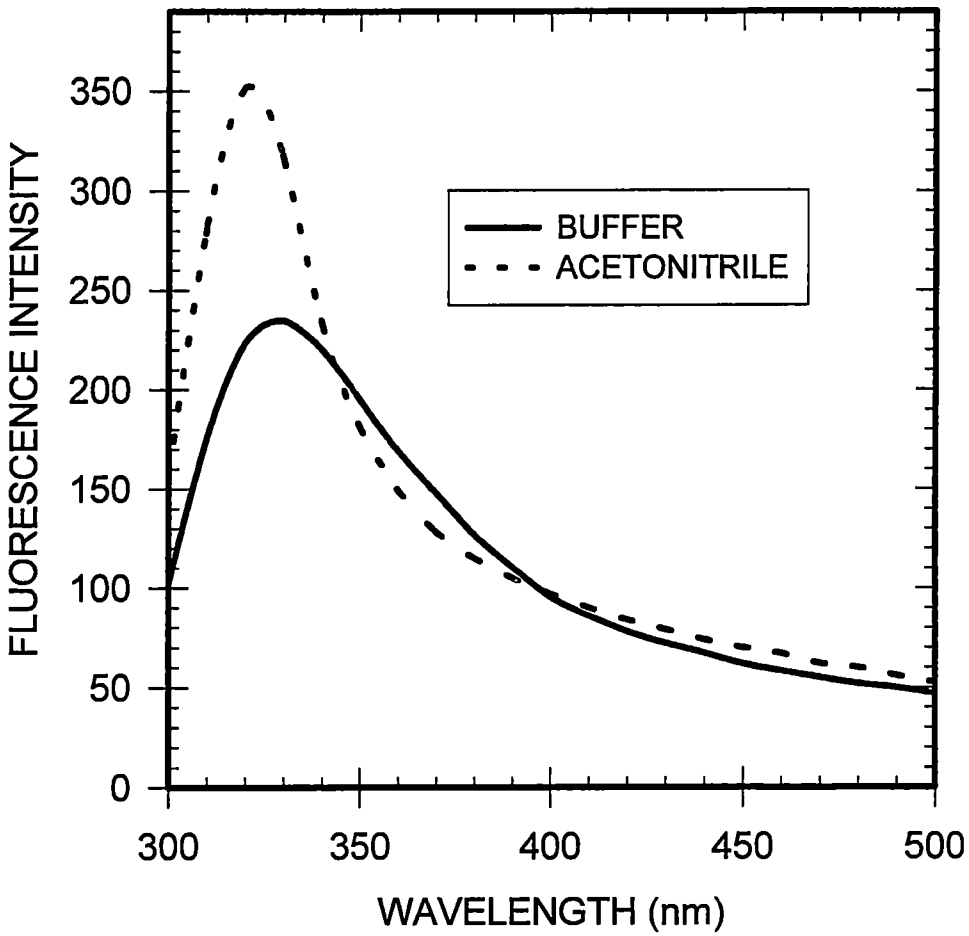


Figure 7
Comparison of the fluorescence spectrum of deoxyguanosine in acetonitrile to that of deoxyguanosine in buffer. The bar indicates the error associated with the fluorescence spectra presented in this study.

Table 1

Comparison of the quantum yields, full-widths-two-thirds maxima of the fluorescence and absorption spectra, tail-to-peak fluorescence spectral ratios γ, and absorption and fluorescence spectral peak locations of deoxyguanosine in the solvents used in the present study.

SOLVENTS:	q	$FWTTM_f$ (cm^{-1})	$FWTTM_a$ (cm^{-1})	tail-to-peak γ	λ_a (nm)	λ_f (nm)
buffer	1	4432	5419	0.25	252	330
acetonitrile	1.2	3048	4883	0 19	255	320
methanol	1.6	3602	4883	0.24	255	320
n-butanol	1.8	4071	5228	0.23	255	325
2-propanol	2.6	4989	4849	0.33	255	325
methylene chloride	21	5408		0.06		330
ethyl acetate	6.3	3944	4776	0.04	255	315
diethyl ether	35	3703		0		305
pH 0.5	88	4981	5408	0.16	252	360
pH 11	9 3	3429		0 07		325

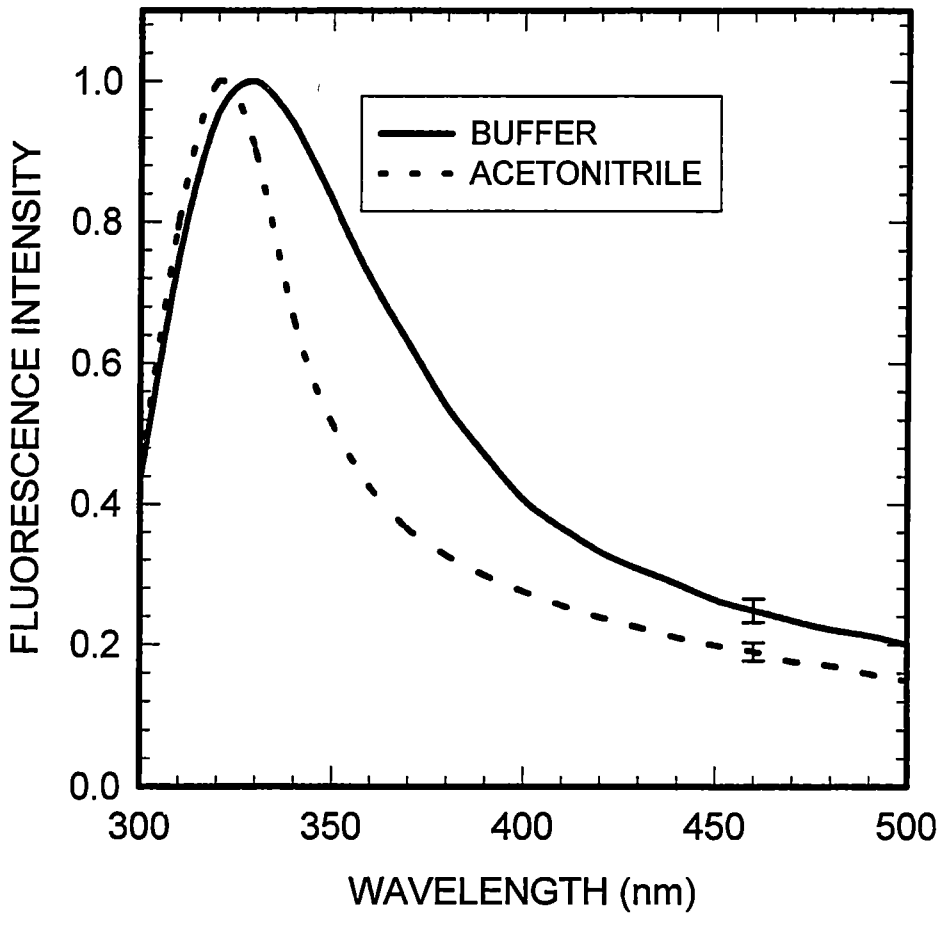


Figure 8
Comparison of the fluorescence spectrum of deoxyguanosine in acetonitrile to that of deoxyguanosine in buffer; the spectra have been normalized at the peak. The bar indicates the of error associated with the fluorescence spectral tail presented in this study.

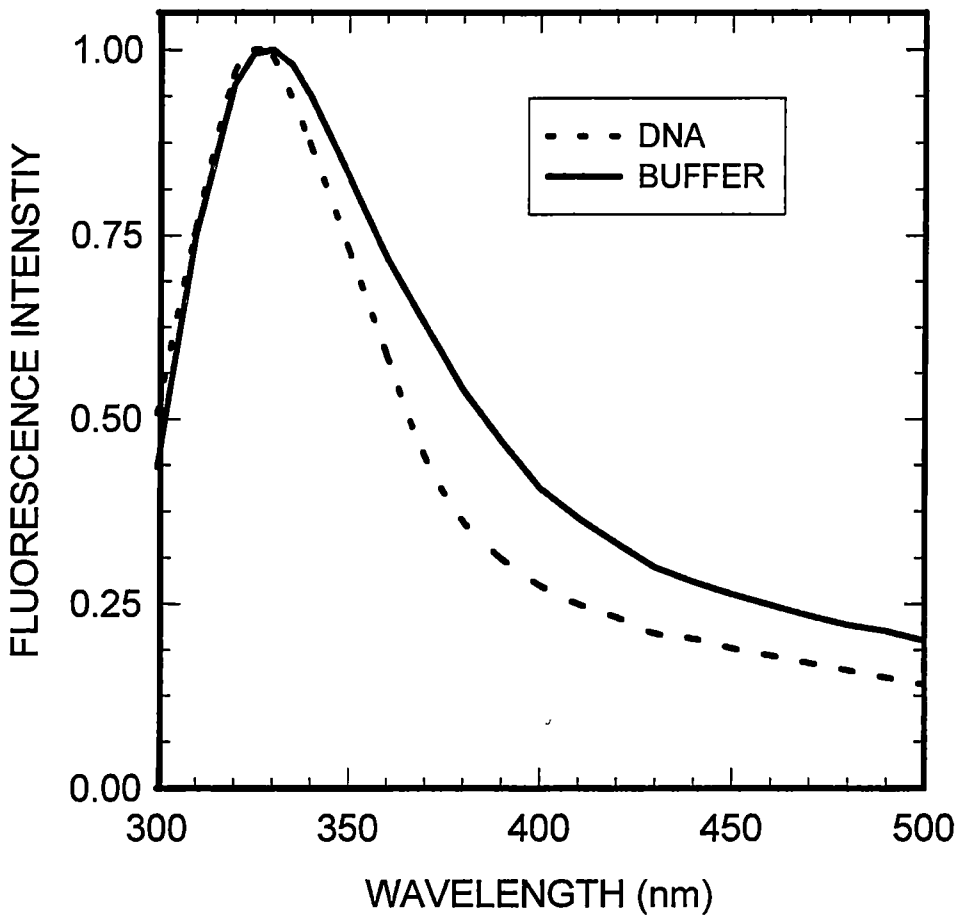


Figure 9
Comparison of the fluorescence spectrum of deoxyguanosine in poly (dG-dC)•poly (dG-dC) to that of deoxyguanosine in buffer, the spectra have been normalized at the peak (data taken from Huang and Georghiou, 1992).

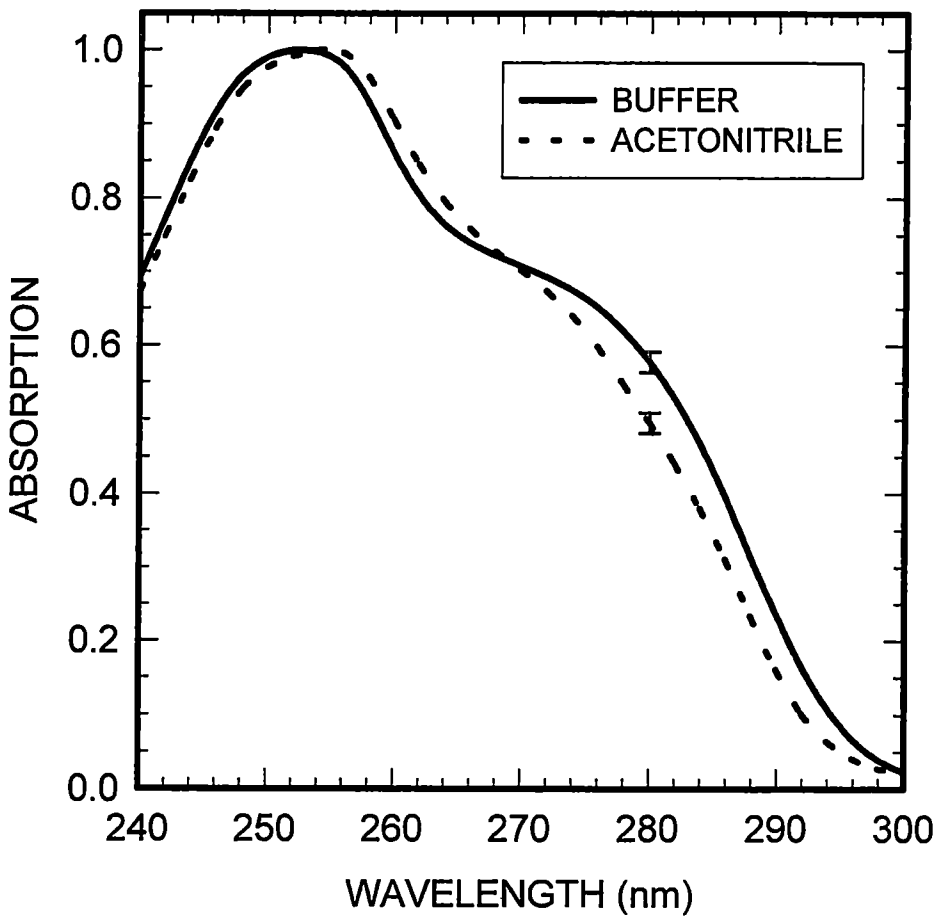


Figure 10
Comparison of the absorption spectrum of deoxyguanosine in acetonitrile to that of deoxyguanosine in buffer; the spectra have been normalized at the peak. The bar indicates the error associated with the absorption spectra presented in this study.

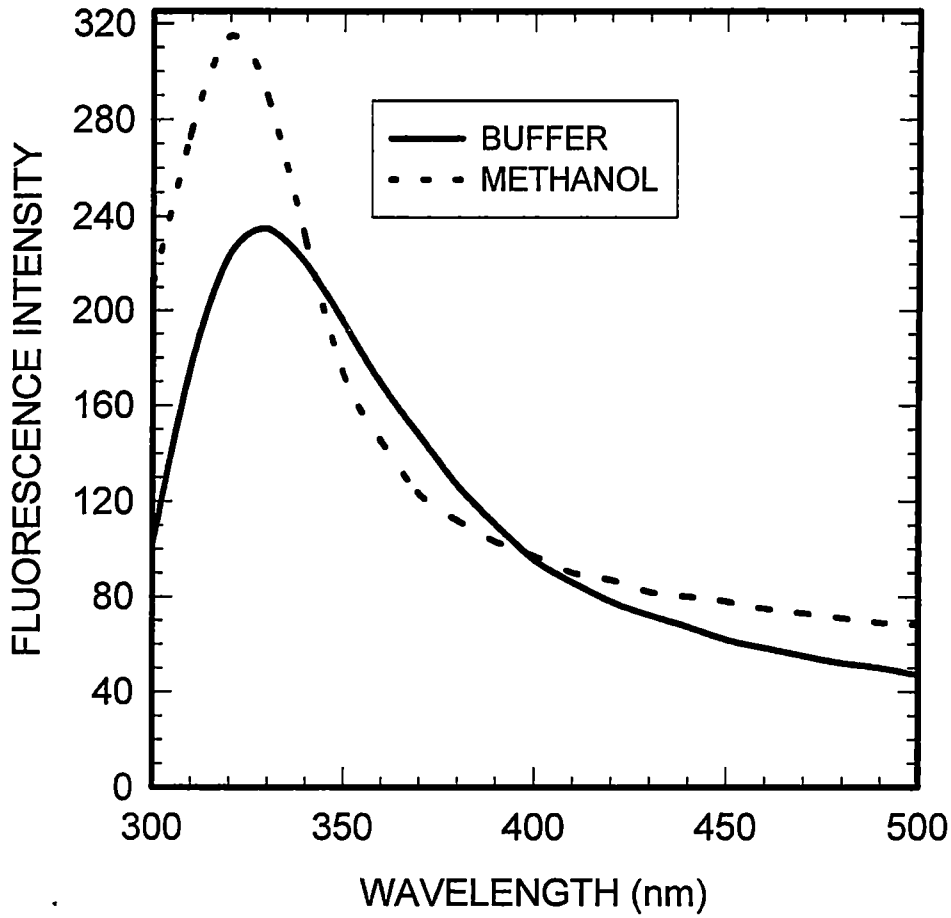


Figure 11
Comparison of the absolute fluorescence spectrum of deoxyguanosine in methanol to that of deoxyguanosine in buffer

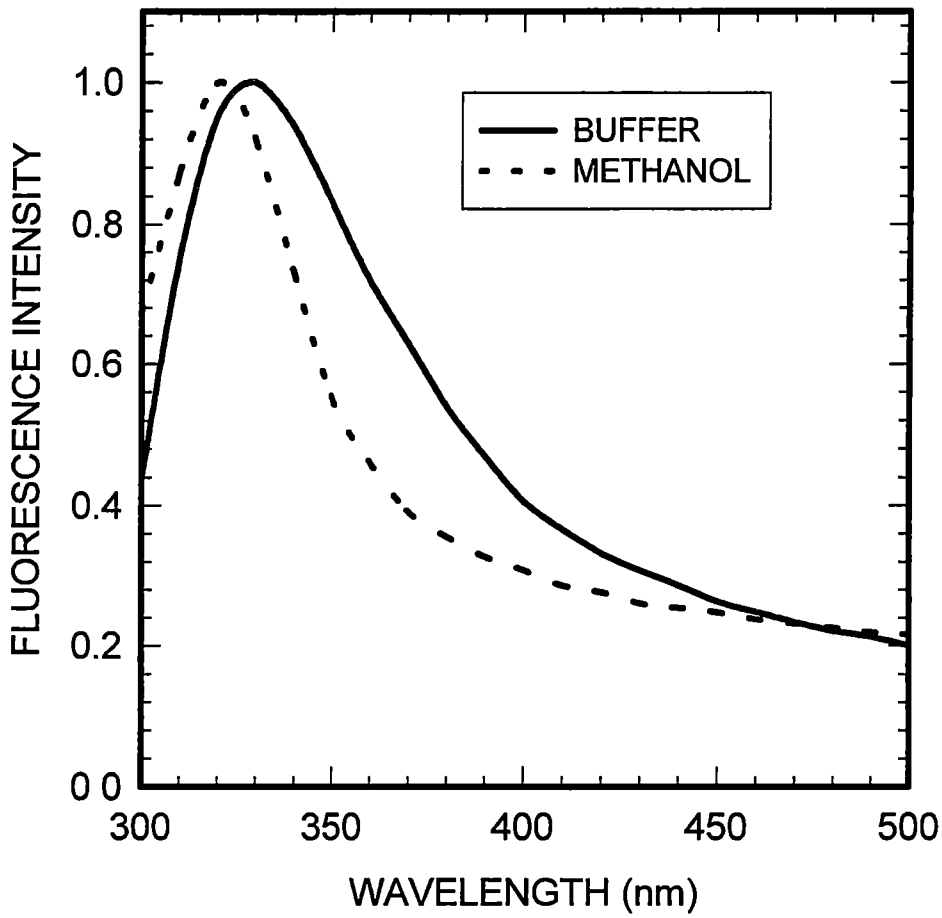


Figure 12
Comparison of the fluorescence spectrum of deoxyguanosine in methanol to that of deoxyguanosine in buffer; the spectra have been normalized at the peak.

an FWTTM value of 4883 ± 293 cm^{-1} (Fig. 13). The quantum yield in 2-propanol is 2.6 (Table 1), and the fluorescence spectrum has a γ ratio of 0.33 (Fig. 14). The fluorescence spectrum is the widest with an FWTTM value of 4989 ± 299 cm^{-1} and peaks at 325 nm (Fig. 15). The absorption spectrum in 2-propanol is reminiscent of those in methanol and acetonitrile peaking at 255 nm with an FWTTM value of 4849 ± 291 cm^{-1}, making it slightly narrower (Fig. 16). The quantum yield in ethyl acetate has a much greater value than those in the solvents discussed so far (Table 1), but the fluorescence spectrum in that solvent has a very small tail: the γ ratio is only 0.04 (Fig. 17). The peak has shifted considerably to shorter wavelengths, to 315 nm, and the spectrum is narrower than that in buffer having an FWTTM value of 3944 ±237 cm^{-1} (Fig. 18). The absorption spectrum, as in the previous solvents, peaks at 255 nm, and has an FWTTM value of 4776 ± 287 cm^{-1} (Fig. 19), which is slightly smaller than those in the other solvents It should be noted here that the solubility of dG in ethyl acetate was not very good. The absorption spectrum was acquired by using a maximum absorbance of 0.07 The quantum yield in diethyl ether has a huge value of 35 (Table 1) and the fluorescence spectrum has absolutely no tail with a γ ratio of 0 (Fig. 20). The peak has shifted dramatically to shorter wavelengths to 305 nm, which is much shorter than the peak wavelength of the fluorescence spectrum of any DNA reported (Ge and Georghiou, 1991, Huang and Georghiou, 1992, Vigny and Ballini, 1977). The FWTTM value is 3703 ± 231 cm^{-1} (Fig 21). In this solvent, dG has insufficient solubility, and so an absorption spectrum could not be obtained.

The quantum yield in methylene chloride is large having a value of 21 (Table 1) The γ ratio has a value of 0 06 (Fig 22). This γ ratio is higher than that in aprotic

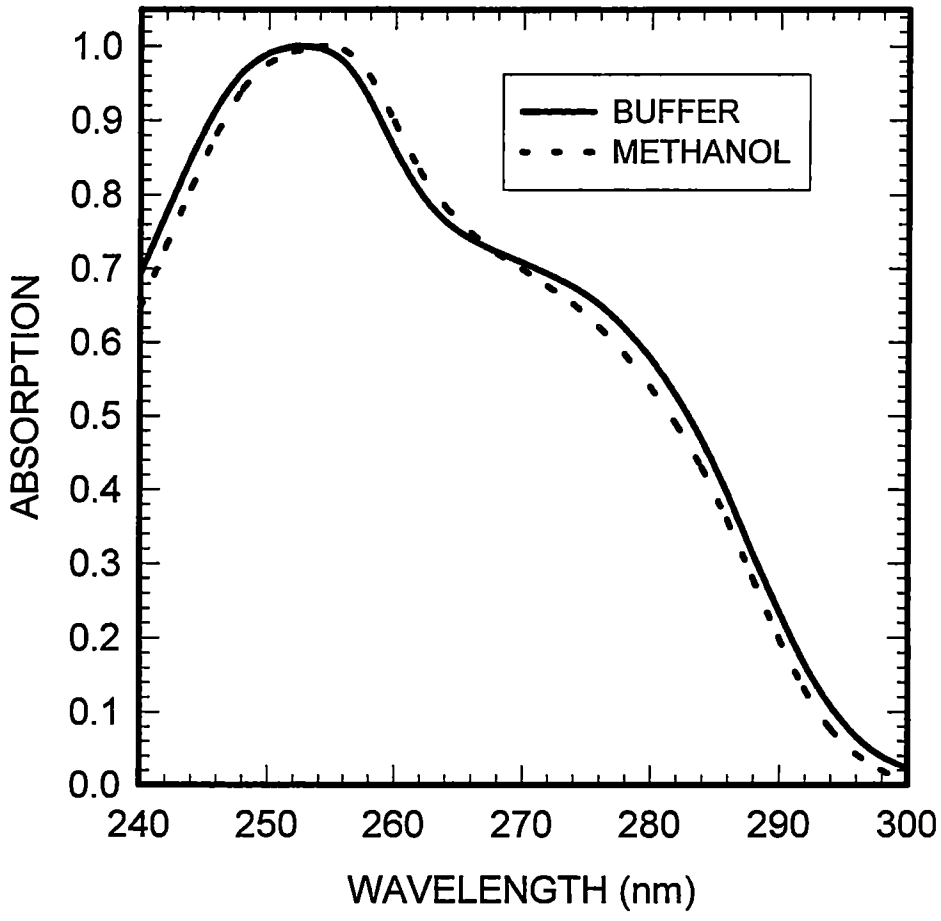


Figure 13
Comparison of the absorption spectrum of deoxyguanosine in methanol to that of deoxyguanosine in buffer; the spectra have been normalized at the peak.

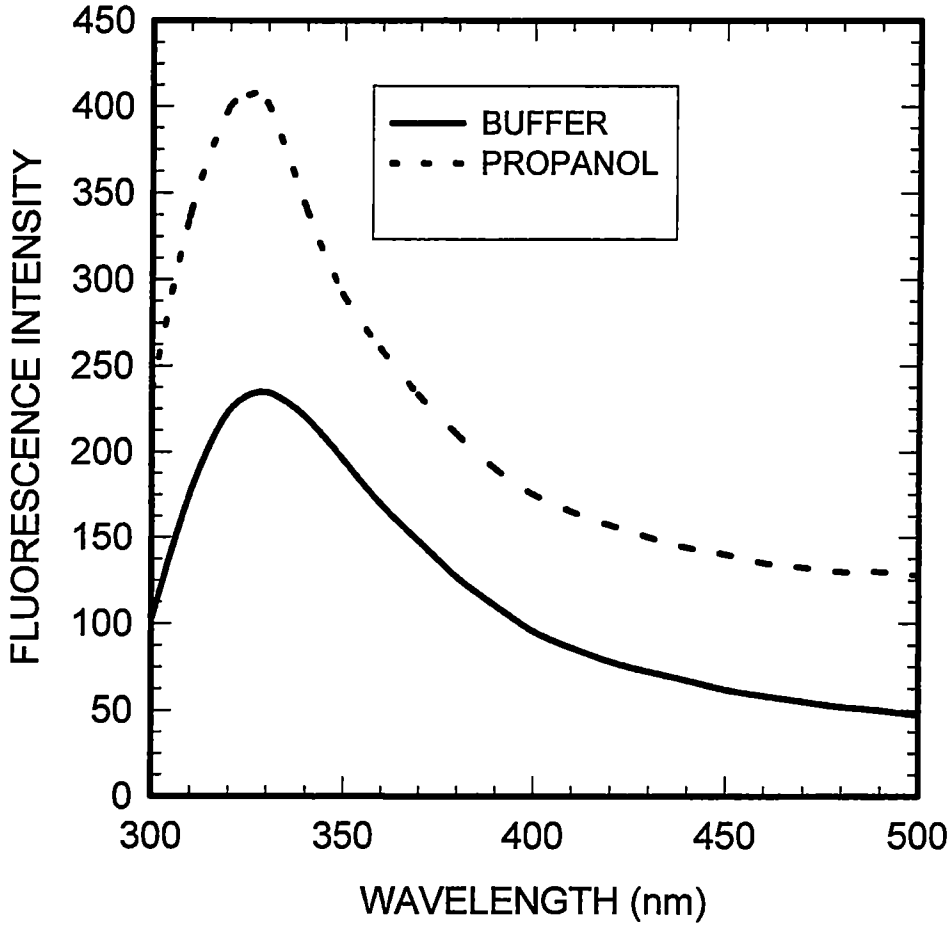


Figure 14
Comparison of the fluorescence spectrum of deoxyguanosine in 2-propanol to that of deoxyguanosine in buffer.

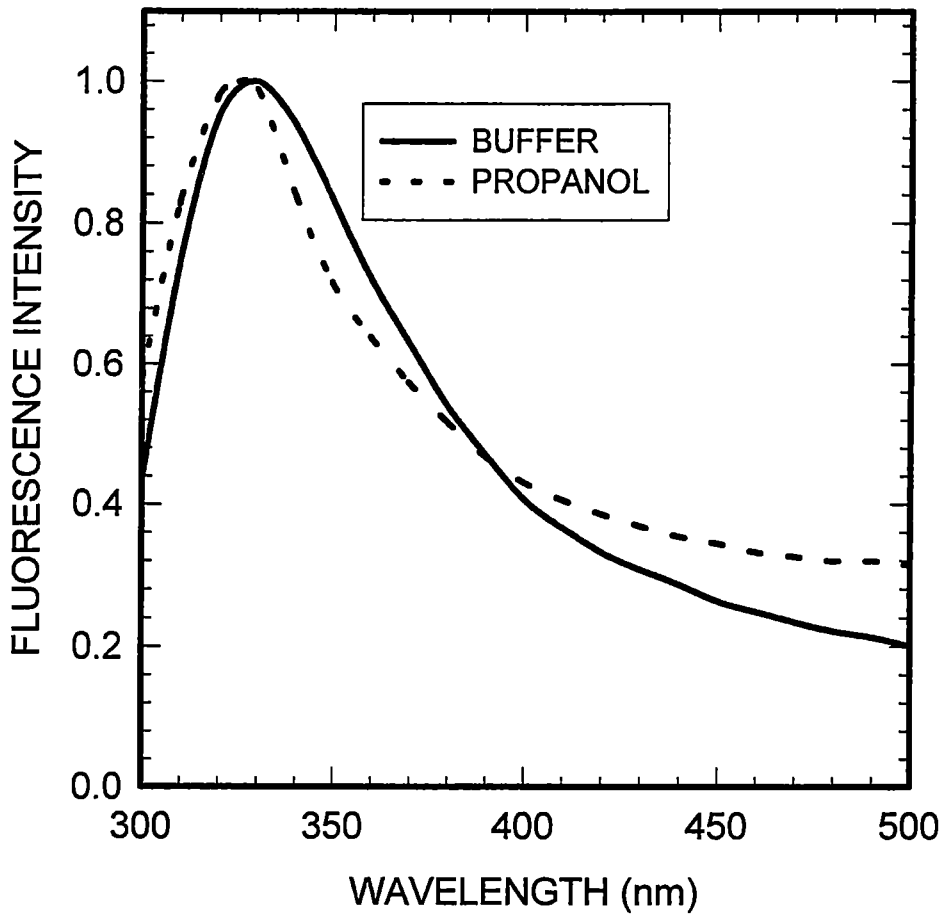


Figure 15
Comparison of the fluorescence spectrum of deoxyguanosine in 2-propanol to that of deoxyguanosine in buffer, the spectra have been normalized at the peak

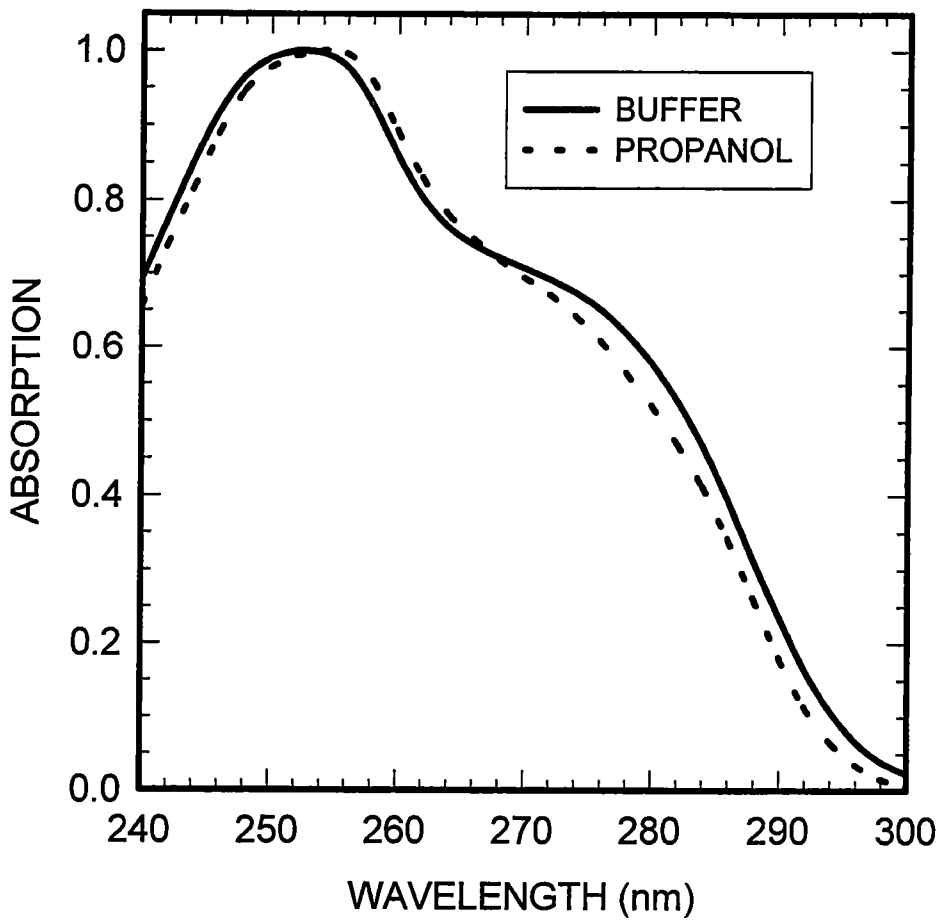


Figure 16
Comparison of the absorption spectrum of deoxyguanosine in 2-propanol to that of deoxyguanosine in buffer, the spectra have been normalized at the peak.

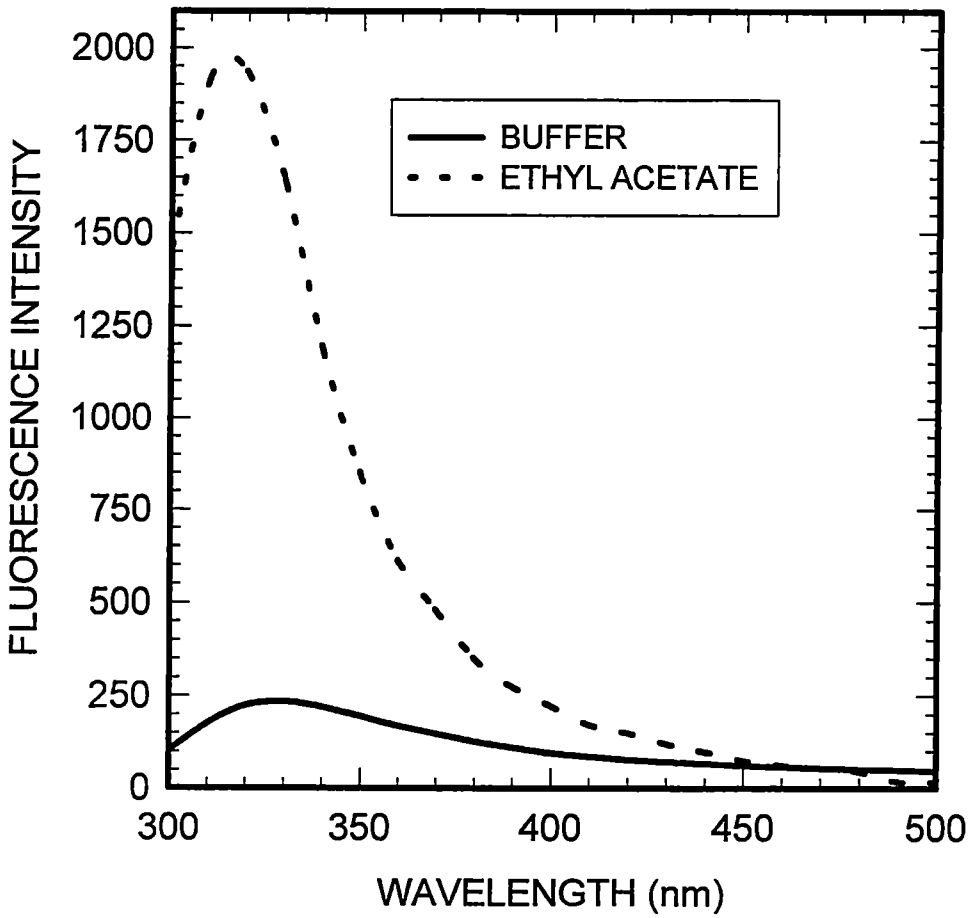


Figure 17
Comparison of the fluorescence spectrum of deoxyguanosine in ethyl acetate to that of deoxyguanosine in buffer.

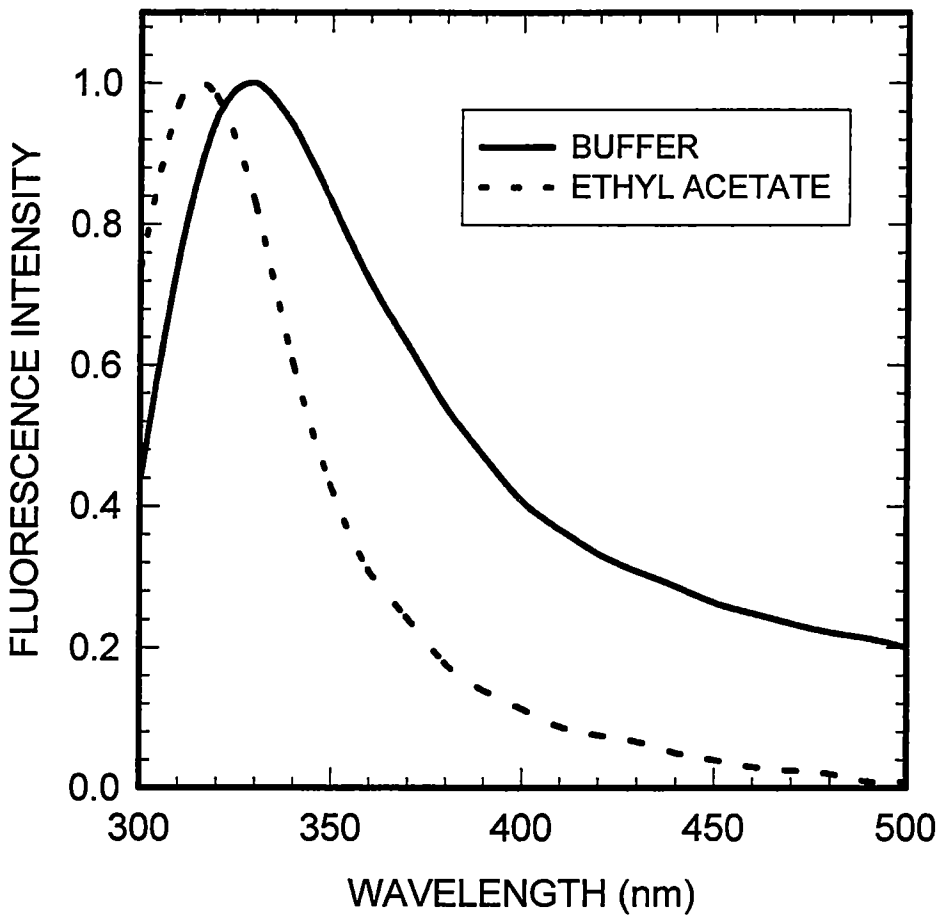


Figure 18
Comparison of the fluorescence spectrum of deoxyguanosine in ethyl acetate to that of deoxyguanosine in buffer; the spectra have been normalized at the peak.

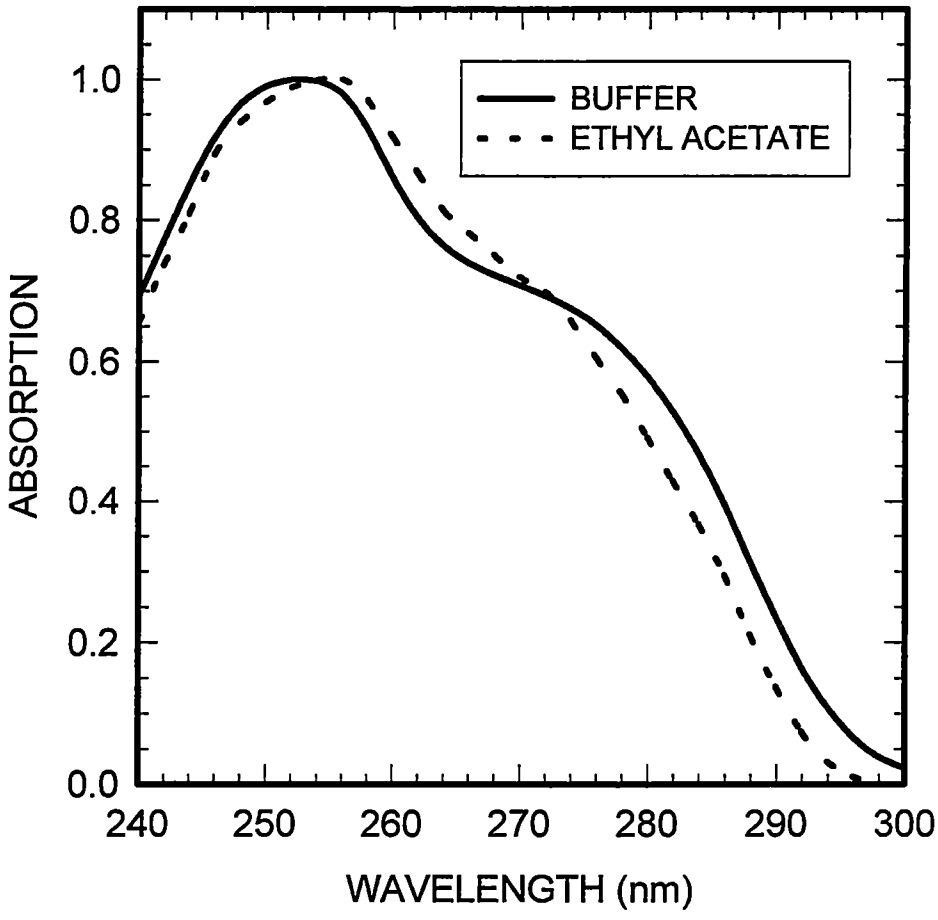


Figure 19
Comparison of the absorption spectrum of deoxyguanosine in ethyl acetate to that of deoxyguanosine in buffer; the spectra have been normalized at the peak

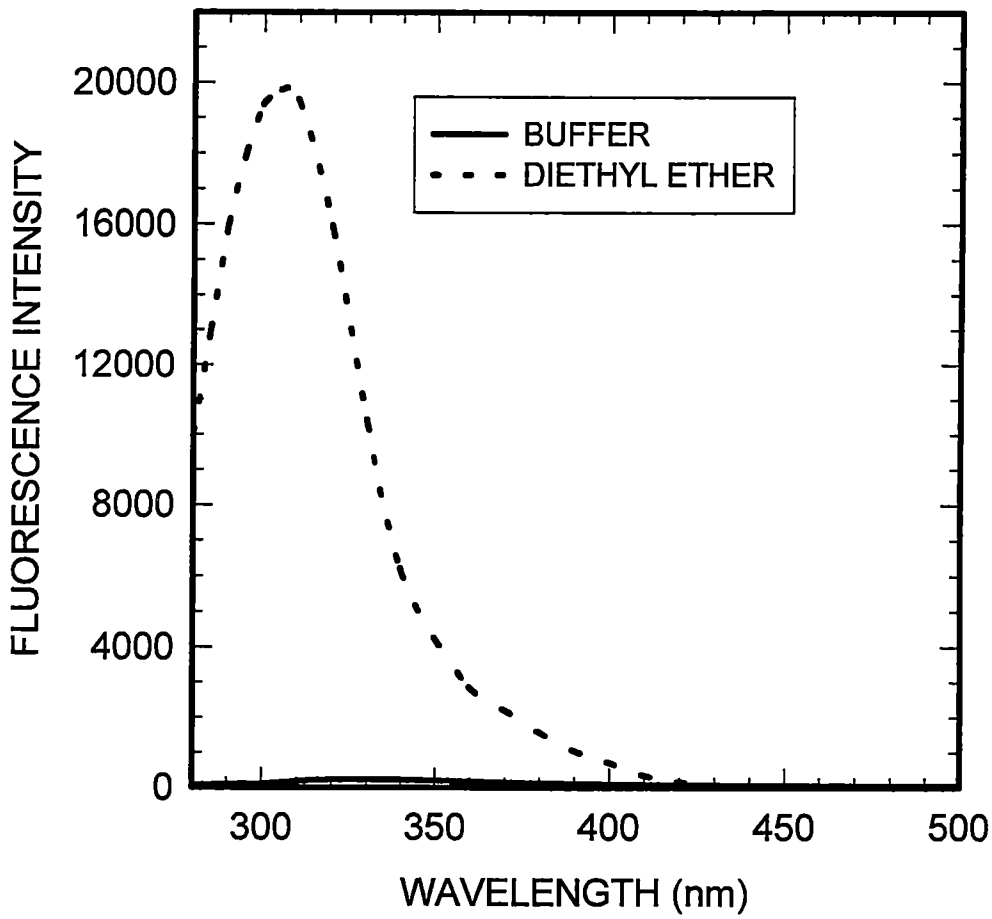


Figure 20
Comparison of the fluorescence spectrum of deoxyguanosine in diethyl ether to that of deoxyguanosine in buffer.

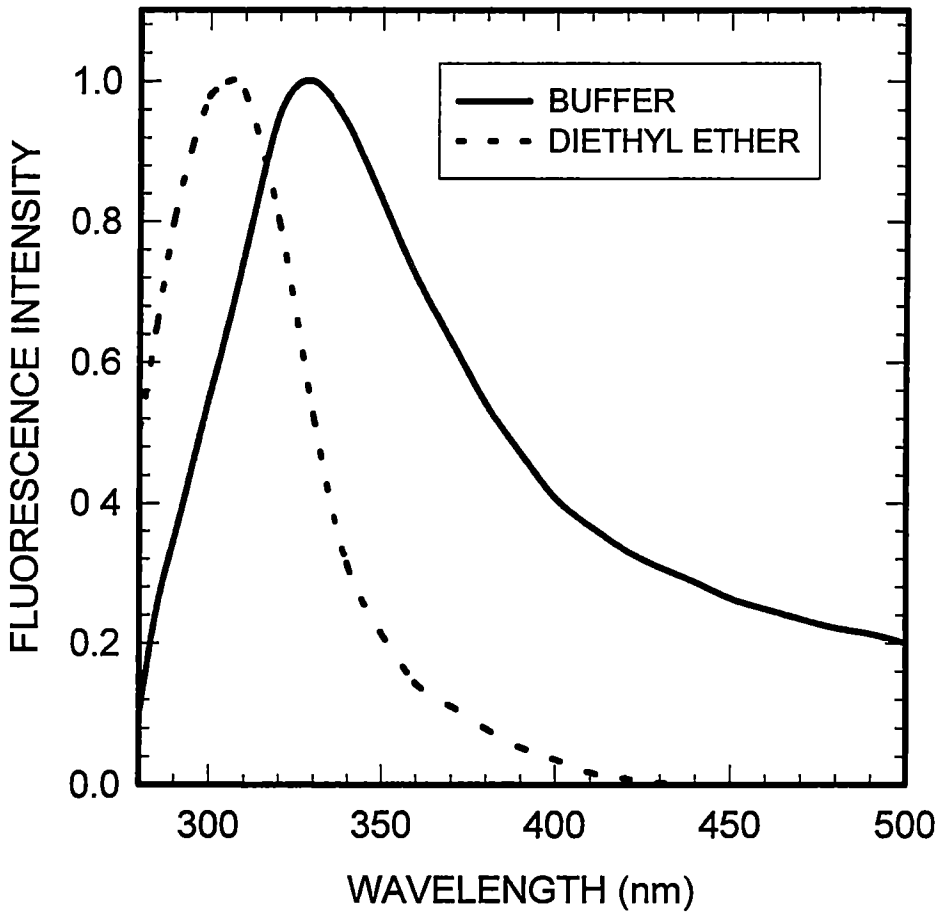


Figure 21
Comparison of the fluorescence spectrum of deoxyguanosine in diethyl ether to that of deoxyguanosine in buffer; the spectra have been normalized at the peak.

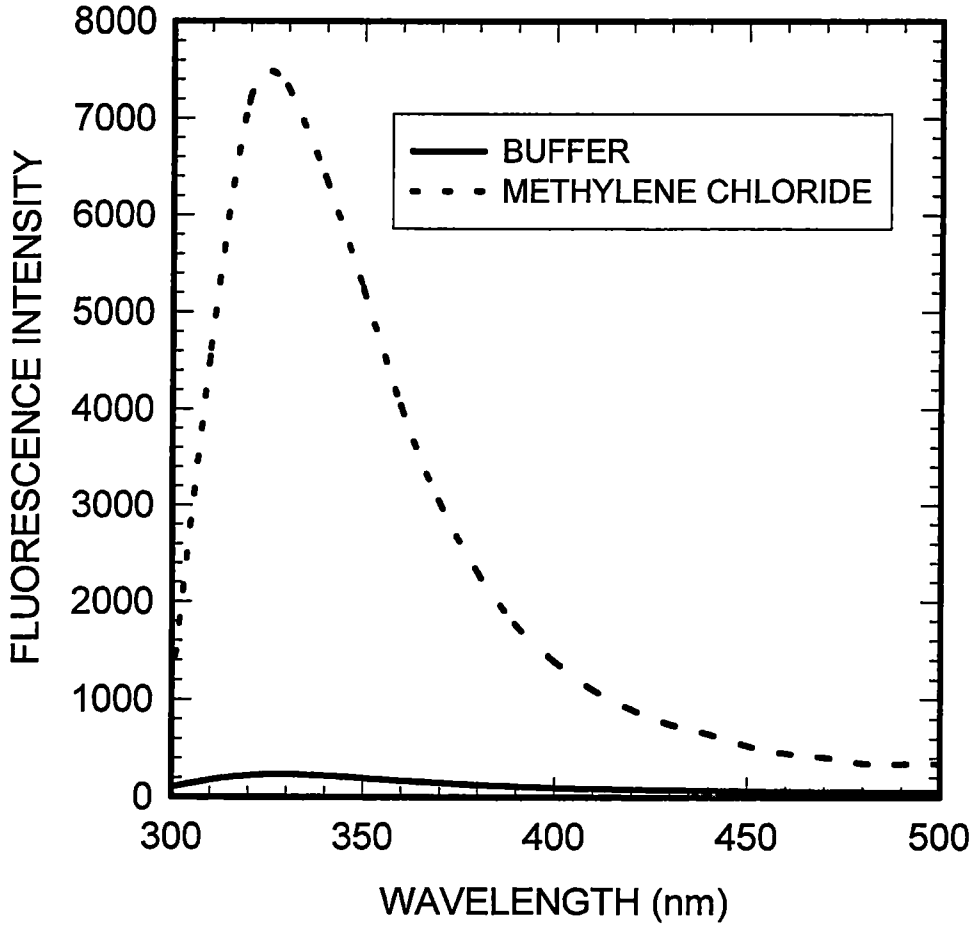


Figure 22
Comparison of the fluorescence spectrum of deoxyguanosine in methylene chloride to that of deoxyguanosine in buffer.

solvents (acetonitrile, ethyl acetate, and diethyl ether), except acetonitrile, and lower than those in the alcohols. The fluorescence spectrum is very narrow having an FWTTM value of 3306 ± 198 cm^{-1} The peak wavelength, 330 nm, is the same as that in buffer (Fig. 23). In this solvent dG also has insufficient solubility and so an absorption spectrum could not be obtained. Relative quantum yields, FWTTM, γ values, and peak locations of the fluorescence and absorption spectra are shown in Table 1 while the polarizabilities, dielectric constants, and E_N^T values for the various solvents are shown in Table 2. We should note in this regard that the solvent parameters varied in this study represent individual contributions to the change in the fluorescence spectra, this is evidenced by the absence of a correlation between the parameters (Figs. 24, 25, and 26).

HYDROGEN BONDING

Other work that has been done in the present study with dG was aimed at simulating the hydrogen bonding that occurs in DNA by using very low and very high pH values. The pK_a for the N7 hydrogen is 2.1 and the pK_a for the N1 hydrogen is 9.2 (Bloomfield *et al* , 1974). We dissolved dG in a 0.0032 M NaOH solution of pH equal to 11 to remove the N1 hydrogen, simulating an extreme case of hydrogen bonding. For the other extreme case, a 0.316 M HCl solution was prepared of pH equal to 0.5. This will serve to protonate the N7. Under basic conditions, the quantum yield is equal to 9, the peak wavelength is 325 nm (Table 1), and the γ ratio is 0.07 (Fig. 27). The spectrum is narrow having an FWTTM value of 3429 ± 206 cm^{-1} (Fig. 28). The absorption spectrum displays a much larger long-wavelength peak, and this may stem from a pH effect on the excited state of dG (Fig. 29). For pH approximately equal to 0.5, the quantum yield is equal to 88, the peak wavelength is 360 nm (Table 1), and the fluorescence spectrum has

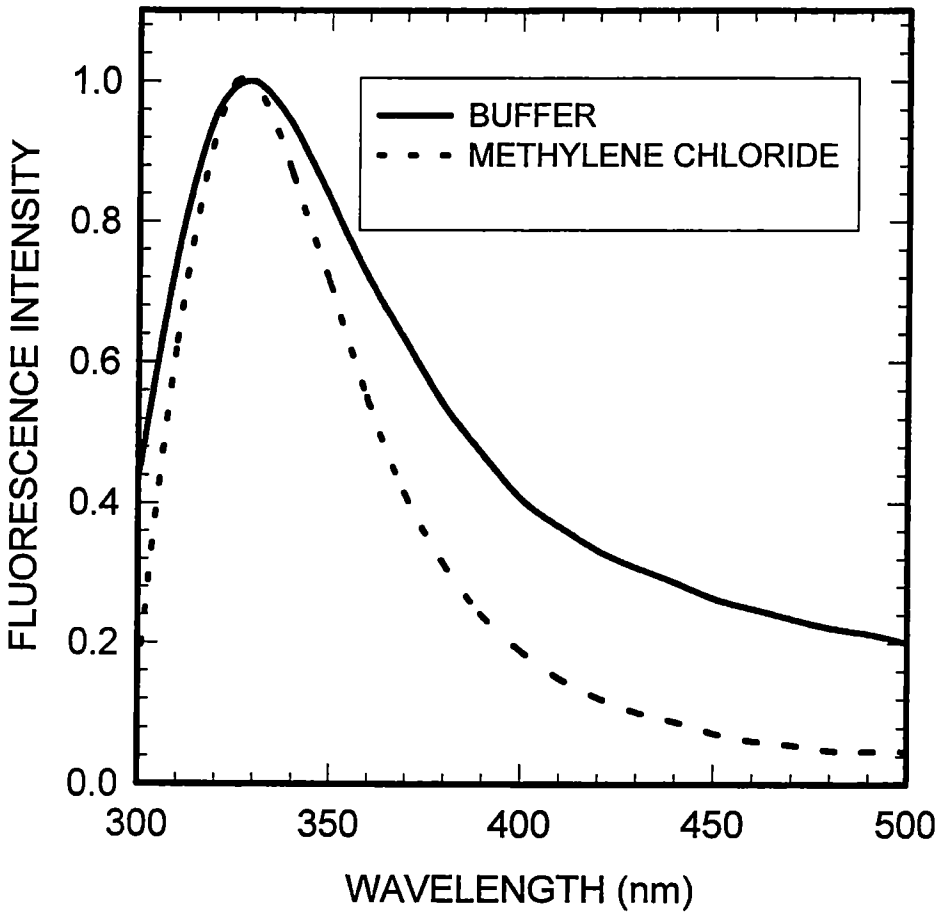


Figure 23
Comparison of the fluorescence spectrum of deoxyguanosine in methylene chloride to that of deoxyguanosine in buffer; the spectra have been normalized at the peak

Table 2

Values of the polarizability, dielectric constant, and solvent polarity empirical parameter E_N^T for the organic solvents used in the present study.

SOLVENTS:	α ($Å^3$)	ε	E_N^T
buffer	1 45	80	1 000
acetonitrile	4.4	38	0.460
methanol	3.3	33	0.762
n-butanol	8.9	18	0 602
2-propanol	7.3	18	0 546
methylene chloride	7.2	9	0.350
ethyl acetate	9.7	6	0.228
diethyl ether	9.5	4	0 117

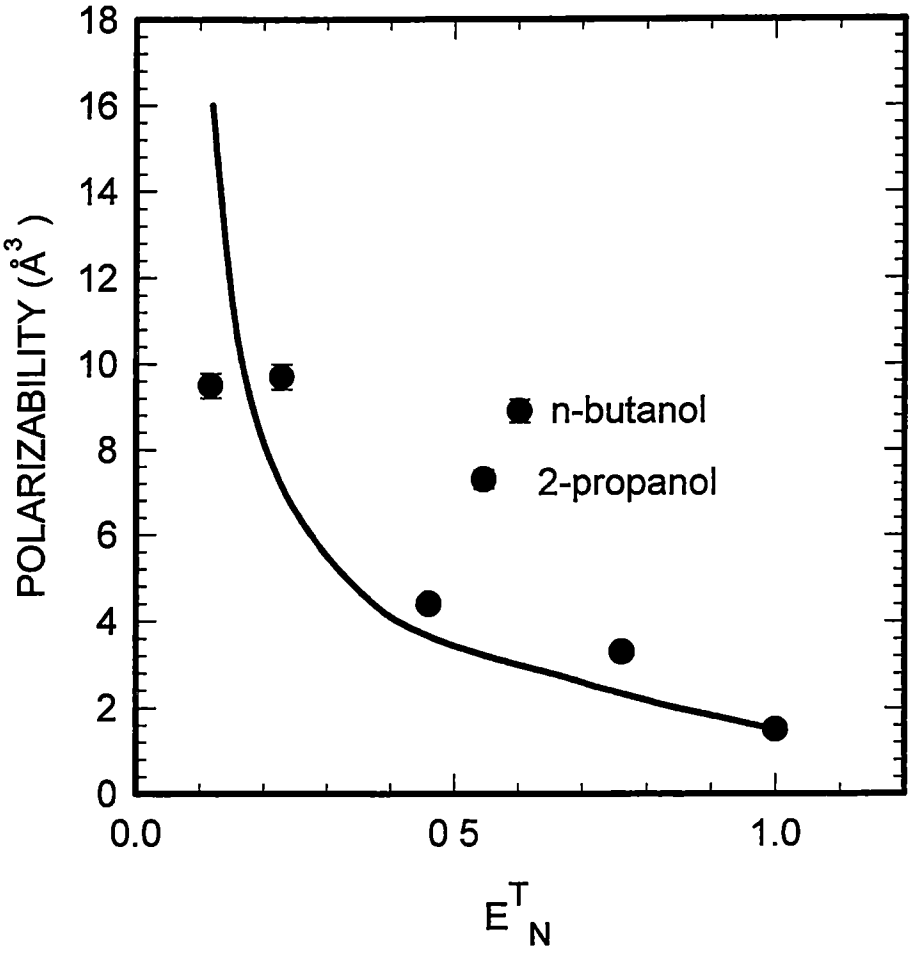


Figure 24
A plot of the polarizability *vs* the solvent polarity according to the E_N^T values for the solvents used in this study

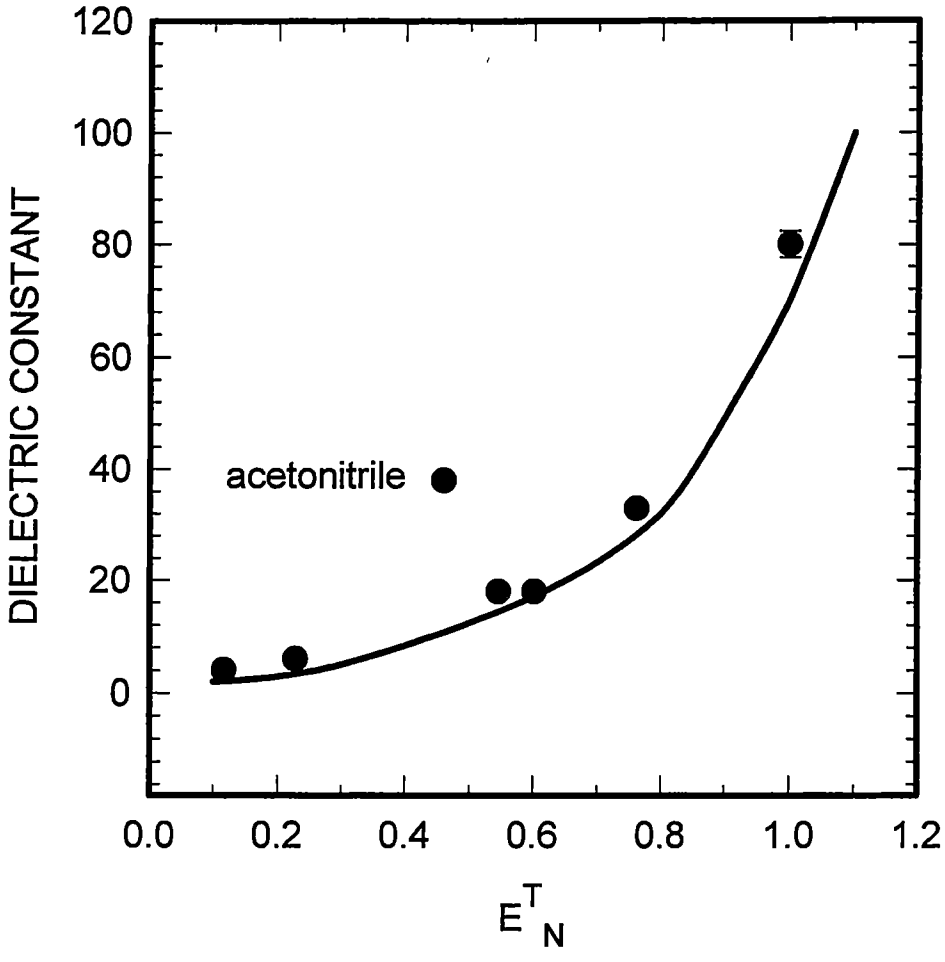


Figure 25
A plot of the dielectric constant *vs* the solvent polarity according to the E_N^T values for the solvents used in this study.

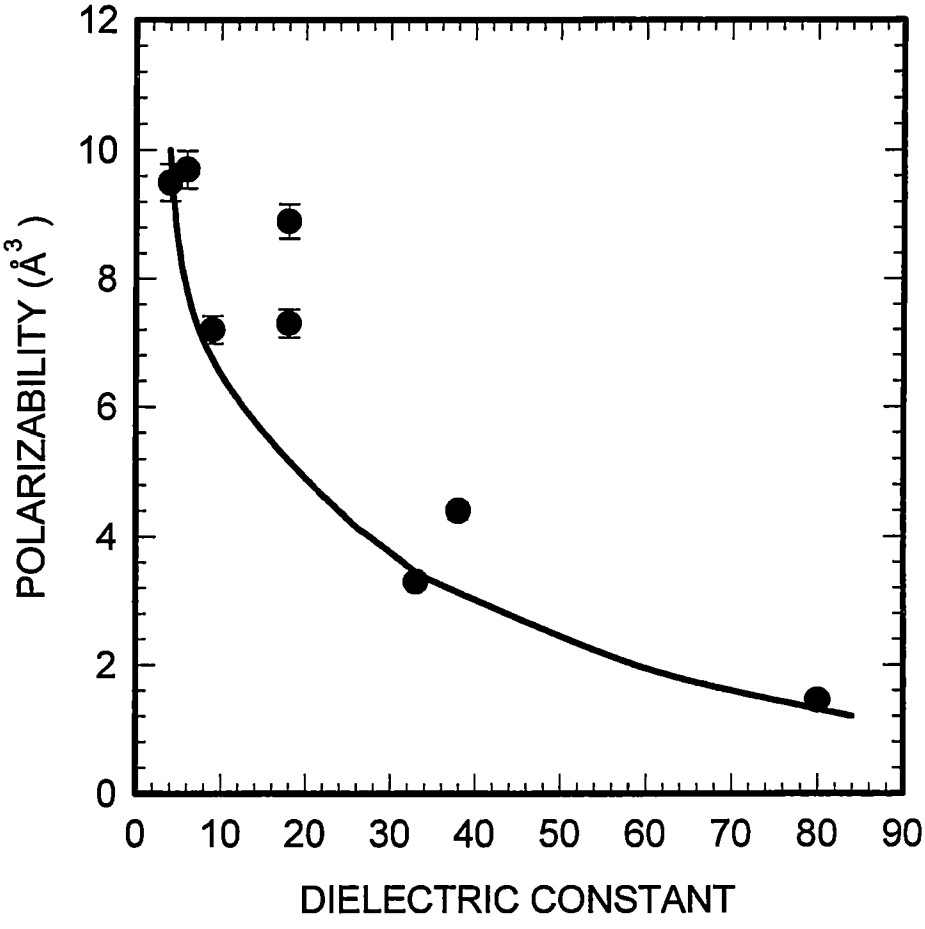


Figure 26
A plot of the polarizability *vs* the dielectric constant for the solvents used in this study.

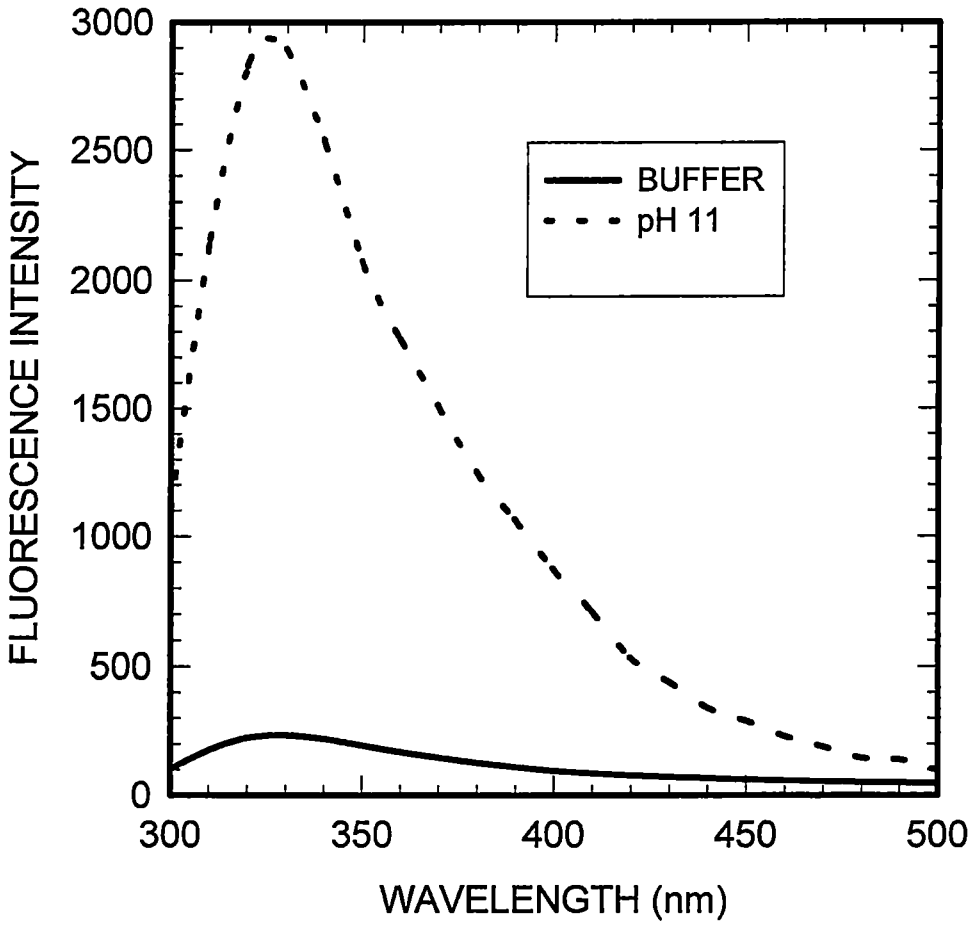


Figure 27
Comparison of the fluorescence spectrum of deoxyguanosine in pH 11 to that of deoxyguanosine in buffer.

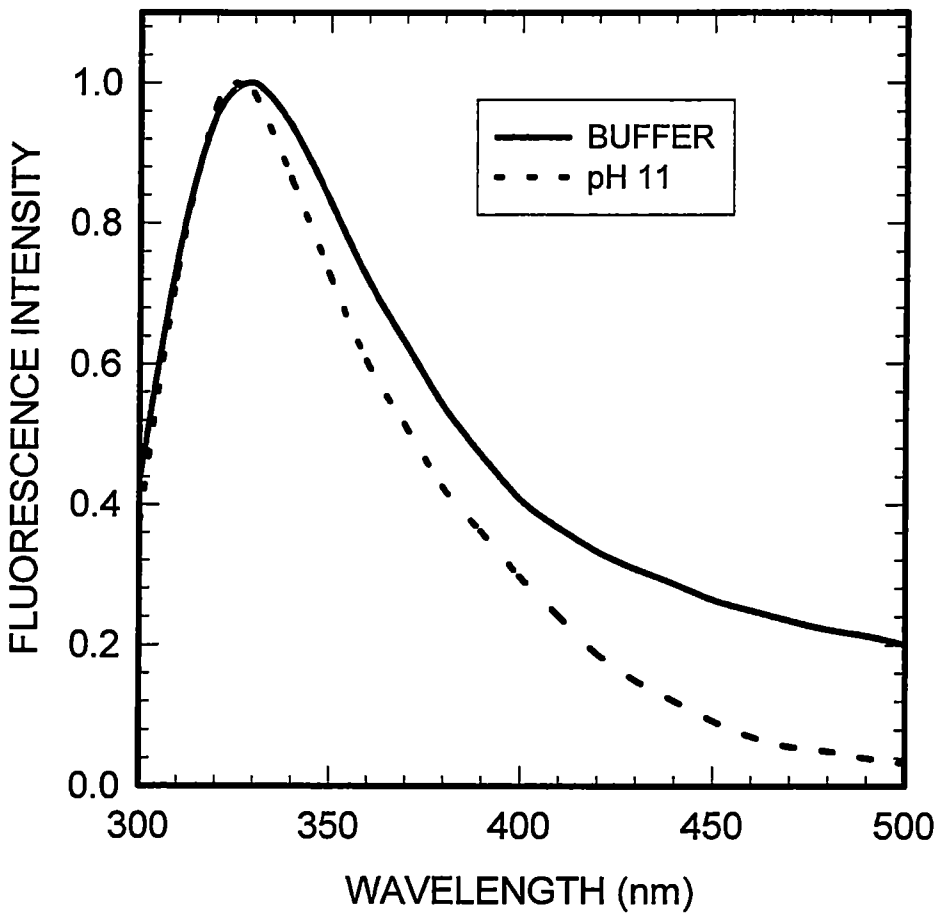


Figure 28
Comparison of the fluorescence spectrum of deoxyguanosine in pH 11 to that of deoxyguanosine in buffer; the spectra have been normalized at the peak.

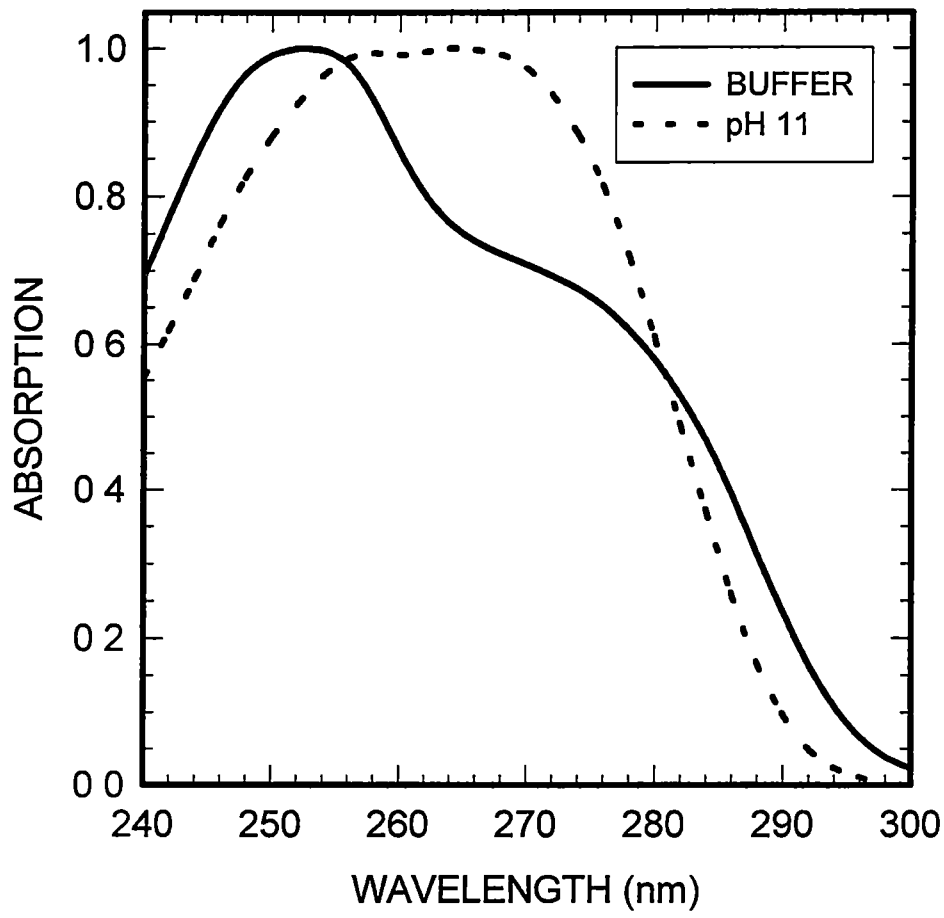


Figure 29
Comparison of the absorption spectrum of deoxyguanosine in pH 11 to that of deoxyguanosine in buffer, the spectra have been normalized at the peak.

a γ ratio of 0.16 (Fig. 30). This spectrum is very wide having an FWTTM value of 4981 ± 299 cm^{-1} (Fig. 31). The absorption spectrum is quite similar to that in buffer in that the peak location is the same but it is somewhat wider having an FWTTM value of 5408 ± 324 cm^{-1} (Fig 32). Previous work done in our laboratory has shown a large increase in the quantum yield with a dramatic shift to a longer wavelength upon methylation of G at position N7 (Ge *et al.*, 1990). Thus, the large fluorescence enhancement we observe at pH 0.5, where a proton is actually added to dG at N7, precludes any conclusion to be drawn regarding the importance of hydrogen bonding at this site, where a proton would be shared.

The N2 and N3 sites are capable of protonation, but cannot be studied due to lack of product availability.

VISCOSITY

All the fluorescence quantum yields of the 60% and 70% sucrose solutions were measured relative to that in buffer. The relative quantum yield of the 60% aqueous solution at 20 °C has been found to be equal to 1.7 (Fig. 33), while that of the 60% solution at 5 °C has been found to be equal to 2.5 (Fig. 34). The viscosities of these solutions are 14 cP and 29 cP, respectively, while the viscosity of buffer at 20°C is about 1 cP. Furthermore, the quantum yield of the 77% solution, for which the viscosity is 58 cP, is 3.7 (Fig. 35), while the quantum yield of the 77% solution at 5 °C, viscosity of 149 cP, is 7.4 (Fig. 36).

The shapes of the fluorescence spectra for both sucrose solutions at room temperature exhibit differences from that in buffer For the 60% solution, the fluorescence spectral peak is located at 335 nm, and the FWTTM of the spectrum is

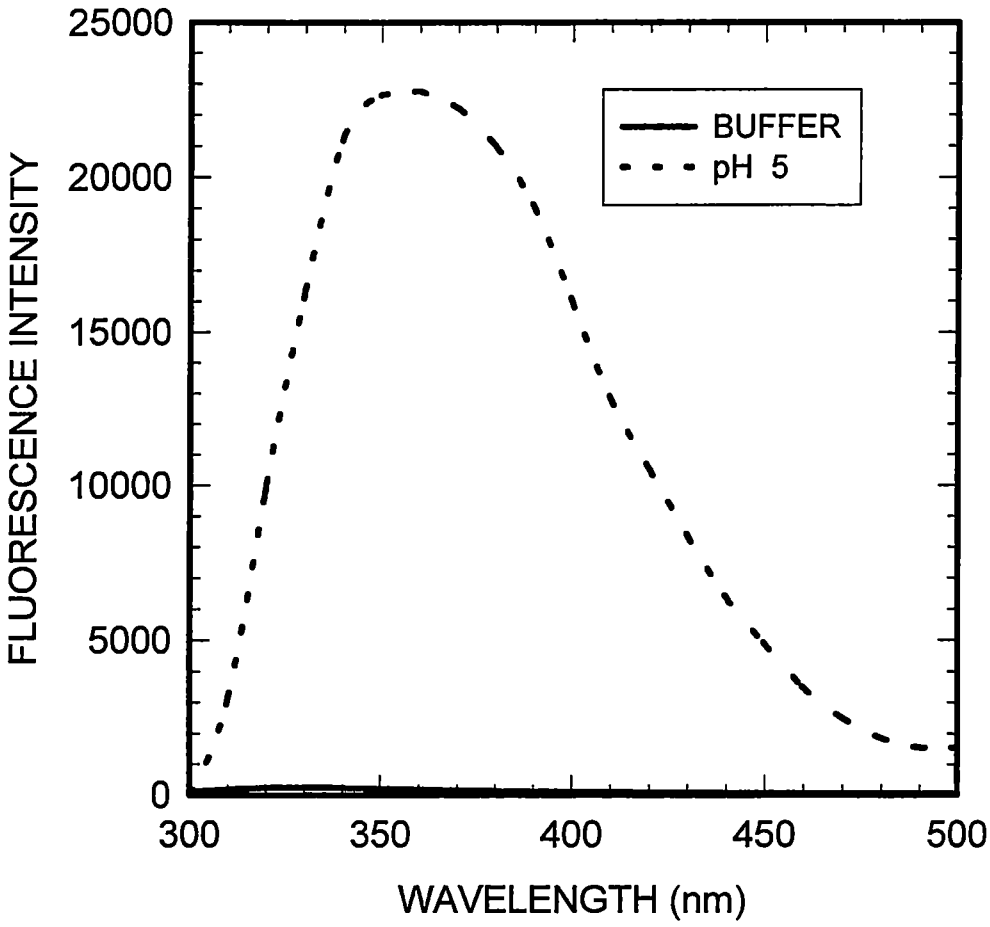


Figure 30
Comparison of the fluorescence spectrum of deoxyguanosine in pH 0 5 to that of deoxyguanosine in buffer.

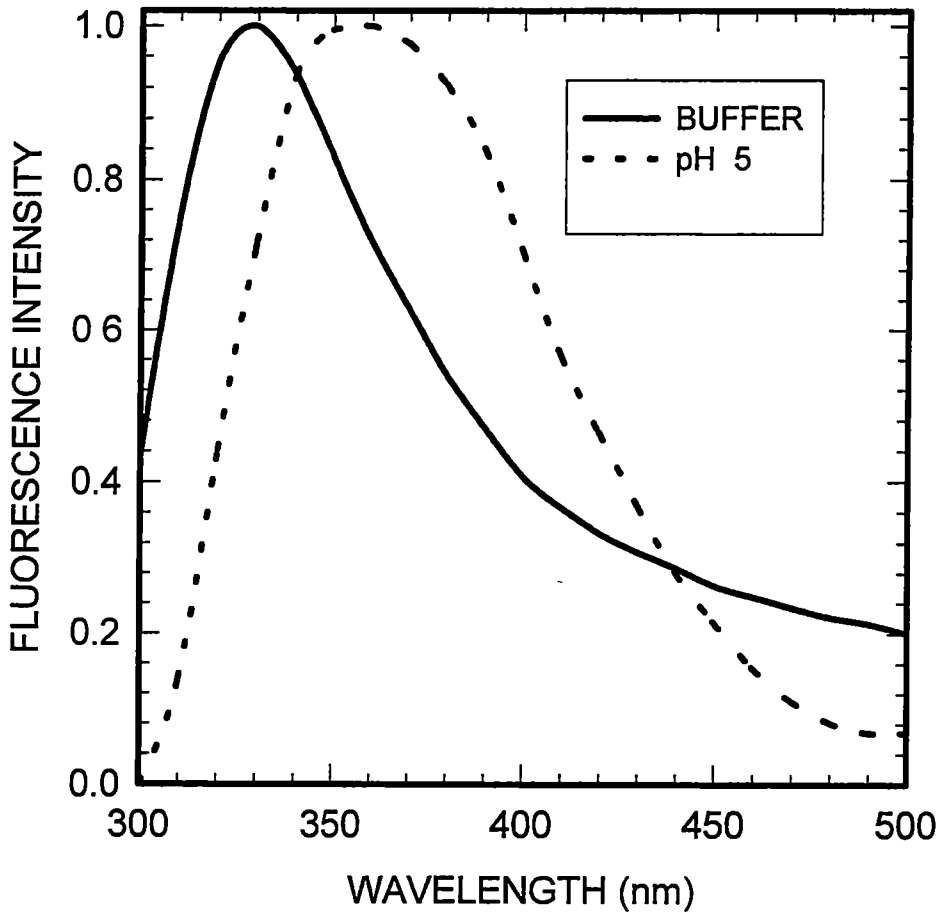


Figure 31
Comparison of the fluorescence spectrum of deoxyguanosine in pH 0.5 to that of deoxyguanosine in buffer; the spectra have been normalized at the peak.

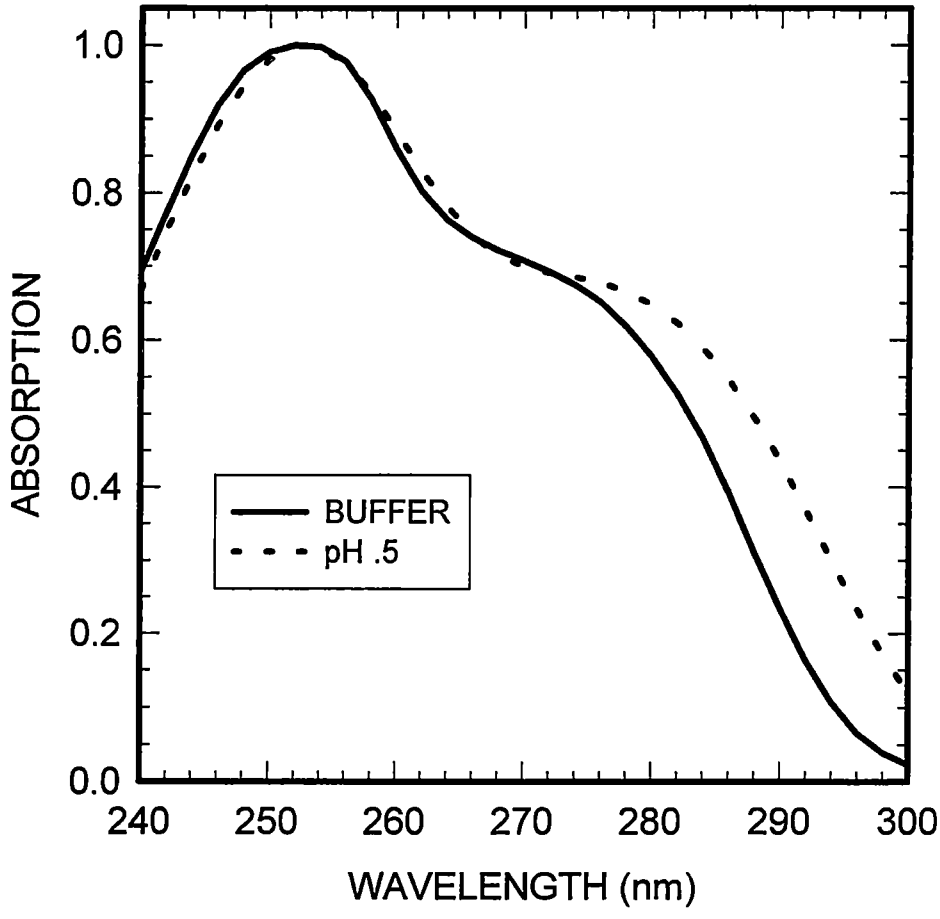


Figure 32
Comparison of the absorption spectrum of deoxyguanosine in pH 0.5 to that of deoxyguanosine in buffer, the spectra have been normalized at the peak.

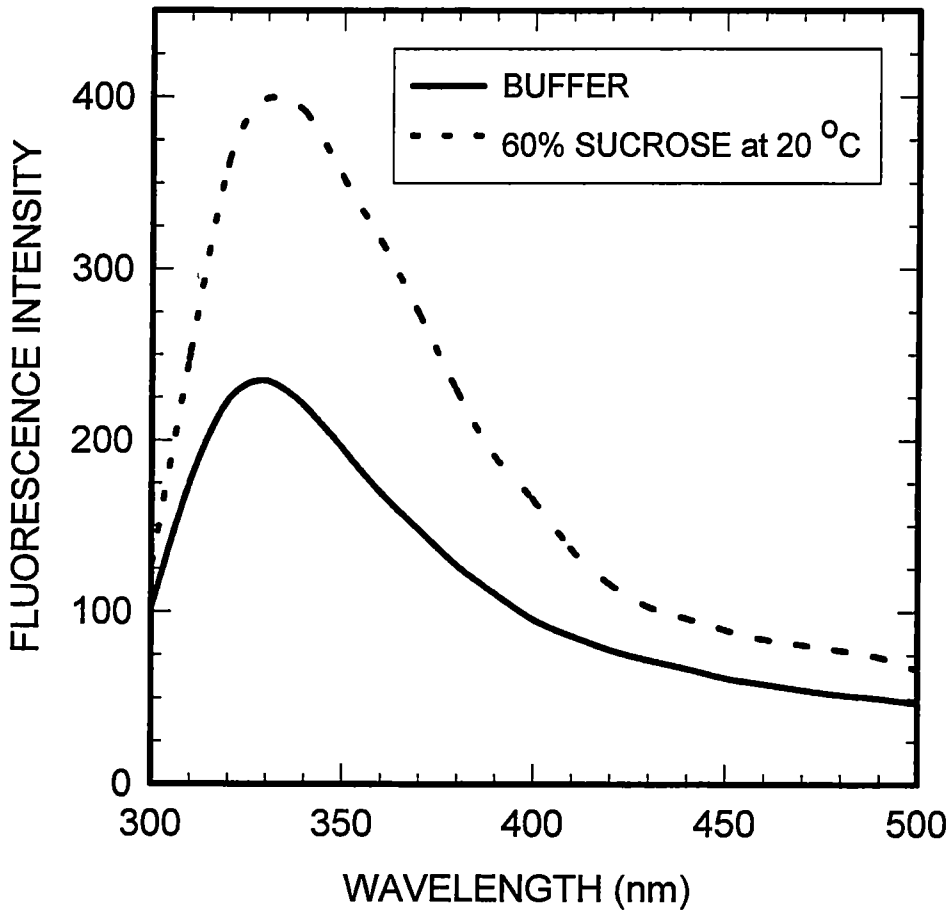


Figure 33
Comparison of the fluorescence spectrum of deoxyguanosine in 60% sucrose solution, with a viscosity of 14 cP, to that of deoxyguanosine in buffer at room temperature.

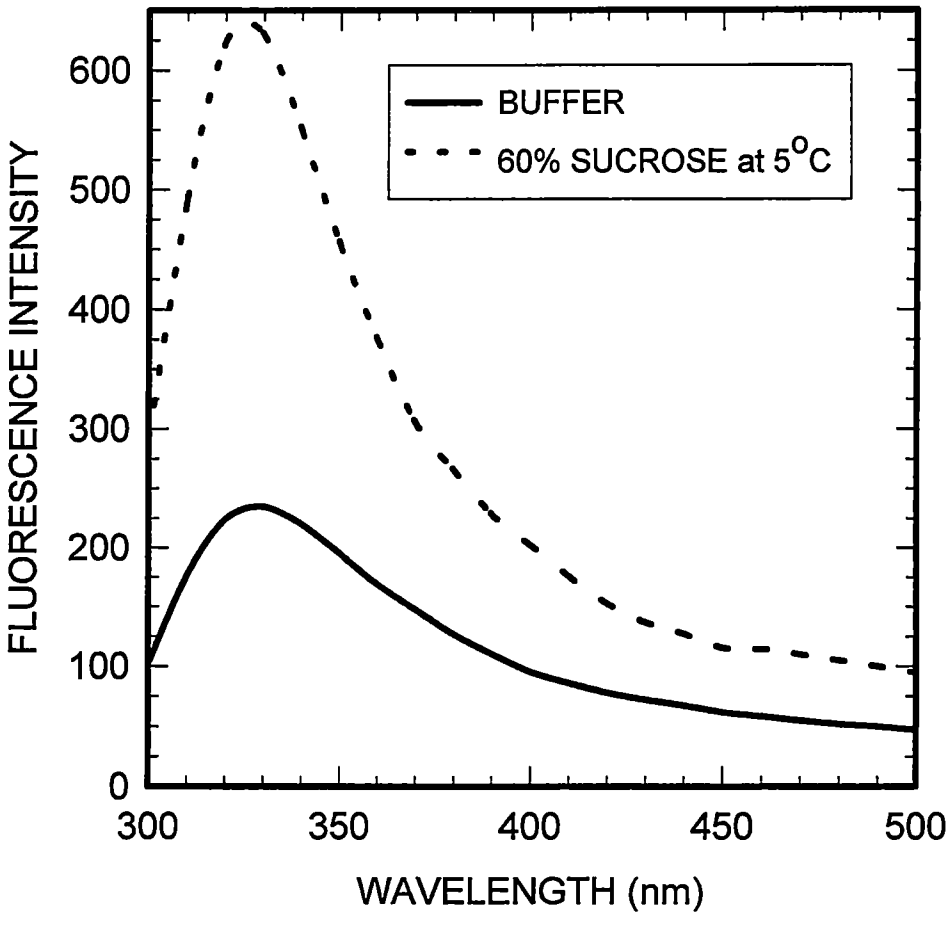


Figure 34
Comparison of the fluorescence spectrum of deoxyguanosine in 60% sucrose solution at 5 °C, with a viscosity of 29 cP, to that of deoxyguanosine in buffer at room temperature.

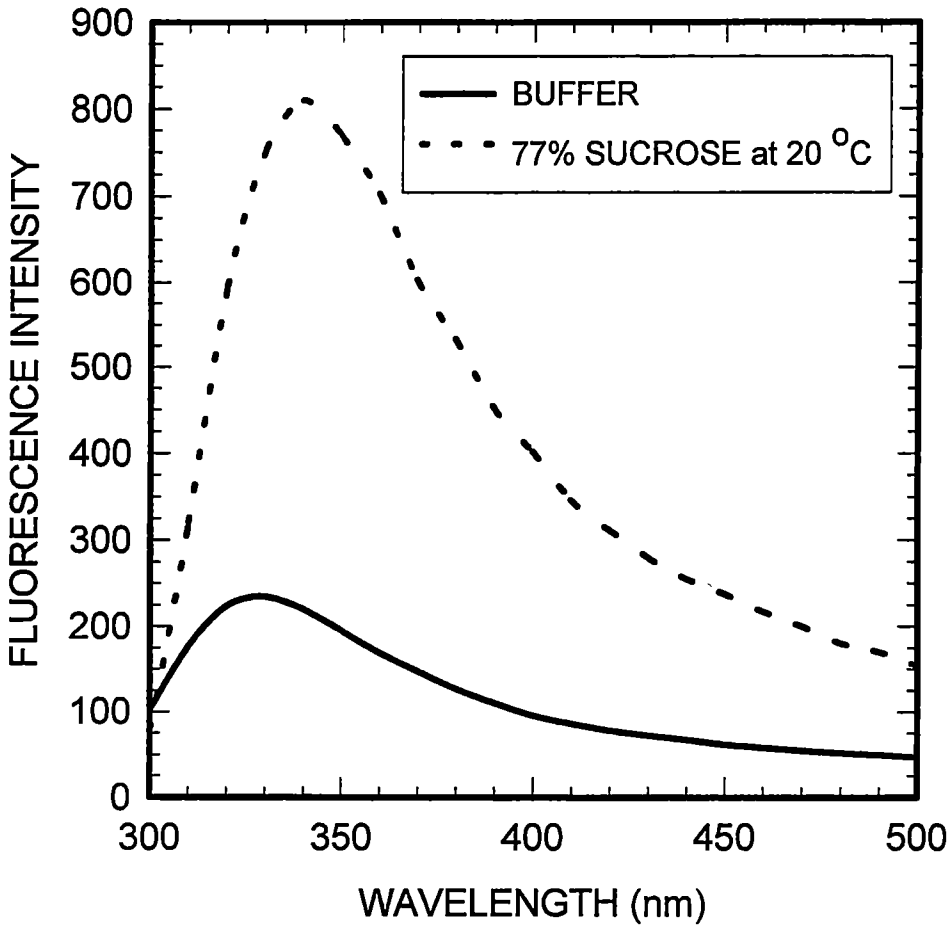


Figure 35
Comparison of the fluorescence spectrum of deoxyguanosine in 77% sucrose solution, with a viscosity of 58 cP, to that of deoxyguanosine in buffer at room temperature.

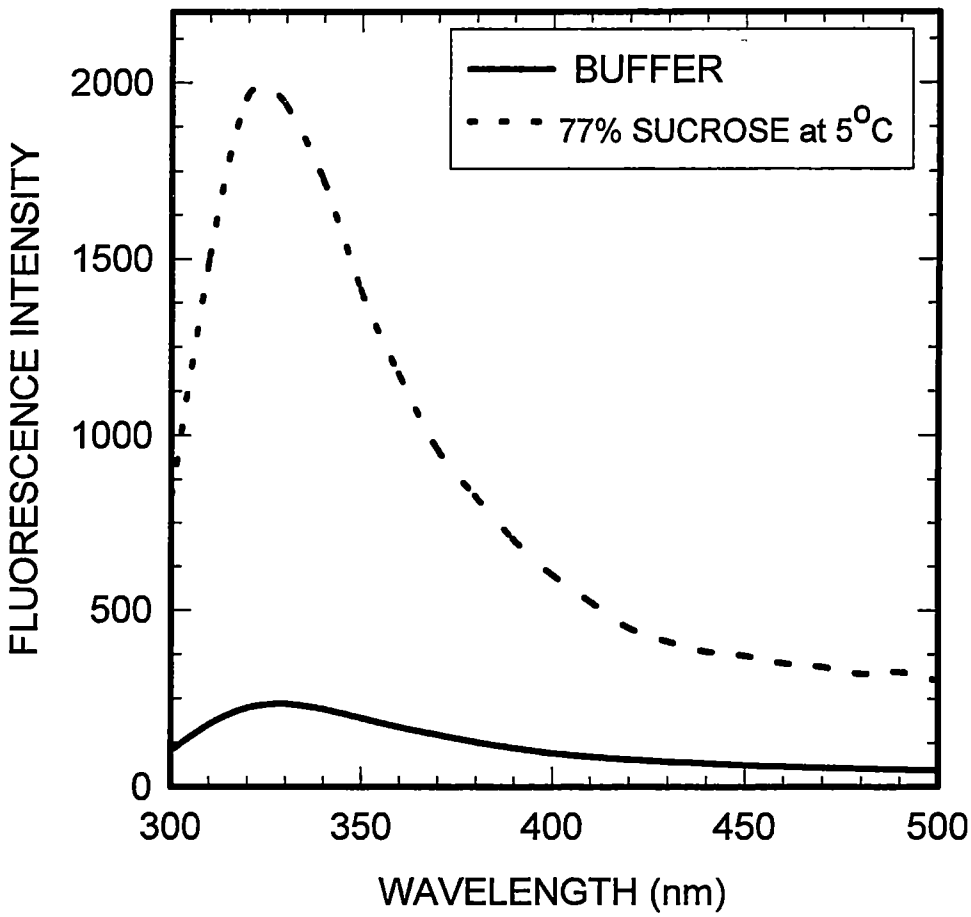


Figure 36
Comparison of the fluorescence spectrum of deoxyguanosine in 77% sucrose solution at 5 °C, with a viscosity of 149 cP, to that of deoxyguanosine in buffer at room temperature.

5525 ± 273 cm^{-1} (Table 3); this compares to an FWTTM of 4432 cm^{-1} for buffer (Table 1). As Fig. 37 shows, the absorption spectrum for this solution is very similar to that in buffer. The tail-to-peak ratio, γ, is 0.20 (Fig. 33, Table 3), while for the buffer solution it is 0.22 (Table 1). The fluorescence quantum yield increases by a factor of 1 7 relative to that in buffer (Table 3). The fluorescence spectral peak location of the 60% sucrose solution at 5 °C is 325 nm, and the spectrum has a γ value of 0.18 (Fig. 34). This solution has an FWTTM value of 4554 ± 122 cm^{-1} (Fig. 34 and Table 3). The spectrum has become narrower by about 970 cm^{-1} compared to that for the room temperature solution and has shifted by 10 nm to shorter wavelengths. The fluorescence quantum yield increases by a factor of 2.5 relative to that in buffer (Table 3). The 77% solution at room temperature has a fluorescence spectral peak located at 340 nm and an FWTTM value of 5190 ± 60 cm^{-1} (Fig. 35, Table 3). The corresponding γ value is 0.27 (Table 3) and the quantum yield is greater by a factor of 3.7 relative to that in buffer (Table 3). The absorption spectrum shows very little change compared to that in buffer (Fig 38) When the temperature of the 77% sucrose solution is lowered to 5 °C, the fluorescence peak location shifts from 340 nm to 325 nm. (This wavelength is identical to that of the 60% sucrose solution at 5 °C.) The spectrum has an FWTTM value of 5018 ± 61 cm^{-1} (Fig. 36) and a quantum yield which is greater by a factor of 7.4 relative to that in buffer (Table 3). The γ value is 0.18 (Table 3), which is the same as that of the 60% solution at 5° C. The absorption spectrum shows very little change as compared to that in buffer (Fig. 39). It should be noted that the absorption spectrum of the solution in buffer exhibits very little change upon going to 5 °C (Fig 40) The tail of the fluorescence spectrum exhibits only a small change whereas the spectrum becomes narrower by about

Table 3

Comparison of the viscosities, fluorescence quantum yields, and fluorescence spectral peak locations for deoxyguanosine in the sucrose solutions used in the present study.

Sucrose solution	q	η (cP)	γ	$FWTTM_f$ (cm^{-1})	λ_f(nm)
0 %	1	1	0.22	4432	330
0 % at 5°C	1.03	1.5	.22	4700	330
60%	1.7	14	0.20	5525	335
60% at 5°C	2.5	29	0.18	4554	325
77%	3.7	58	0.27	5190	340
77% at 5°C	7.4	149	0.18	5018	325

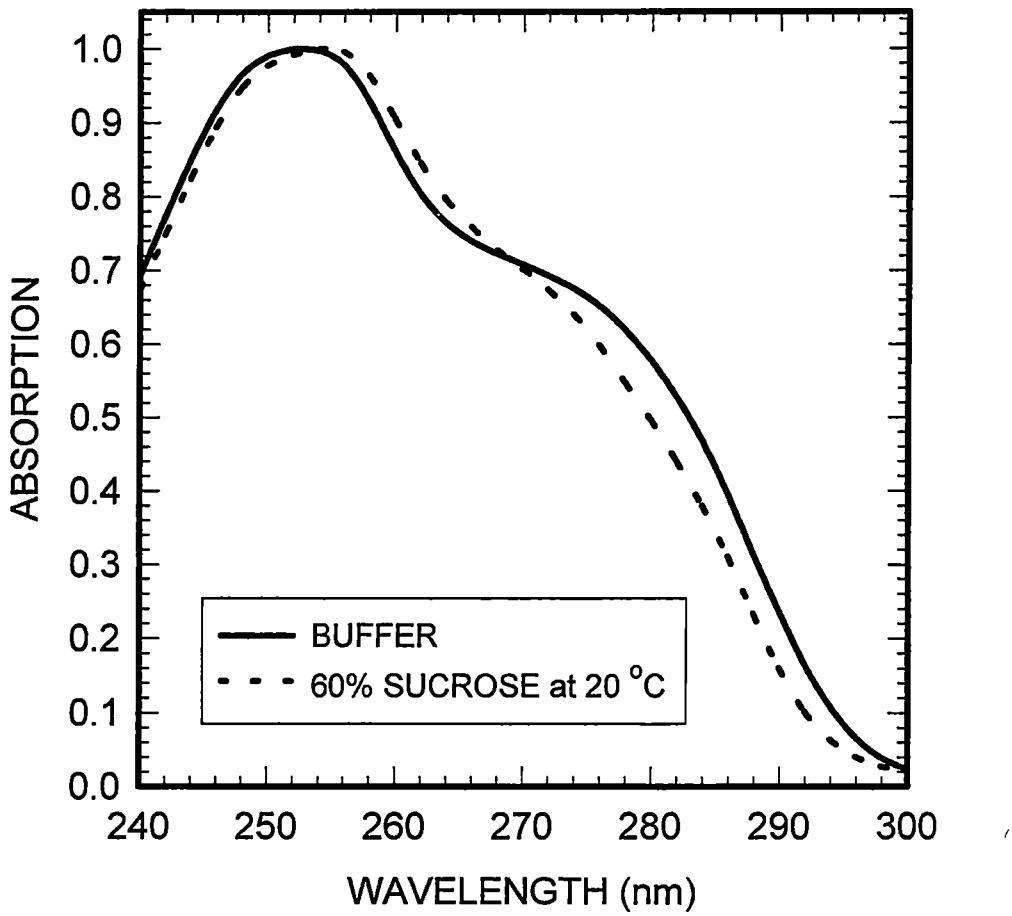


Figure 37
Comparison of the absorption spectrum of deoxyguanosine in 60% sucrose solution to that of deoxyguanosine in buffer at room temperature, the spectra have been normalized at the peak.

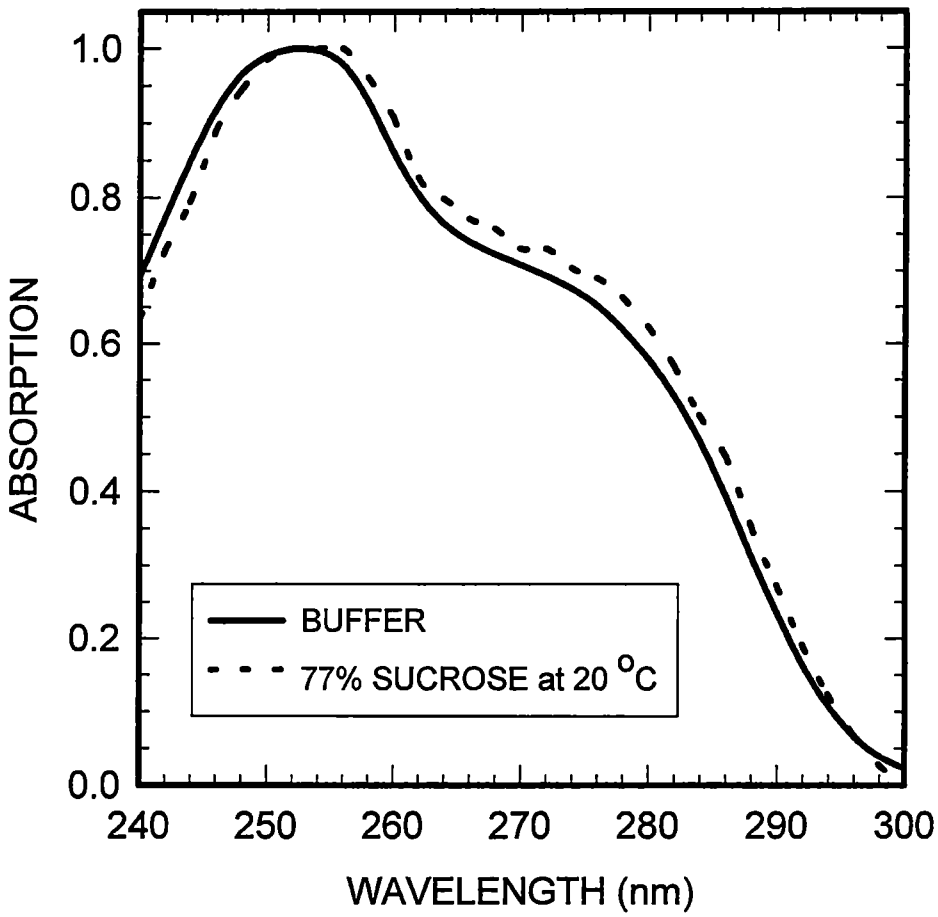


Figure 38
Comparison of the absorption spectrum of deoxyguanosine in 77% sucrose solution to that of deoxyguanosine in buffer at room temperature; the spectra have been normalized at the peak.

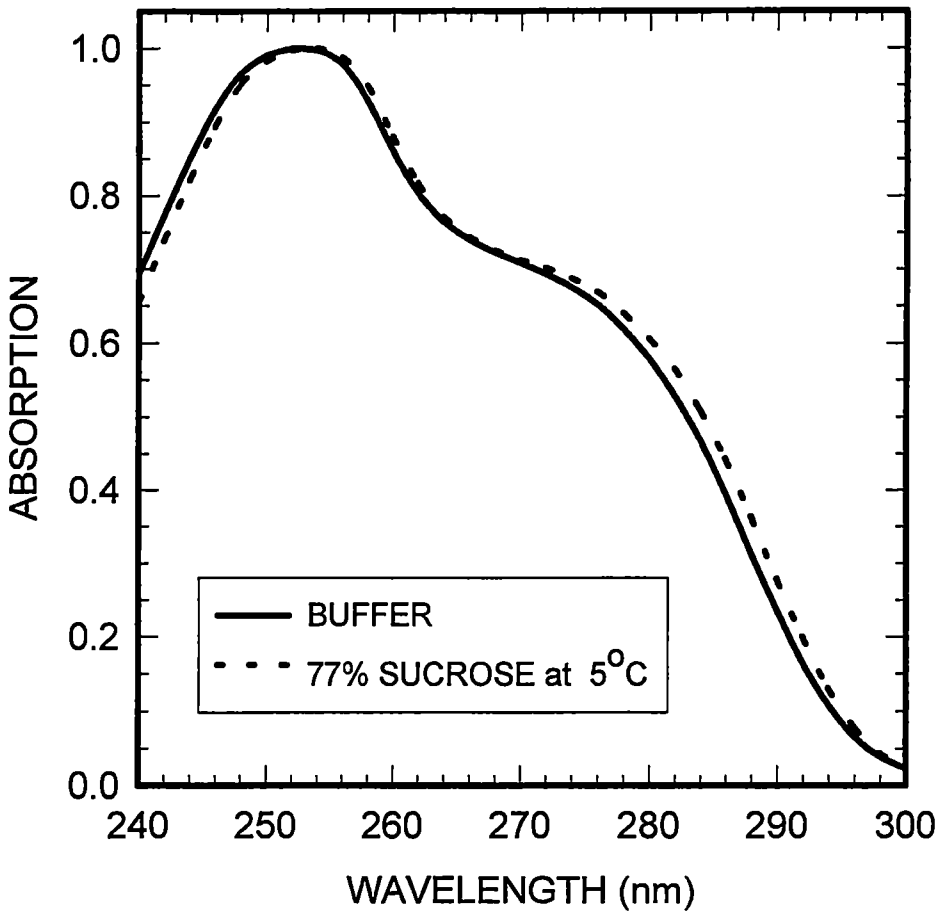


Figure 39
Comparison of the absorption spectrum of deoxyguanosine in 77% sucrose solution at 5 °C to that of deoxyguanosine in buffer at room temperature.

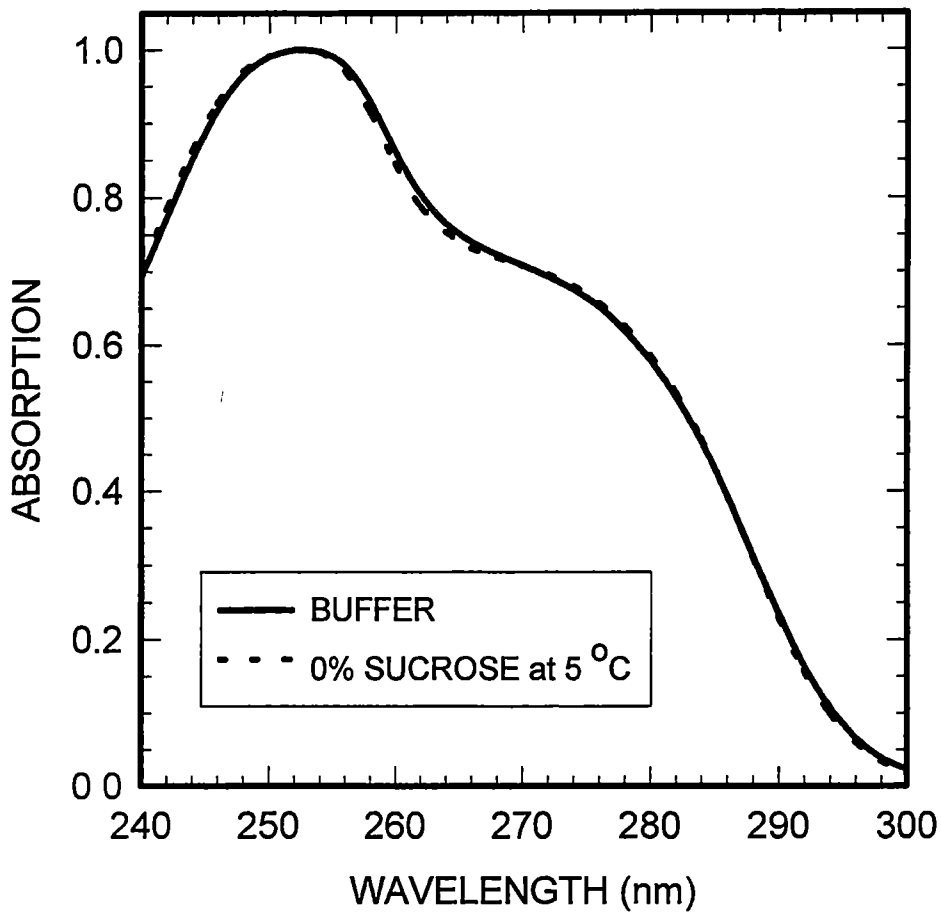


Figure 40
Comparison of the absorption spectrum of deoxyguanosine in buffer at room temperature to that at 5 °C.

270 cm^{-1} (Fig. 41); the peak intensity increases by about 20 %, but the peak wavelength does not change. The fluorescence quantum yield, however, increases only by about 3% (Table 3). Therefore, for the sucrose solutions, upon going to 5 °C the observed fluorescence spectral shifts and the increase in the quantum yield are effects that stem from viscosity, not from temperature. On the other hand, the observed narrowing of the spectra, which is very similar to that observed upon cooling the solution in buffer (Table 3), most probably stems from temperature effects. A comparison of the fluorescence spectra for all the measurements for the different viscosities is shown in Fig 42, and a plot of the fluorescence quantum yield *vs* viscosity is shown in Fig. 43.

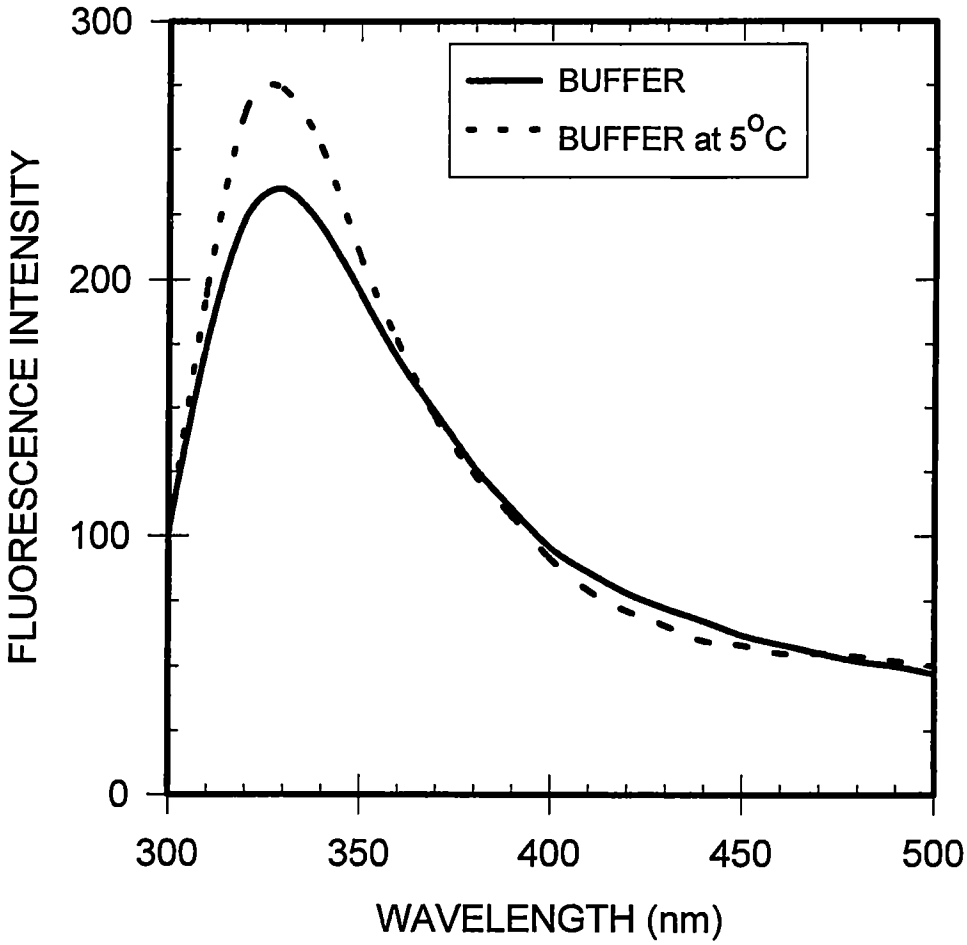


Figure 41
Comparison of the fluorescence spectrum of deoxyguanosine in buffer at room temperature to that of deoxyguanosine in buffer at 5 °C.

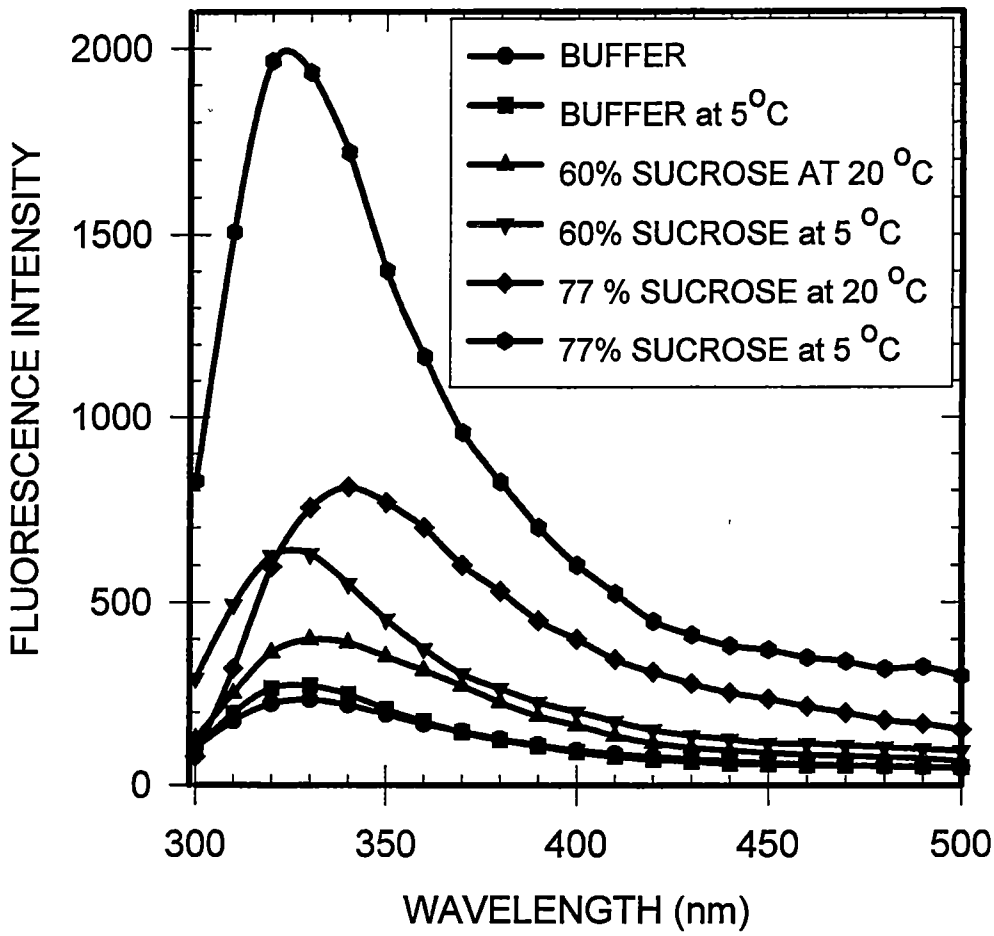


Figure 42
Comparison of the fluorescence spectra of deoxyguanosine in 0% sucrose solution at 5 °C, 60% sucrose solution at room temperature, 60% sucrose solution at 5°C, 77% sucrose solution at room temperature, and 77% sucrose solution at 5 °C, to that of deoxyguanosine in buffer at room temperature.

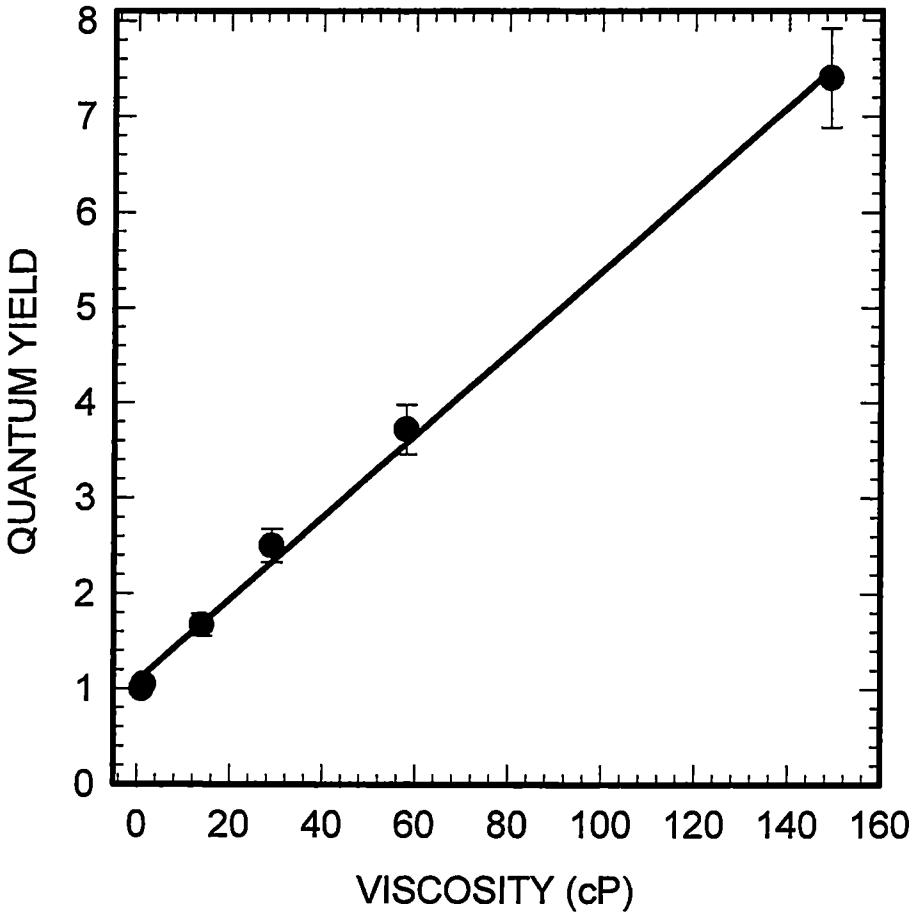


Figure 43
A plot of the fluorescence quantum yield of deoxyguanosine as a function of viscosity of the various sucrose solutions used in the present study

IV. DISCUSSION

SOLVENTS

In an effort to understand the variation of the fluorescence quantum yield with the solvent physical properties, we have considered the dielectric constant, ϵ, which is a measure of the ability of the solvent to screen charges from one another. If a solvent such as water has a high ϵ, then the energy of attraction or repulsion between electric charges in solute molecules is lower than that in vacuum. We have plotted the fluorescence quantum yield, q, *vs.* ϵ in Fig. 44. This plot is seen to be nonlinear; nevertheless, q decreases as ϵ is increased which suggests that the dielectric constant affects the photophysical properties of dG. (The point for methylene chloride is an exception, and a possible explanation is discussed below) In this regard we have considered the Lippert's function which has been used as a measure of polarity in connection with the difference between the wavenumbers of the fluorescence and the absorption maxima. We show in Fig. 45 a plot of the difference in the peak wavenumbers of the absorption and the fluorescence spectra (ν_a - ν_f) *vs* the Lippert's function; the plot is seen to be linear This suggests that polar interactions effect the photophysical properties of dG (see also below) This strong correlation leads us to consider polarity effects on the quantum yield. Although there exists no theoretical equation expressing the fluorescence quantum yield q as a function of the refractive index or the dielectric constant, it is customary, on an empirical basis, to plot q *vs* the Lippert's function. This plot is shown in Fig. 46. As the Lippert's function increases, the quantum yield is seen to decrease. This suggests that polar interactions have an effect on the quantum yield. Despite all of this, the solvent polarity needs to be defined and quantified. This is not a simple task because it cannot be

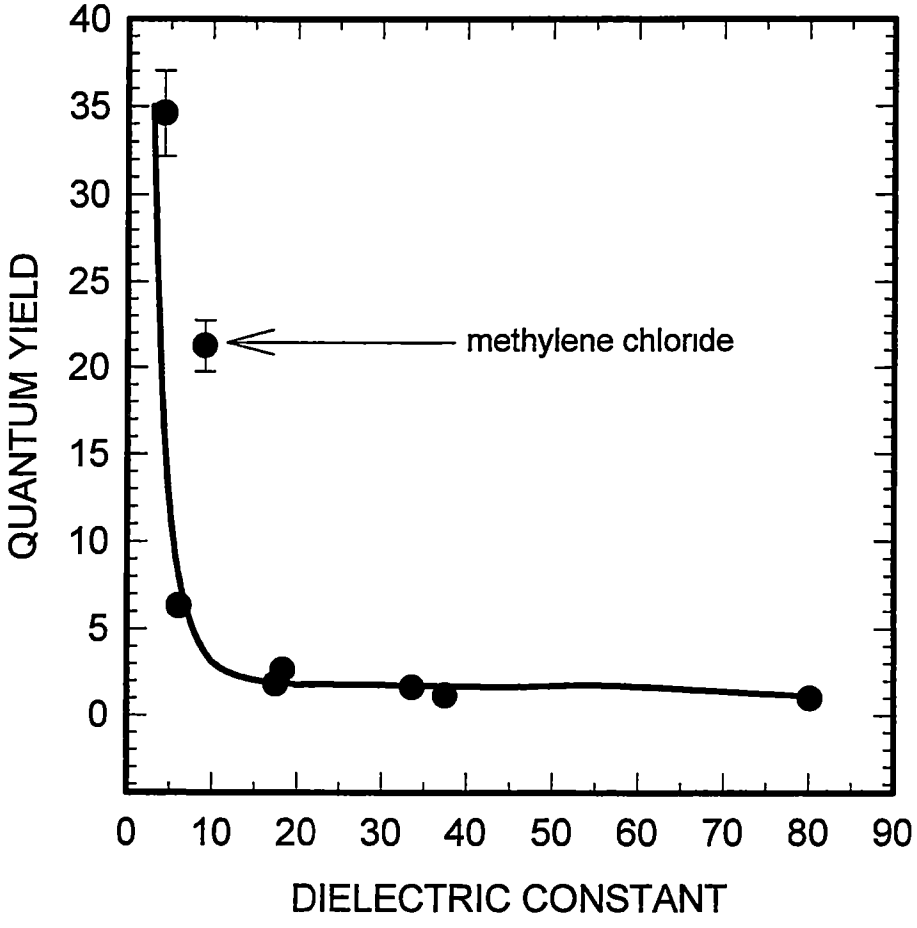


Figure 44
Plot of the fluorescence quantum yield of deoxyguanosine as a function of solvent dielectric constant

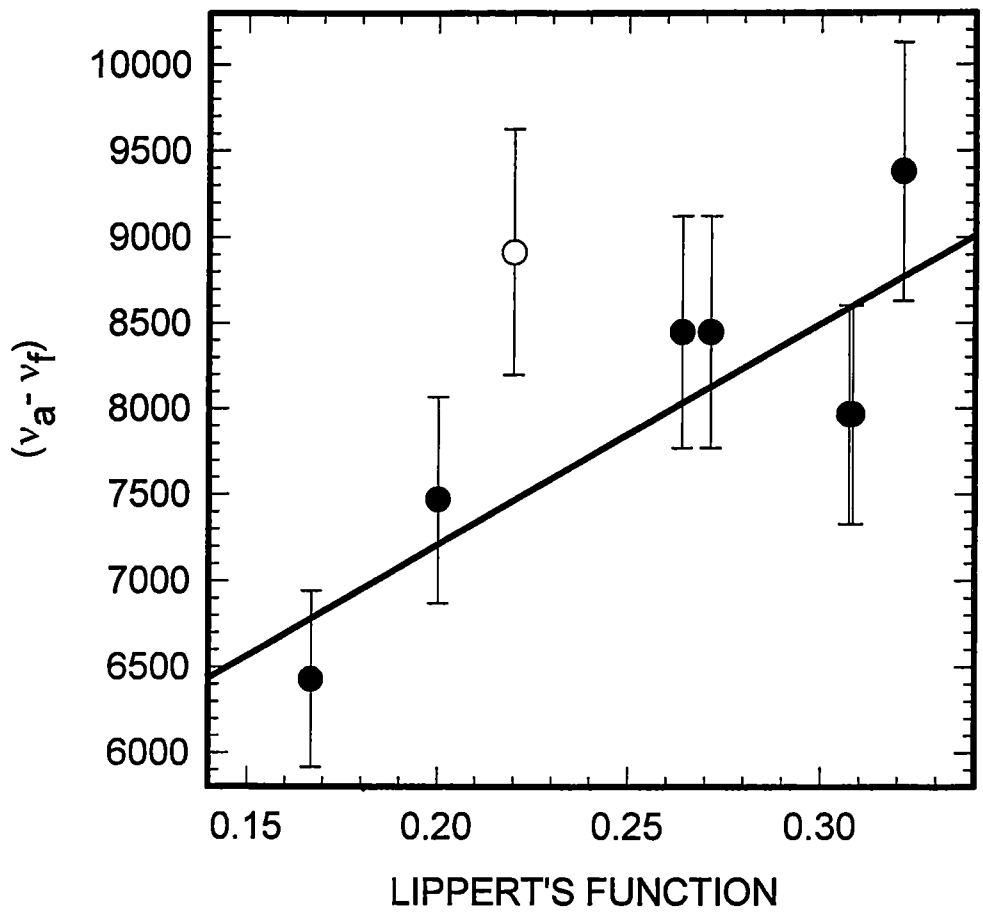


Figure 45
Plot of the difference between the wavenumbers of the maxima of the absorption and fluorescence spectra (ν_a - ν_f) of deoxyguanosine as a function of solvent polarity according to Lippert's function, the open symbol pertains to methylene chloride.

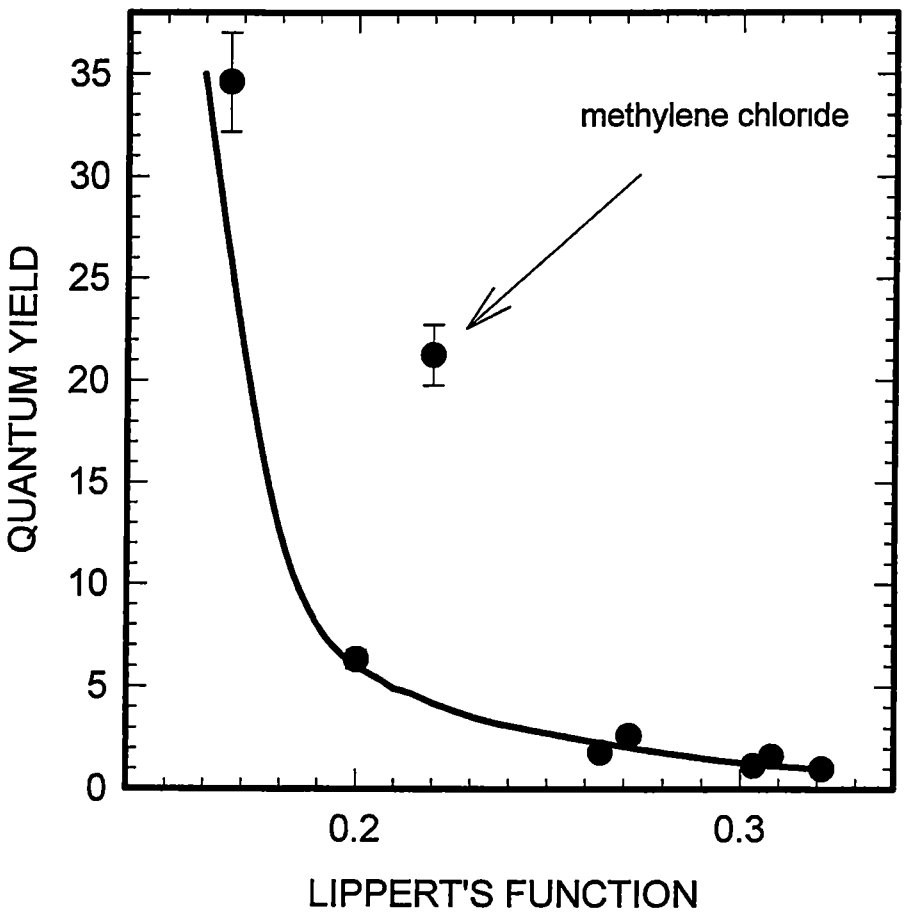


Figure 46
Plot of the fluorescence quantum yield of deoxyguanosine as a function of solvent polarity according to Lippert's function.

defined by one variable alone such as the dielectric constant. Qualitatively, solvent polarity is a measure of the solvating power of the solvent (Reichardt, 1994). However, quantitatively there are a number of scales of empirical solvent polarity of which E_N^T is the most widely used (Suppan and Ghoneim, 1997). In this scale, high values of the empirical parameter of solvent polarity correspond to high values of solvent polarity, such as water that has an E_N^T value of 1 (the highest value on this normalized scale). The plot of the fluorescence quantum yield q as a function of E_N^T for the present study is shown in Fig. 47, and can be seen that it is nonlinear; nevertheless, it follows a trend: as the E_N^T increases, q decreases following the same pattern as the plot of q *vs.* ϵ (Fig 44). Therefore, the solvent polarity does have an effect on the quantum yield. We next need to consider the effect of the solvent polarizability, α. We have plotted q *vs.* α and this plot is shown in Fig. 48. Although the plot is nonlinear, the quantum yield increases as the polarizability is increased indicating that polarizability also affects the photophysical properties of dG. Thus, solvent polarity serves to diminish the quantum yield, while solvent polarizability serves to enhance it We have also plotted the quantum yield as a function of viscosity (Fig. 49). It is seen that, for small viscosities, the quantum yield decreases sharply as the viscosity is increased, and then slowly increases as the viscosity increases. This sharp decrease is difficult to understand because typically an increase in viscosity is known to reduce the deformation of the structure of an emitting molecule through viscous damping by the solvent and to result in an increase in the quantum yield. We should note that in this plot the point for methylene chloride exhibits a regular behavior; this is not the case for the plots as a function of ϵ, Lippert's function, E_N^T, and polarizability (Figs 44, 46, 47, and 48). This behavior may be related to the high

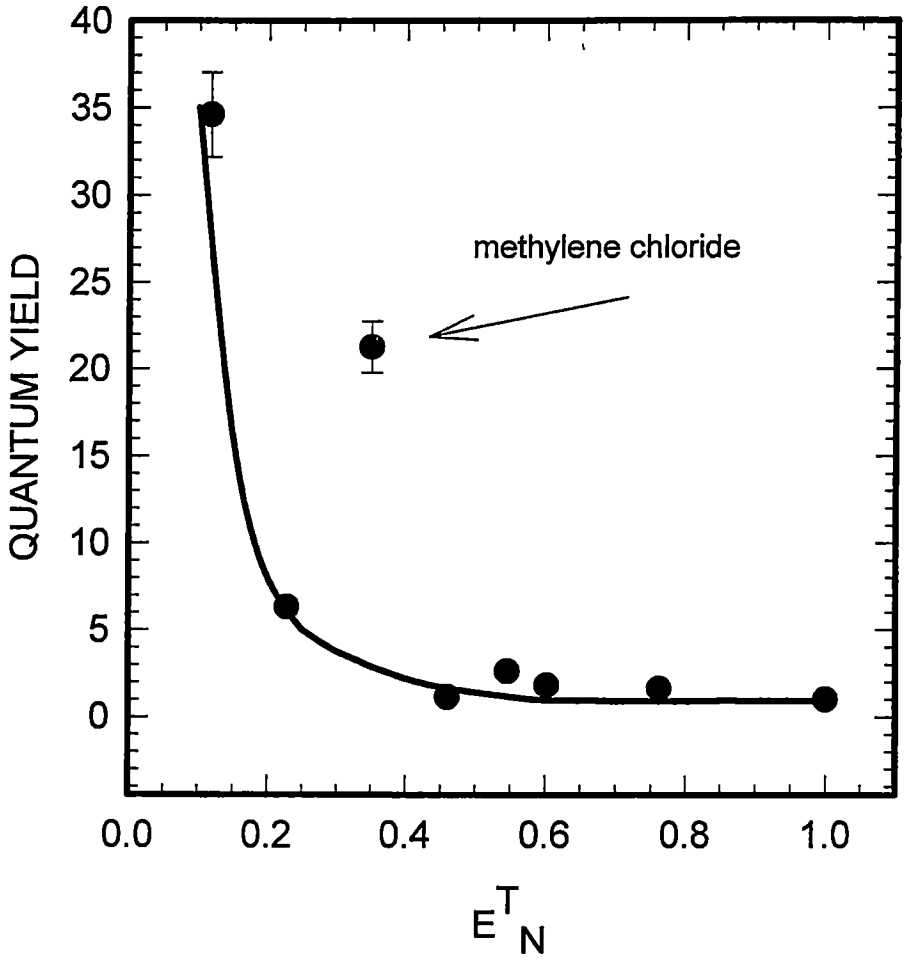


Figure 47
Plot of the fluorescence quantum yield of deoxyguanosine as a function of the empirical measure of solvent polarity according to E_N^T values.

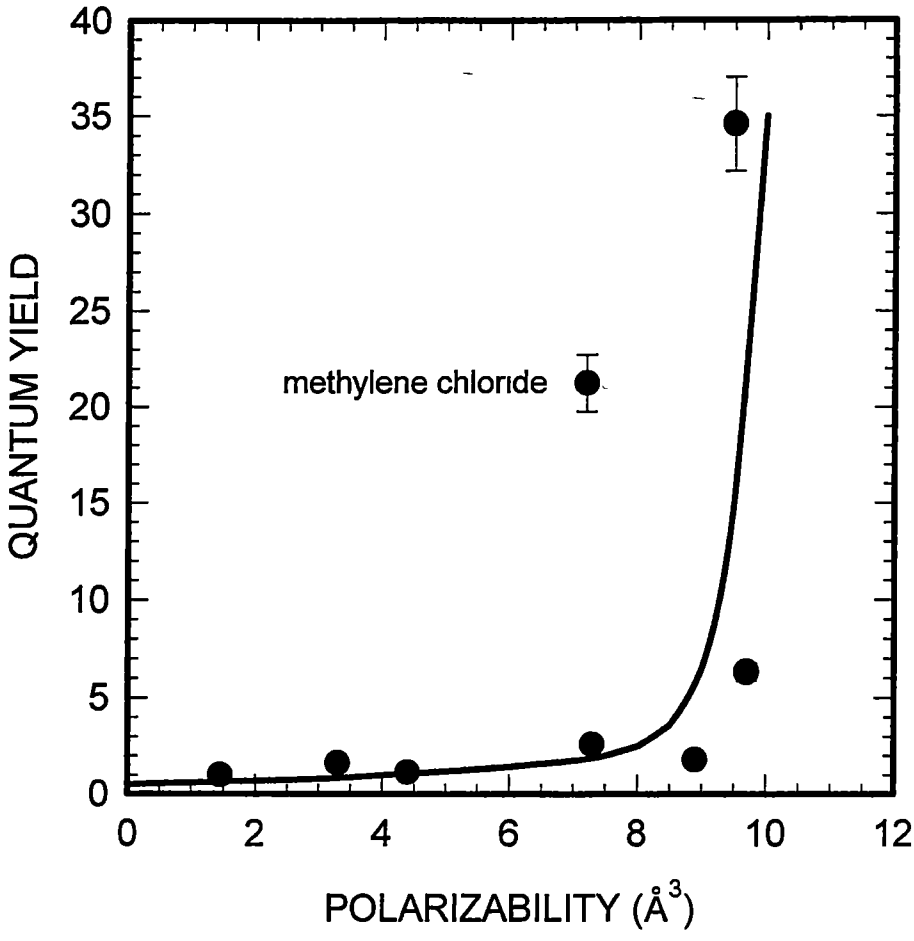


Figure 48
Plot of the fluorescence quantum yield of deoxyguanosine as a function of solvent polarizability.

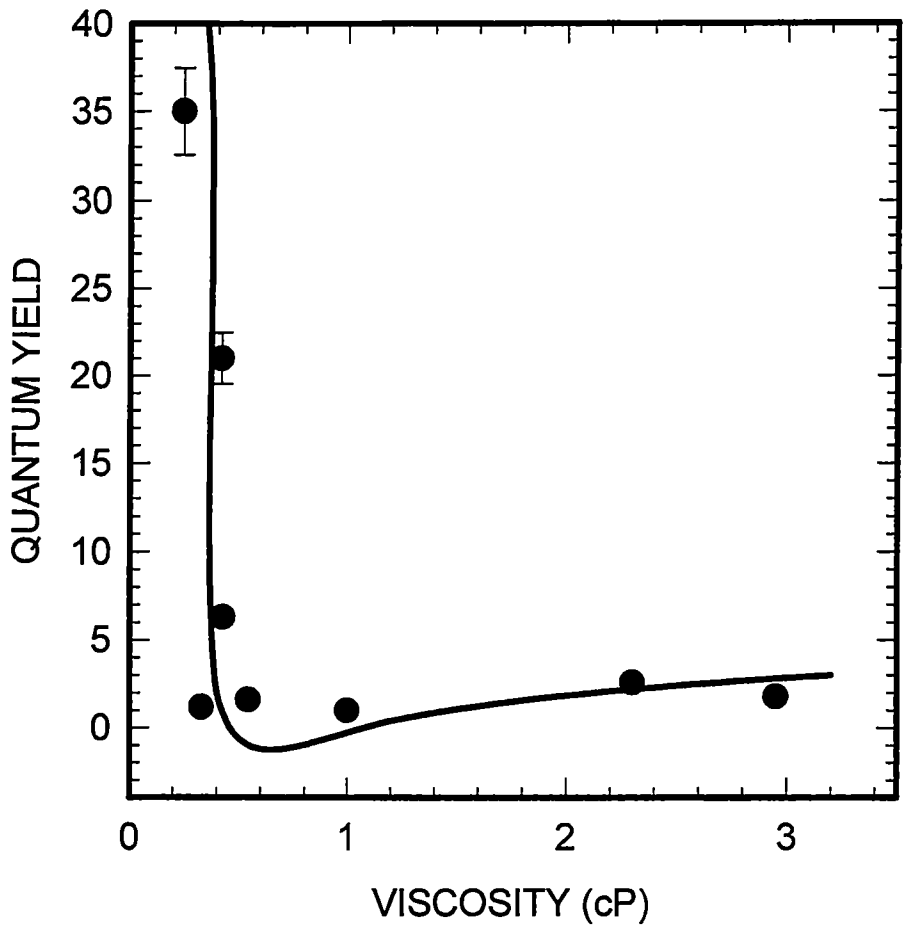


Figure 49
Plot of the fluorescence quantum yield of deoxyguanosine as a function of the solvent viscosity.

electronegativity of chlorine in a way that currently is not clear.

Lippert has developed an equation that relates his function (in terms of the solvent ϵ and the refractive index n) to the change in the wavenumber of the maximum of the absorption spectrum, ν_a, and the wavenumber of the maximum of the fluorescence spectrum, ν_f, which follows below.

$$\bar{\nu}_a - \bar{\nu}_f = \frac{2(\mu_e - \mu_g)^2}{hcR^3}\left[\frac{\epsilon - 1}{2\epsilon + 1} - \frac{n^2 - 1}{2n^2 + 1}\right] + constant$$

In this function, μ_g and μ_e are the permanent dipole moments of dG in the ground and in the excited state, respectively, h is Planck's constant, c is the speed of light in vacuum, and R is the cavity radius in Onsager's theory of the reaction field, which is calculated to be 3.1 Å (Edwards, 1970). A plot of (ν_a - ν_f) *vs.* the bracketed function (Lippert's function) is shown in Fig 45, and can be seen to be linear. From the slope of this plot we can calculate $\Delta\mu$, which is the difference between the dipole moments of the excited and the ground states for dG. From this, since μ_g is known, 6.9 D (Alyoubi and Hilal, 1995), μ_e can be calculated. We find a value of 9.7 D for the dipole moment of dG in the excited state. The fact that this value is larger than that in the ground state means that dG becomes more polar upon excitation. Thus, shifts in the fluorescence spectra relative to the spectrum in diethyl ether, which is the most inert solvent we have used in the present study, are expected to be greater than those in the absorption spectra. As can be seen from Table 1, this expectation is born out. Another potential source of spectral shifts is hydrogen bond formation. With reference to a non-hydrogen bonding solvent, shifts to longer wavelengths in the fluorescence spectra are observed when the hydrogen bond is

stronger in the excited state (Pimentel, 1957; Georghiou, 1981). Although dG is not soluble in a completely non-hydrogen bonding solvent, the solution in diethyl ether can be taken as an approximate reference; this is the most inert solvent in this study. With this reference, it can be seen that shifts are to longer wavelengths and, therefore, dG does form stronger hydrogen bonds upon excitation. However, because dG is not soluble in nonhydrogen-bonding solvents, the hydrogen bond strengths in the different solvents cannot be quantified.

For the solvents used in the present study, there is no clear trend with regard to the spectral widths. For the fluorescence spectra, as the dielectric constant is decreased or the polarizability is increased, changes are observed but there are no clear correlations (Table 1 and 2). Also, within the experimental error, no changes are found in the spectral widths of the absorption spectra in all the solvents with the exception of that in buffer, which is slightly larger (Table 1).

The results of the present study indicate that dielectric and polarization interactions greatly influence the fluorescence quantum yield and the location of the fluorescence spectral peaks; however, no clear correlation has been found between the widths of the fluorescence spectra and the solvent dielectric constant or the polarizability. In this regard, we need to investigate the contribution of the breaking or forming of hydrogen bonds and to explore the change in the shape of the spectra regarding the fluorescence spectrum tail; this is done below.

FLUORESCENCE SPECTRUM TAIL

A characteristic property of poly(dG-dC)•poly(dG-dC) is the pronounced tail in its fluorescence spectrum (Fig 9). To investigate the origin of this formation, we have

plotted the γ ratio *vs.* the solvent dielectric constant ϵ, E_N^T, and the polarizability α It can be seen from Fig 50 that the γ ratio increases as the dielectric constant increases, and the same holds true for the plot of the γ ratio *vs.* E_N^T (Fig. 51). In contrast, it can be seen from Fig. 52 that an increase in the solvent polarizability results in a reduction in the γ ratio. As can be seen in all three plots (Figs. 50-52), 2-propanol is the exception to the goodness of the fit. A plot of the γ ratio *vs.* the quantum yield (Fig. 53) finds that there is no correlation between these two parameters. On the other hand, a plot of γ *vs.* viscosity, η (Fig. 54) finds that there is a good correlation. γ increases sharply from zero (in diethyl ether) as η is slightly increased for small values of η: as η is increased further, the plot reaches a plateau at $\gamma \approx 0.24$ In sucrose solutions, the values of γ are not very different from this plateau value: $\gamma = 0.20$ for $\eta = 14$ cP and $\gamma = 0.27$ for $\eta = 149$ cP (see Table 3). We conclude that there is some contribution of viscosity to the magnitude of the tail of the spectrum at small viscosities.

We need to explore whether hydrogen bonding affects the photophysics of this system, and this is discussed in the next section.

HYDROGEN BONDING

We have tested the importance of hydrogen bonding groups at the N1 and N7 positions in the optical properties of dG. The N1 position is involved in interbase hydrogen bonding in DNA. The pK_a of the N7 position is 2.1 and the pK_a for the N1 position is 9.2 (Bloomfield *et al*, 1974). dG was dissolved in solutions of very low pH, 0.5, and very high pH, 11, and both the fluorescence and the absorption spectra were measured. In the pH 0.5 solution, where a proton is added to dG at the N7 position, the changes in the fluorescence spectrum were so dramatic (see Results) they precluded any

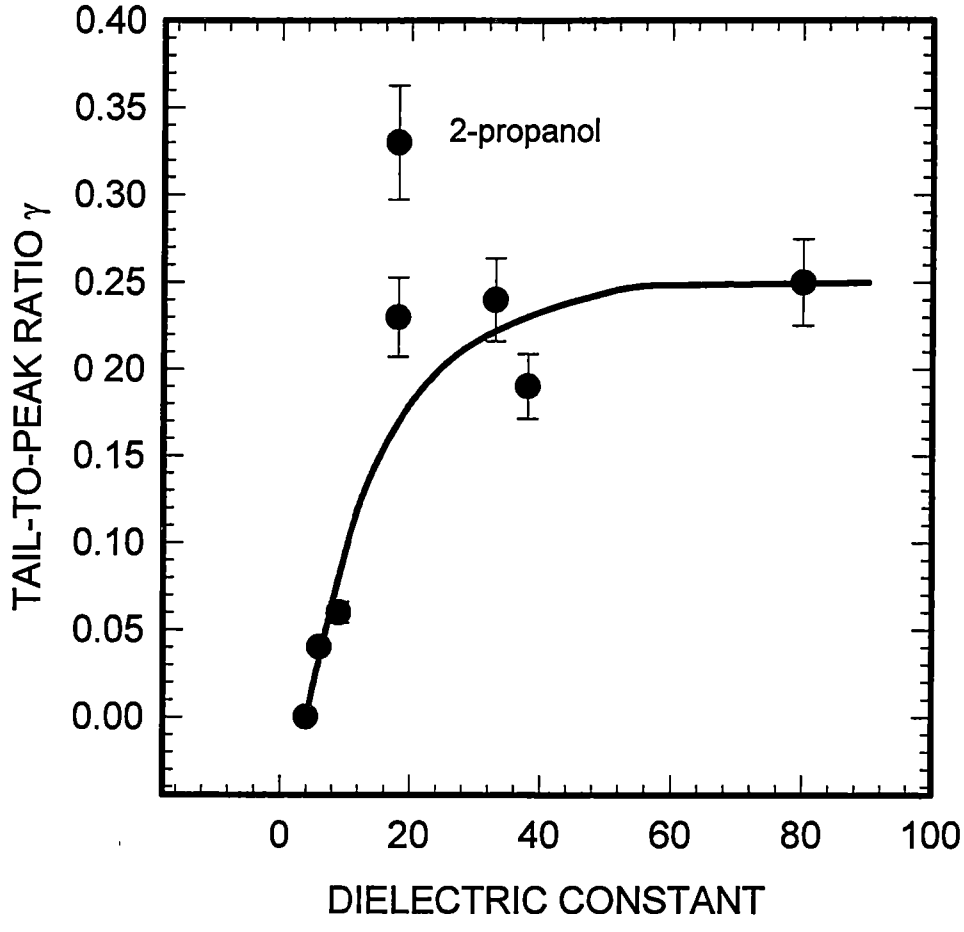


Figure 50
Plot of the fluorescence tail-to-peak ratio of deoxyguanosine as a function of the solvent dielectric constant.

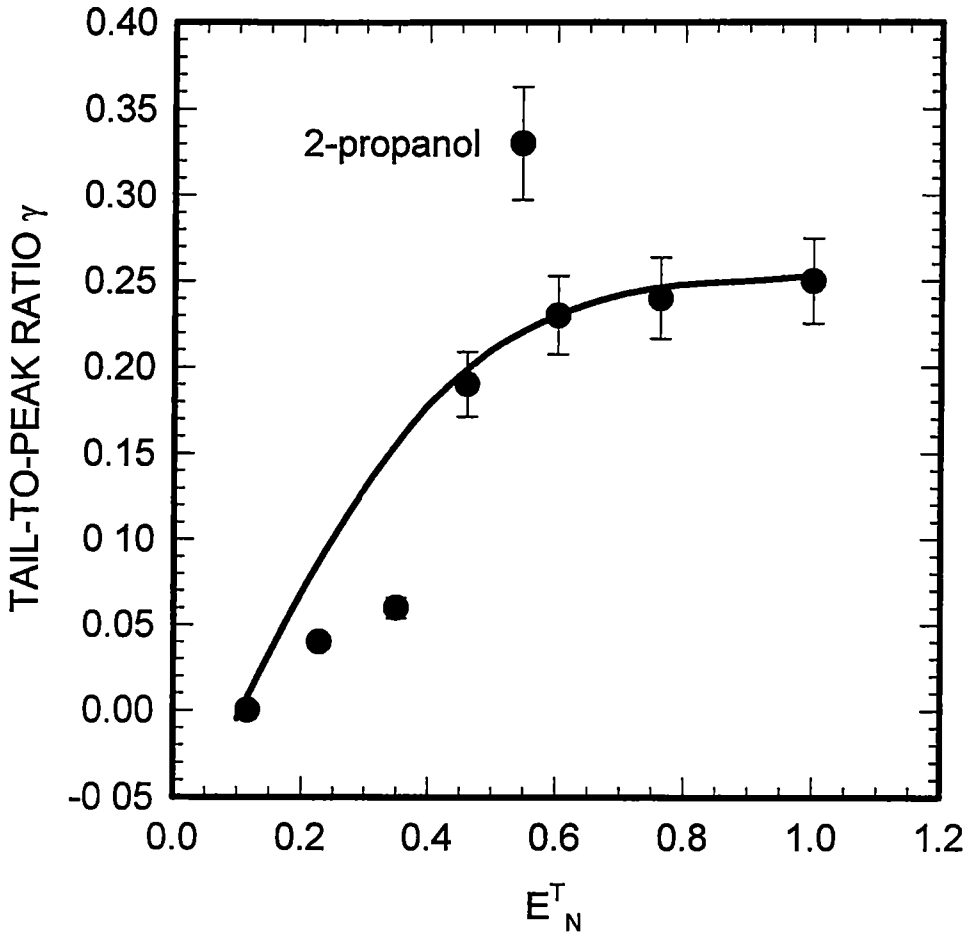


Figure 51
Plot of the fluorescence tail-to-peak ratio of deoxyguanosine as a function of the solvent polarity according to the values of the E_N^T scale.

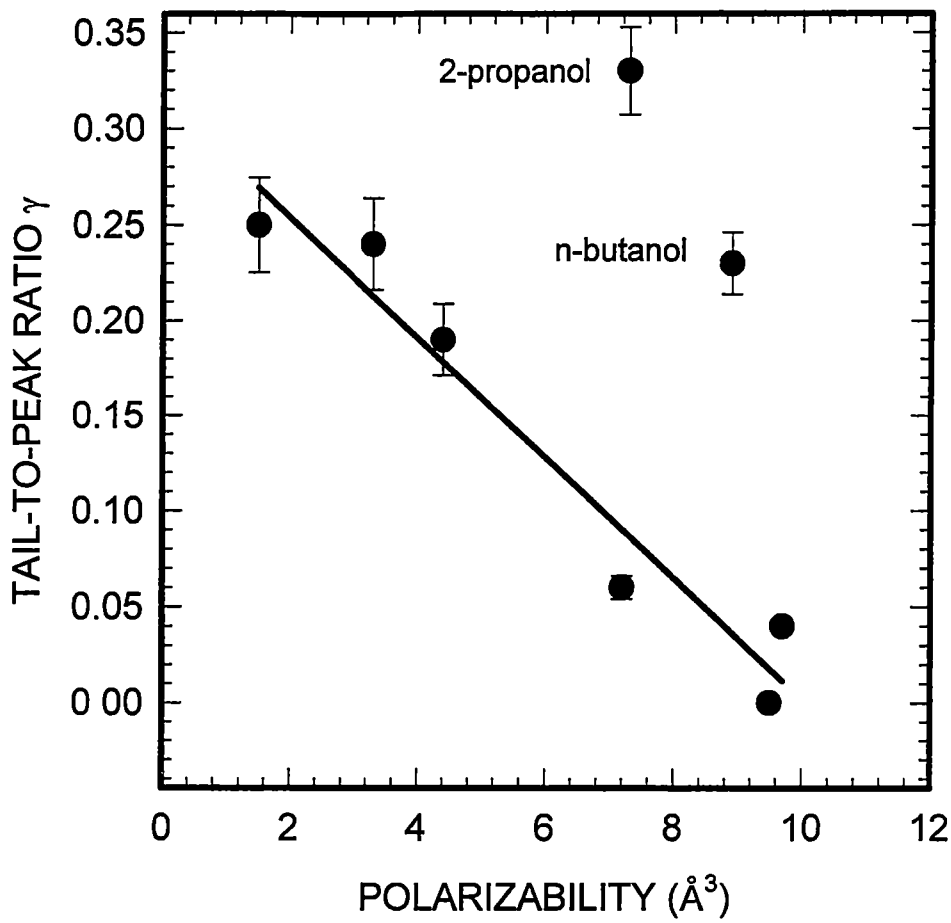


Figure 52
Plot of the fluorescence tail-to-peak ratio of deoxyguanosine as a function of the solvent polarizability.

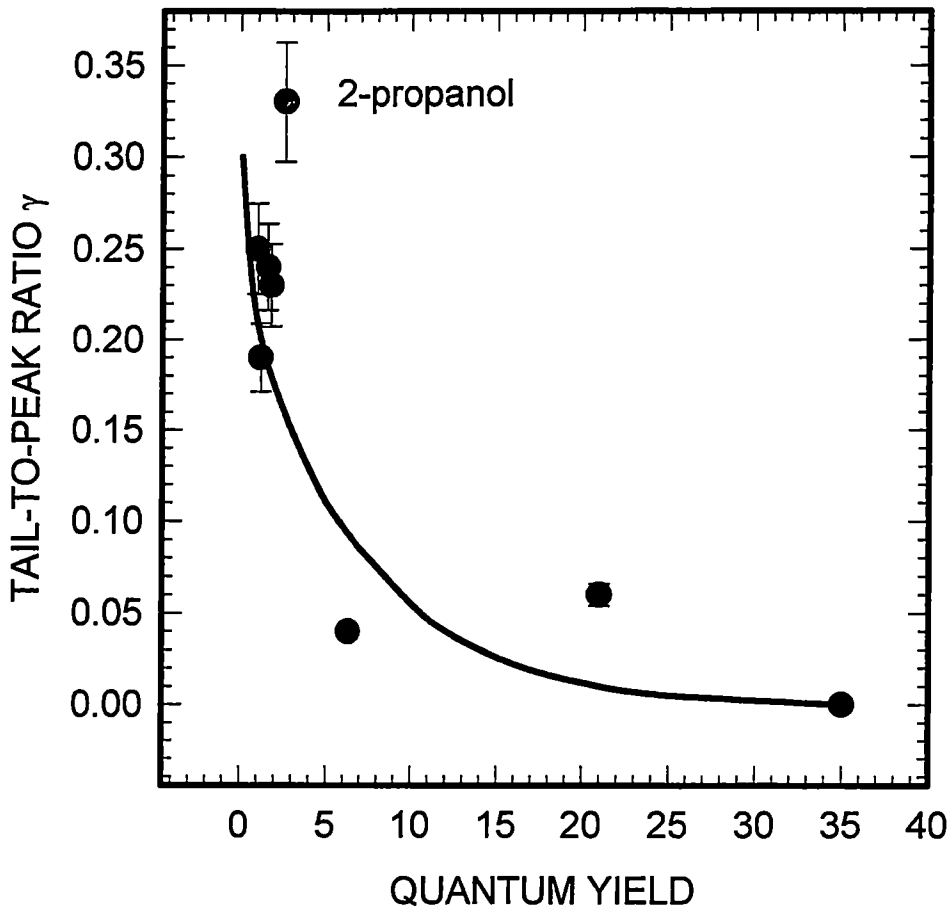


Figure 53
Plot of the fluorescence tail-to-peak ratio of deoxyguanosine as a function of the fluorescence quantum yield.

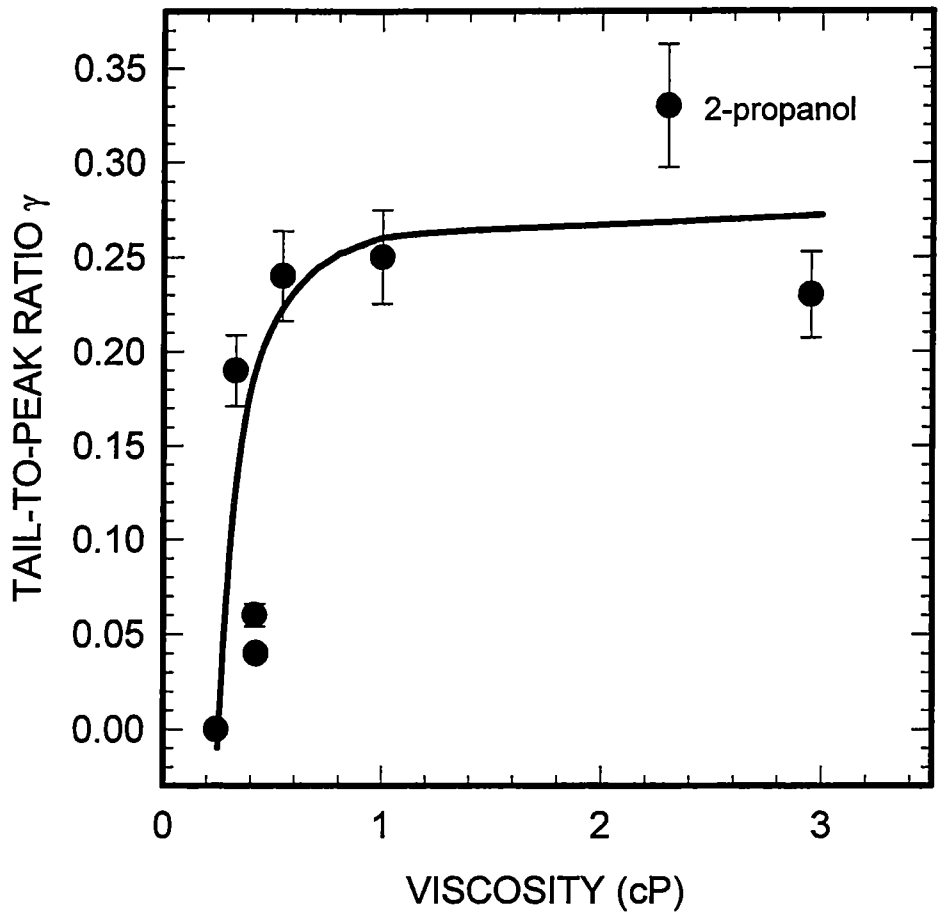


Figure 54
Plot of the fluorescence tail-to-peak ratio of deoxyguanosine as a function of the solvent viscosity.

conclusions to be drawn regarding the photophysics of the hydrogen bonding at this position where a proton would actually be shared. Supporting this is previous work done in our laboratory that has shown a large increase in the quantum yield with a dramatic shift of the fluorescence spectrum to longer wavelengths upon methylation of guanosine at the N7 position (Ge *et al.*, 1990).

At pH 11, the fluorescence spectrum is seen to display a very large enhancement. the fluorescence quantum yield is 9.3 times larger than that in buffer (Fig. 27 and Table 1). The absorption spectrum, however, displays large broadening which may suggest a large perturbation of the excited electronic surface. This perturbation is the result of a complete transfer of proton to dG at position N1 [$pK_a = 9.2$ (Bloomfield *et al.*, 1974)]. In DNA, position N1 is involved in interstrand hydrogen bonding. The fact that the absorption spectrum of DNA has a shape which is very similar to that of an equimolar mixture of bases (Gueron *et al.*, 1974) suggests that hydrogen bonding at position N1 of dG, that involves sharing of proton rather than complete transfer, does not greatly perturb the electronic structure.

The N2 and N3 positions are also capable of protonation, but cannot be studied due to lack of product availability.

The question arises as to how well we can simulate the photophysical properties of the dG residue in DNA on the basis of the results of the present experiments that are based on the photophysical properties of dG in aqueous buffer, in the absence and in the presence of sucrose, and in organic solvents. The large increase in the fluorescence quantum yield, q, with viscosity (Fig. 42) as well as that in solvents that are not very polar, *i.e.* diethyl ether and ethyl acetate (Table 1), suggests that the increase of the

rigidity of dG and of the hydrophobic nature of its environment, which occur when dG becomes part of DNA, are not responsible for the very small value of q in DNA: 0.8×10^{-5} (Huang and Georghiou, 1992) as compared to that of 0.8×10^{-4} for free dG in water (Vigny and Ballini, 1977) We should note that of these two increases in the quantum yield, the one caused by the hydrophobicity of the environment is by far the largest, by a factor of 35 (Table 1). It is not known how rigid the interior of DNA is, but were we to assume that it corresponds to a viscosity of 29 cP, the increase in the quantum yield would be by a factor of only 2.5 (Table 3) We propose instead that the quenching of the fluorescence of dG in DNA stems from specific interactions between polar groups of dG in the grooves, N7 and O6 in the major groove, and N2 and N3 in the minor groove, with the aqueous environment. Support for this proposal was obtained from the experiments described in "Affinity of dG for Water" (see below) which suggest that a network of water is formed around free dG in an 8% water/butanol mixture; this network is found to affect profoundly the photophysical properties of free dG. The difficulty then in the simulation stems from the inability to describe the hydration network in terms of those formed around dG in the organic solvents. We should recall that the O6, N1, and N2 positions are involved in interstrand hydrogen bonding in DNA, whereas these positions in free dG are available for hydrogen bonds in solution. We should note that the solvent effects on the fluorescence quantum yield of dG, either free or in DNA, are most probably stemming from effects on the rate constant of internal conversion: this inference is based on the observation that intersystem crossing is inefficient for nucleic acids, with internal conversion being very efficient (Gueron, *et al* , 1974).

AFFINITY OF DEOXYGUANOSINE FOR WATER

We have also attempted to quantify the effects of hydrogen bonding on the photophysical properties of dG by using aqueous mixtures of organic solvents Specifically, we wanted to look at small percentages of water so that the bulk properties of the solvent would not be changed. We should note in this regard that attempts were made at utilizing water mixtures with methanol or 2-propanol. The results in these solvents were found to be independent of the sequence of steps in which the solutions were prepared. The reason for this appears to stem from the fact that these solvent compete well with water in forming hydrogen bonds For this purpose, we chose n-butanol because it is a weak alcohol, *i e* it does not form strong hydrogen bonds As a consequence of this, the maximum miscibility of water in this alcohol is only 20% (Merck, 1983). In the process, it was discovered that the results depended on the sequence of the steps used in preparing the solution. We prepared the butanol/water solutions using three different methods. In the first method, which we call "injected", we started with dG dissolved in butanol and we then added 8% water. In the second method, which we call "pre-mixed", we first mixed butanol with 8% water and then added the (solid) dG. The third method, which we call "carried its own water," utilized a high concentration of dG dissolved in water. This concentration was specific because an 8% addition from it to pure butanol in the cuvette gave the correct absorbance of about 0.05 at the excitation wavelength of 265 nm. We have found that these three different methods of solution preparation gave different results Figure 55 shows the results. It is seen that dG in the "pre-mixed" solution shows a large fluorescence enhancement, by about a factor of about 2.5, relative to the solution in pure butanol By contrast, the

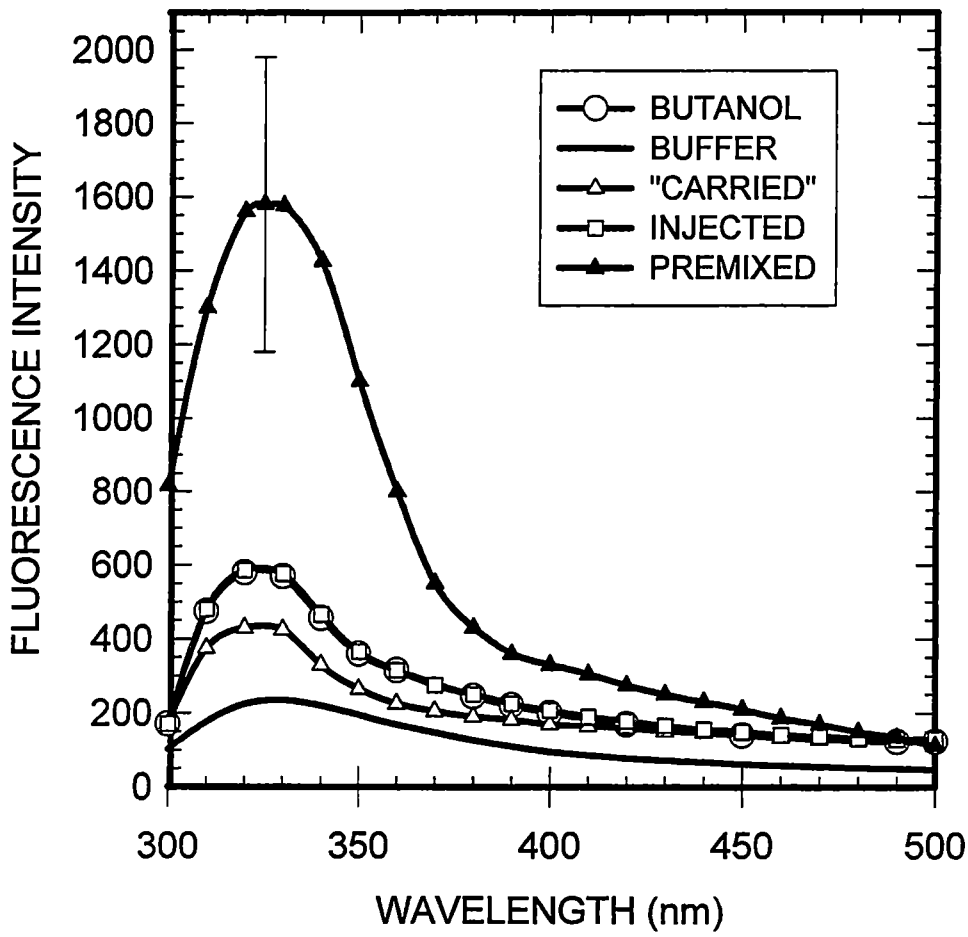


Figure 55

Comparison of the fluorescence spectrum of deoxyguanosine in 8% water/butanol mixtures in which the water was added using three different methods: "carried its own water," where deoxyguanosine was dissolved in water and then added to butanol, "injected," where water was added to butanol that already contained deoxyguanosine, and "premixed" where water and butanol were mixed, and then deoxyguanosine was dissolved in the mixture. The error bar pertains to the measurement for the "premixed" solution; this is a rather large error which may have its origin in the sensitivity of the fluorescence signal to relatively small variations in the hydration pattern of water around deoxyguanosine.

"injected" solution shows virtually no change Finally, the "carried its own water" solution exhibits fluorescence quenching by about 40% relative to the pure butanol solution.

We presume that in the "premixed" solution different solvation sites are occupied by water molecules and/or by butanol molecules, depending on the affinity of the sites. In order to test this supposition, we ran a series of experiments in which the solution was heated for 10 minutes, allowed to cool to room temperature, and then have its fluorescence tested The results are shown in Fig. 56. It is seen that the fluorescence intensity is reduced as the incubation temperature is increased. The spectrum for 40 °C is virtually identical with that for pure butanol This indicates that in the "premixed" solution at room temperature the dG has a network of water formed around it which is disrupted at higher incubation temperatures, leaving only butanol to occupy the solvation sites. This desolvation of dG was further quantified by considering this process to follow an Arrhenius behavior of the form

$$I = I_o e^{-\frac{\Delta E}{RT}}$$

Here, R is the gas constant = 1.987 x 10^{-3} kcal/mol·K, T is the incubation absolute temperature, ΔE is the activation energy, and I_0 is a constant. This equation yields

$$\ln I = \ln I_0 - \frac{\Delta E}{RT}$$

A plot of the ln I as a function of 1/T is shown in Fig. 57. The plot is seen to be linear with a slope = (3.3 ± 0.7) x 10^3 K. Therefore, ΔE = - (3.3 ± 0 7) x 10^3 K x 1.987 x 10^{-3}

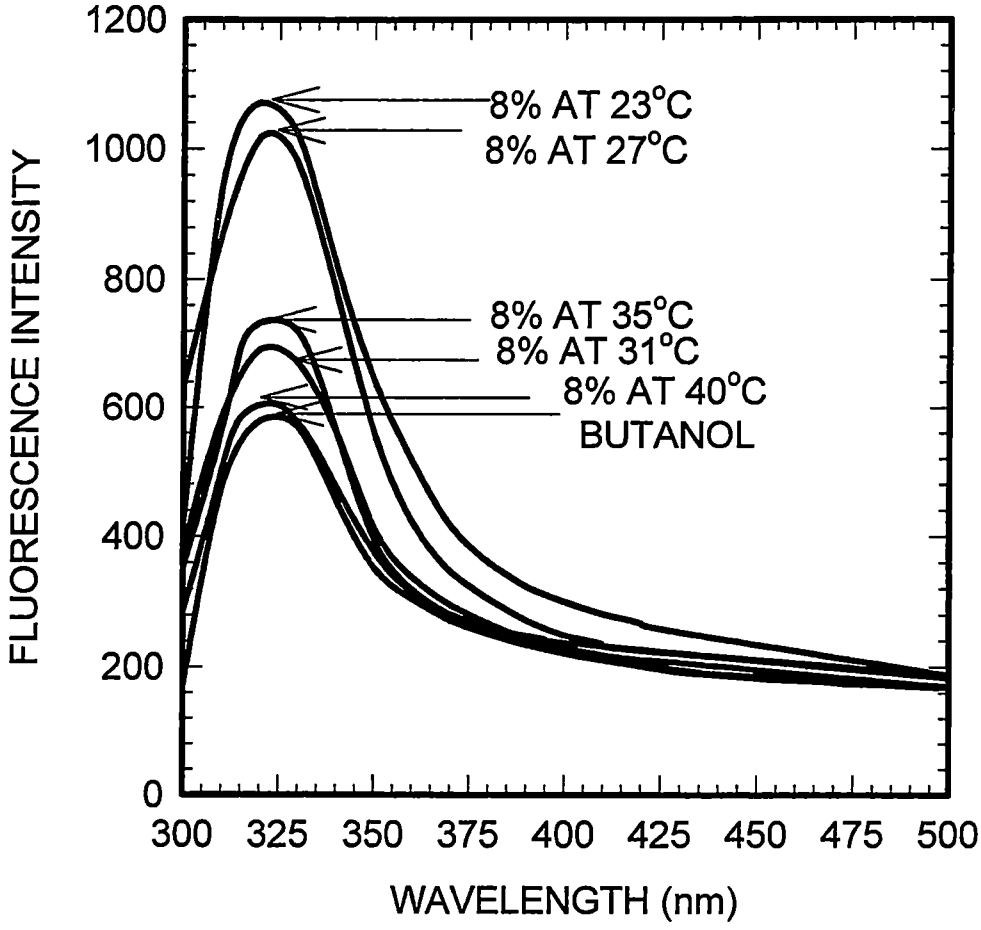


Figure 56
Comparison of the fluorescence spectrum of deoxyguanosine in an 8% water/butanol solutions in which water and butanol were mixed before dissolving the dG in it. The deoxyguanosine solutions were then heated to 27 °C, 31 °C, 35 °C, and 40 °C, and the fluorescence spectra were measured after the solutions reached room temperature.

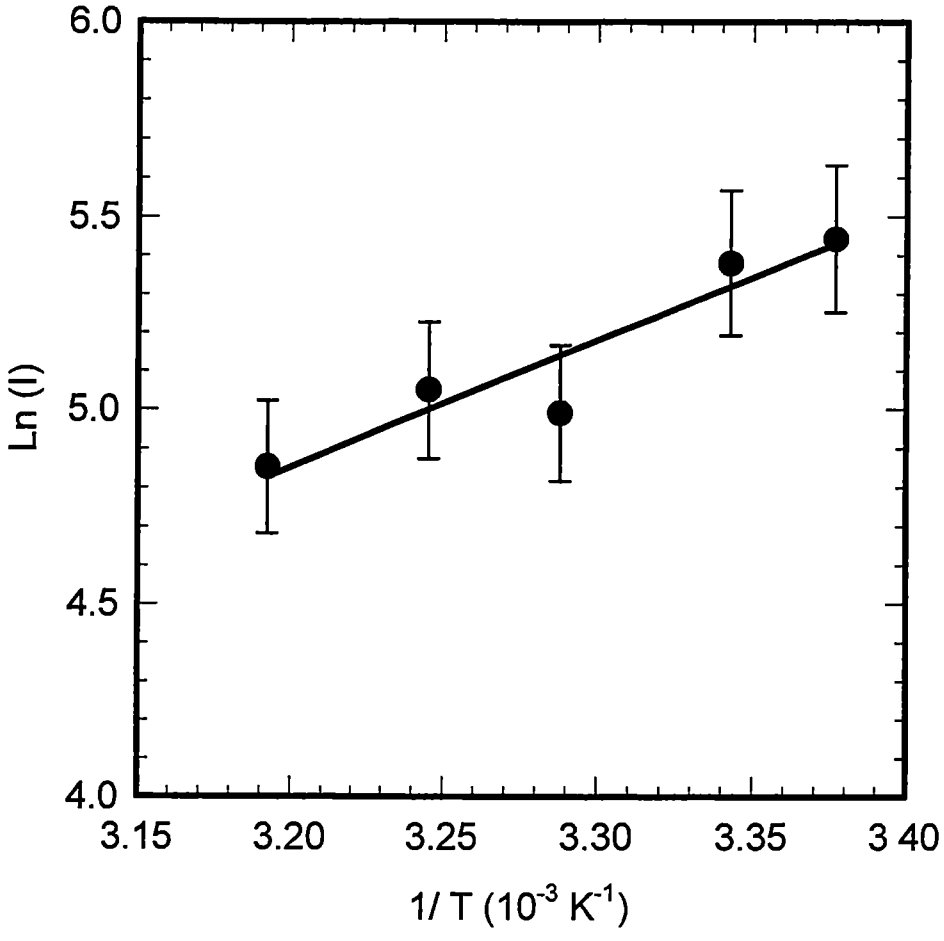


Figure 57
A plot of the natural logarithm of the intensity I of the fluorescence spectra of deoxyguanosine *vs.* 1/absolute temperature for the measurements described in the caption to Fig. 56.

kcal/mol·K = - 6 ± 1 kcal/mol. ΔE may be considered to represent the enthalpy ΔH of the desolvation process. The solvation free energy ΔG for guanine is quite large, approximately - 20 kcal/mol (Bash *et al.*, 1987; Mohan *et al.*, 1992; Elcock and Richards, 1993) ΔG relates to ΔH and to the entropic change ΔS of the desolvation process through the following equation

$$\Delta G = \Delta H - T\Delta S$$

where T is the absolute temperature. This yields TΔS ≈ 14 kcal/mol as the entropic contribution to the desolvation process. At room temperature, 293 K, this value yields ΔS ≈ 48 cal/mol·K This result implies that there is a very large entropic contribution to the desolvation process, which is about twice as much as the enthalpic contribution.

For the "carried its own water" solution, water being the sole solvator induces fluorescence quenching compared to the spectrum of pure butanol: this is in line with the quenching of the fluorescence of dG in buffer (Fig. 55). In the case of the "injected" solution, dG already has a butanol network formed around it which water cannot disrupt because of the preponderance of butanol; as a consequence, the fluorescence spectrum is very similar to that in pure butanol. It should be noted that in all the aqueous mixtures, the fluorescence spectrum has a tail contribution which is similar to that in pure butanol (Fig 56). This suggests that the bulk properties of butanol make a significant contribution to the shape of the fluorescence spectra.

These results suggest that at room temperature dG tends to retain the solvent network initially formed around it. Let us now consider dG in DNA. The sites of hydration are N7, O6, and N3 (Pullman and Pullman, 1981; Schneider and Berman,

1995). Thermal fluctuations are known to transiently break the intermolecular hydrogen bonds of the DNA base pairs in the millisecond range (Leroy *et al.*, 1988), allowing the bases to swing into the aqueous environment. For free dG (Fig. 1), the sites involved in interbase bonding (N1, N2, and O6) can become hydrated, while for dG in DNA only the O6 site can be hydrated (Pullman and Pullman, 1981). Therefore, when the interstrand hydrogen bonds of dG break, allowing it to swing into the aqueous environment of the major or minor groove, the sites N1, N2, and O6 would become hydrated. Theoretical studies report that guanine has a very high free energy of hydration, approximately -20 kcal/mol (Bash *et al.*, 1987; Mohan *et al* , 1992; Elcock and Richards, 1993). Cytosine has a comparable free energy. However, adenine and thymine have free energy values that are smaller by about 10 kcal/mol (Bash *et al* , 1987; Mohan *et al.*, 1992; Elcock and Richards, 1993). Thermodynamic studies also report that GC base pairs are more strongly hydrated (Chalikian *et al* , 1994). Thus, guanine (and presumably cytosine), once exposed to the aqueous environment, will have a network of water formed around it. The results of the present study suggest that guanine will tend to preserve this network As a consequence, the intermolecular hydrogen bonds in DNA that involve that particular guanine residue would tend to remain broken. *We therefore infer that at any instant there will be a number of GC open base pairs along the DNA double helix.* Thus, DNA appears to have "unzipped" segments along its helix. Because of the coupling between base pair opening and bending (Manning, 1983; Ramstein and Lavery, 1988), DNA would bend very easily. Thus, the GC base pairs are sites of locally bent DNA. Presumably, collisions with energetic solvent molecules would disrupt the hydration network and allow the guanine residues to reform the intermolecular hydrogen bonds

Also, in the cell interactions with proteins would result in water removal from the solvent-exposed guanine residues. This picture raises the question of the ability of single strands to form double-stranded DNA in solution: if the GC base pairs are hydrated and unable to form hydrogen bonds, a double-stranded structure would not be formed It is known, however, that single-stranded DNA is highly compacted and its bases are exposed to water to a much smaller extent than the bases of double-stranded DNA (Watson *et al* , 1988) This preserves the ability of the bases of single-stranded DNA to form a hydrogen bonded double-helical structure. In order to make double-stranded DNA, the single strands are annealed to a high temperature. As we have found in the present study, under those conditions water is "shaken off" the guanine residues. Judging from the similarity of the free energy for desolvation of cytosine to that of guanine (Bash *et al.*, 1987; Mohan *et al.*, 1992, Elcock and Richards, 1993), a similar "shake off" would be expected to happen to its water as well.

REFERENCES

Alyoubi, A.O. and R.H. Hilal, Biophys. Chem., **55**, 231, 1995.

Barber, E.J., National Cancer Institute Monograph, **21**, 219, 1966.

Bash, P.A , U.C. Singh, R. Langridge, and P.A. Kollman, Science, **236**, 564, 1987

Bloomfield, V.A., D.M. Crothers, and I. Tinoco, Phys. Chem. Nucl. Acid., Harper and Ro, New York, 1974.

Chalikian, T.V., A.P. Sarvazyan, G.E. Plun, K.J. Breslauer, Biochemistry, **33**, 2394, 1994.

Dean, J.A., Lange's Handbook of Chemistry, 1992, McGraw Hill, New York.

Edwards, J.T., J. of Chem Ed., **47**, 261, 1970.

Elcock, A.H., and W G. Richards, J Am. Chem. Soc., **115**, 7930, 1993.

Ge, G. and S. Georghiou, Photochem. Photobiol, **54**, 301, 1991.

Ge, G. and S Georghiou, Photochem. Photobiol, **54**, 477, 1991.

Ge, G., S. Zhu, T.D. Bradrick, and S. Georghiou, Photochem. Photobiol., **51**, 557, 1990.

Georghiou, S and A.M Saim, Photochem. Photobiol. **44**, 733, 1986.

Georghiou, S in Modern Fluorescence Spectroscopy, Vol 3, 1981, ed by E.L. Wehry, Plenum Press, New York

Gueron M., J Eisinger, and A.A. Lamola in Basic Principles in Nucleic Acid Chemistry, Vol 1, 1974, editor P.O.P. Ts'o, Academic Press, New York.

Huang C.R and S Georghiou, Photochem. Photobiol., **56**, 95, 1992.

Leroy, J.L , M Kochoyan, T. Huynh-Dinh, and M Gueron, J. Molec. Biol., **200**, 223, 1988

Lide, Editor, CRC Handbook of Chemistry and Physics, 73rd Edition, 1992-1993, Chemical Rubber Publishing Co , Cleveland, Ohio.

Manning, G.S , Biopolymers, **22**, 689, 1983.

The Merck Index, 10th Edition, Merck and Co., Rahway, New Jersey, 1983.

Mohan, V , M.E. Davis, J.A. McCammon, and B.M. Pettitt, J. Phys. Chem., **96**, 6428, 1992

Pimentel, G.C., J. Am Chem. Soc., **79**, 3323, 1957.

Pullman, A. and B. Pullman, Quart. Rev. Biophys., **14**, 289, 1981.

Ramstein J and R. Lavery, Proc. Natl. Acad Sci., **85**, 7231, 1988.

Reichardt, C., Chem Rev., **94**, 2319, 1994.

Schneider, B. and H.M. Berman, Biophys. J., **69**, 2661, 1995.

Suppan, P., Solvatochromism, 1997, The Royal Society of Chemistry, Cambridge.

Taylor-Gerke L.S., Master's Thesis, University of Tennessee, 1996.

Vigny, P. and J.P. Ballini, in Excited States in Organic Chemistry and Biochemistry, 1977 (Edited by B. Pullman and N. Goldblum), D. Reidel, Boston.

Watson, J.D., N.C. Hopkins, J.W. Roberts, J.A. Steitz, and A.M. Weiner, Molecular Biology of the Gene, 4th edition, 1988, Benjamin/Cummings Publishing Company, Menlo Park, CA.

PART II:
ELECTROSTATIC INTERACTIONS IN DNA

I. INTRODUCTION

Customarily, the effect of the medium on Coulomb interactions is taken into account by treating it as a continuum with a screening dielectric constant. This description, however, breaks down at short distances where pairwise non-additive polarization effects that take place in the medium make a considerable contribution to the total interaction (Buckingham and Pople, 1955; Warshel, 1978; Stone, 1996). The need for incorporating polarization effects in electrostatic interactions has long been recognized and a number of studies have been carried out (Stone, 1996) Jarque and Buckingham (1989; 1992) used the Padé Approximant method to carry out a Monte Carlo simulation of many-body effects in a polarizable medium with two ions embedded in it. In the present study, we employ the results of their analysis to calculate the contribution the polarization effects make to the electrostatic interaction between phosphates in DNA. These effects are found to greatly diminish the contribution of the Coulomb interaction to the total interaction between the phosphates across the minor groove; their contribution, however, across the major groove is much smaller The results are found to shed considerable light on several aspects of the structure-dynamics relationship in DNA.

II. THEORY

DNA

The intrastrand separation between adjacent phosphates on the same DNA strand varies considerably, *e.g* from about 5.9 Å to 7.2 Å for a series of four dodecamers; a similar distance span for each dodecamer was also observed (Saenger, 1986). As a consequence of this variation, the strength of the repulsive Coulomb interactions would change depending on the sequence. Also, because of the much smaller width of the minor groove (about 6 Å) relative to that of the major groove (about 11.6 Å) (Neidle, 1994), the repulsion would be greater for the former case. The corresponding Coulomb interaction potentials V_{coul} for two charges q_1 and q_2 at distances r of 6 Å and 11.6 Å are calculated from $V_{coul} = q_1q_2 /4\pi\epsilon_o r$, where ϵ_o is the permittivity of free space, and found to be about 55.2 kcal/mol and 28.6 kcal/mol, respectively. However, shielding of the charges by counterions reduces them by about 50% (Padmanabhan *et al.*, 1988; Jayaram *et al.*, 1990, Ramstein and Lavery, 1990; Gurlie and Zakreskwa, 1998). This reduces the aforementioned potential values by a factor of 4 to about 13.8 and 7 1 kcal/mol for the interactions across the minor groove and the major groove, respectively.

With reference to the theoretical analysis of Jarque and Buckingham (1989, 1992), the parameters used are the reduced polarizability, $\alpha^* = \alpha/\beta^3$, where α and β are the polarizability of the medium (in $Å^3$) and the nearest neighbor distance (in Å), respectively, and δ which is given by $\delta = s/\beta$; here, s is the distance between the two charges. For water, $\alpha = 1.45$ $Å^3$ (Lide, 1992) For the DNA base residues, $\alpha \approx 11.8$ $Å^3$ (Miller and Sachik, 1979; Lymann, 1982). For the backbone sugar residue, $\alpha \approx 9\ 5$ $Å^3$ (Miller and Sachik, 1979; Lymann, 1982) DNA and its environment are not a

homogeneous medium. Therefore, in applying the theoretical analysis of Jarque and Buckingham, we need to take averages over the polarizabilities and the nearest neighbor distances for the different components of the system. The above polarization values yield for the average polarizability $<\alpha> \approx 7.6$ Å^3 The approximate distances are: 3 4 Å for adjacent bases on the same strand, 5 Å for bases across the two strands, 5Å for adjacent sugars, 1.5 Å for a sugar-base set, and 2.85 Å for water (Saenger, 1984, Jeffery, 1997). This yields an average nearest neighbor distance $<\beta> \approx 3.5$ Å. Thus, $\alpha^* = <\alpha>/<\beta>^3 \approx 7.6/3.5^3 \approx 0.18$. Shown in Fig. 58 are the results of the analysis by Jarque and Buckingham (1992) regarding two negative charges embedded in a polarizable medium for α^* values of 0.05, 0.1, and 0.5. By using an interpolation computer program based on Lagrange's method, values for the effective potential $V_{eff}(\alpha^*)$ for α^* were obtained from the following equation:

$$V_{eff}(\alpha^*) = y_1 \frac{(\alpha^* - \alpha^*_2)(\alpha^* - \alpha^*_3)}{(\alpha^*_1 - \alpha^*_2)(\alpha^*_1 - \alpha^*_3)} + y_2 \frac{(\alpha^* - \alpha^*_1)(\alpha^* - \alpha^*_3)}{(\alpha^*_2 - \alpha^*_1)(\alpha^*_2 - \alpha^*_3)} + y_3 \frac{(\alpha^* - \alpha^*_1)(\alpha^* - \alpha^*_2)}{(\alpha^*_3 - \alpha^*_1)(\alpha^*_3 - \alpha^*_2)}$$

Here, y_1, y_2, and y_3 are the values of the effective potential V_{eff} for a particular δ obtained from the data of Jarque and Buckingham (Fig. 58) for the three values of α^*: $\alpha^*_1 = 0.05$, $\alpha^*_2 = 0\,1$, and $\alpha^*_3 = 0.5$ Such a curve is presented for $\alpha^* = 0.18$ in Fig. 58. For the minor groove, the average value, <s>, is 6 Å. Thus, $\delta = <s>/<\beta> = 6/3.5 \approx 1.7$, for which a relative value of -0.43 is obtained from Fig. 58 for the polarization potential; this yields a value of -40.7 kcal/mol for the absolute polarization potential, V_{pol} (see caption to Fig. 58). With the charge reduced to –0.5 e, this potential is about –10.2 kcal/mol This

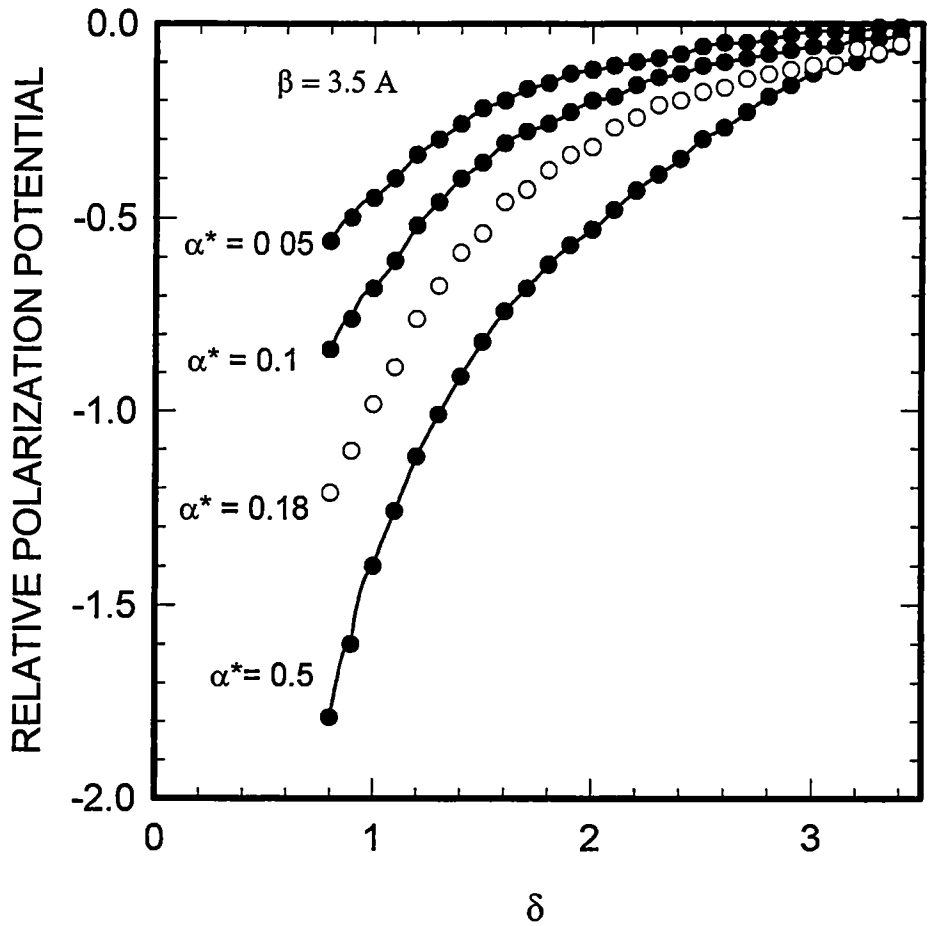


Figure 58

A plot of the relative polarization potential for electrostatic interactions as a function of $\delta = s/\beta$, where s is the distance between two ions of the same sign and β is the nearest neighbor distance, for the reduced polarizability α^* values of 0.05, 0.1, and 0.5. α^* is defined as α/β^3, where α is the polarizability of the medium. The open circles are data obtained by using an interpolation computer program based on Lagrange's method to obtain data for $\alpha^* = 0.18$. These values of the potential must be multiplied by $2.3 \times 10^{-18}/\beta$, with β in Å, for converting their units to Joules.

compares with the value of 13.8 kcal/mol for V_{coul}. Thus, the effective interaction potential, V_{eff}, which is the sum of the Coulomb and the polarization potentials, is equal to about 3 6 kcal/mol. It is seen that the polarization interaction makes a large contribution to the effective potential. This contribution is shown for other values of the groove width in Fig. 59, which compares plots of V_{coul}, V_{eff}, and V_{pol} for $\beta = 3.5$ Å.

Other values of β have also been used in the present calculations, ranging from 3.1 to 5 Å. As can be seen from Figs 60 and 61, in the range of 3.1-3.7 Å, V_{eff} is quite sensitive to the β values, decreasing considerably as β is decreased. This decrease is the result of the large contribution to V_{eff} which is made by the attractive polarization interaction (Fig. 58). This is particularly pronounced for small widths By contrast, for larger β values, ~ 4.1 - 5 Å, and small widths the Coulomb interaction predominates; V_{eff} exhibits a relatively large increase as the width is decreased, which is more pronounced as β is increased (Figs. 60 and 61). It is also seen that for large widths, all the curves tend to converge practically to the same plateau value. This implies that for the major groove, width ≈ 11.6 Å, V_{eff} is insensitive to the width of the groove.

We recall that the effective force F is given by $F = - dV_{eff}/ds$, where s is the groove width, this derivative can be approximated by the slope of the tangent line. We have done this by approximating the curves for the effective potential using the following polynomial

$$f(x) = c_1 + c_2 x + c_3 x^2$$

Using a χ^2 analysis of the following form

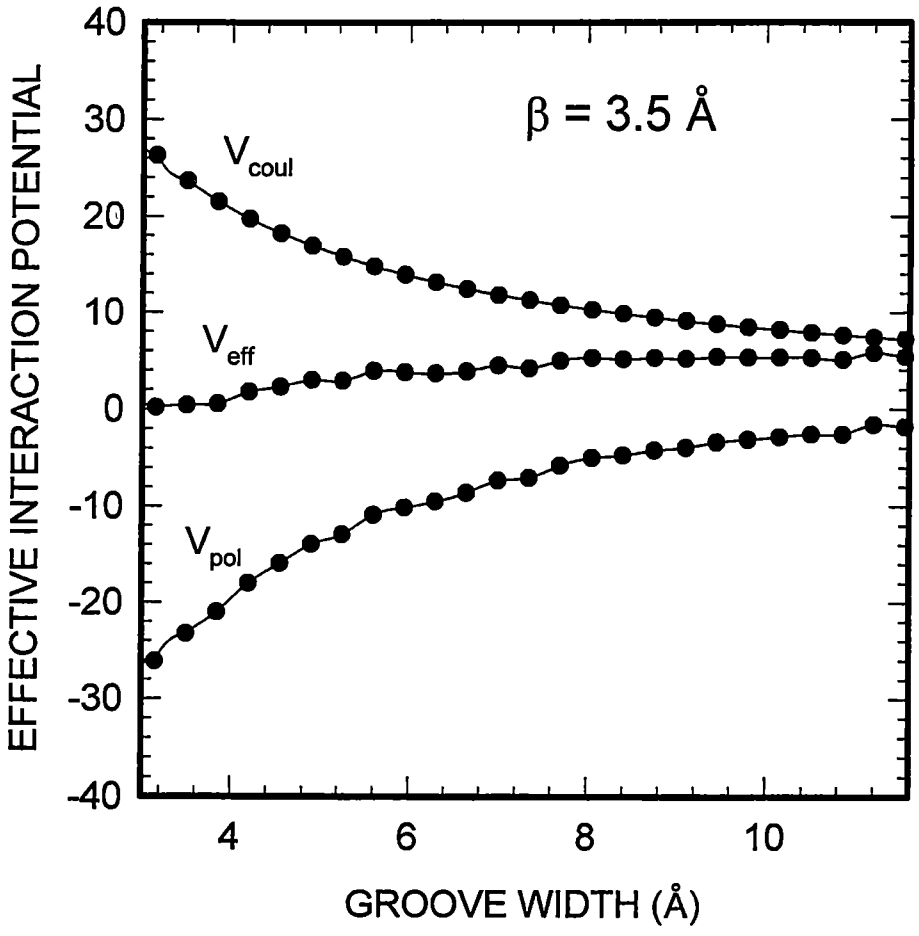


Figure 59
A plot of the Coulomb potential, V_{coul}, the polarization potential, V_{pol}, and the effective potential, $V_{eff} = V_{coul} + V_{pol}$, for a nearest neighbor distance of $\beta = 3.5$ Å and a reduced polarizability $\alpha^* = 0.18$, as a function of groove width s

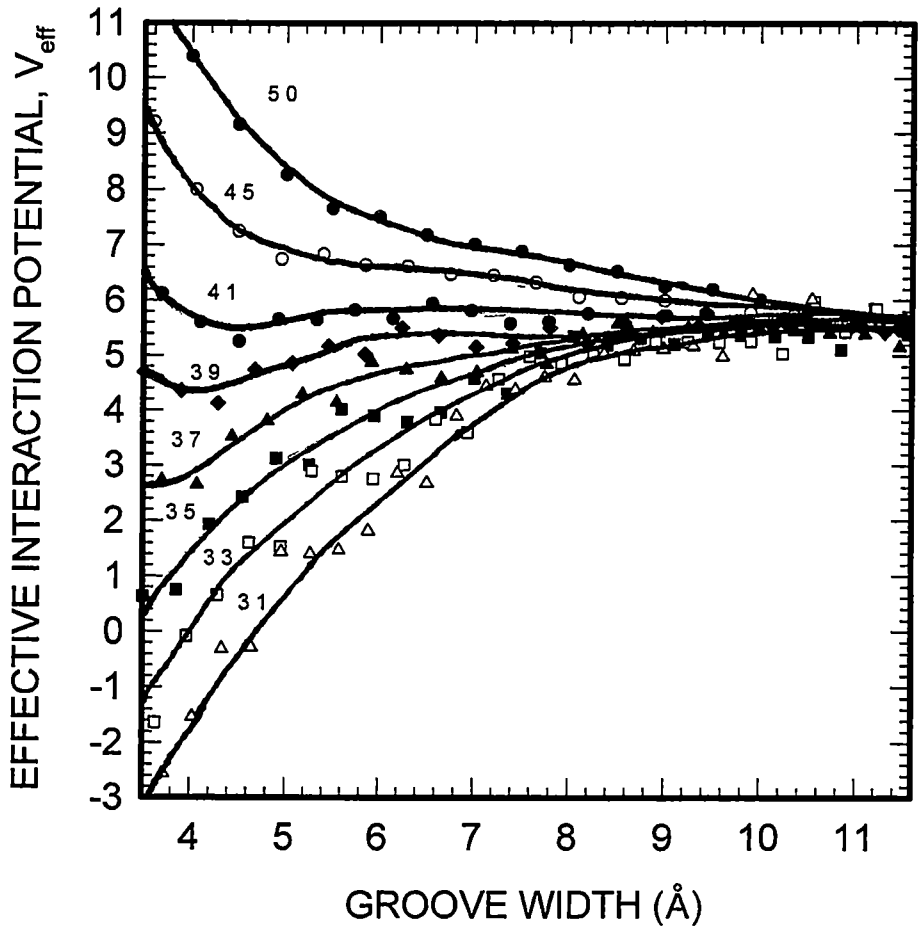


Figure 60
A plot of the effective interaction potential $V_{eff} = V_{coul} + V_{pol}$ as a function of groove width for different odd nearest neighbor values β as indicated on the curves.

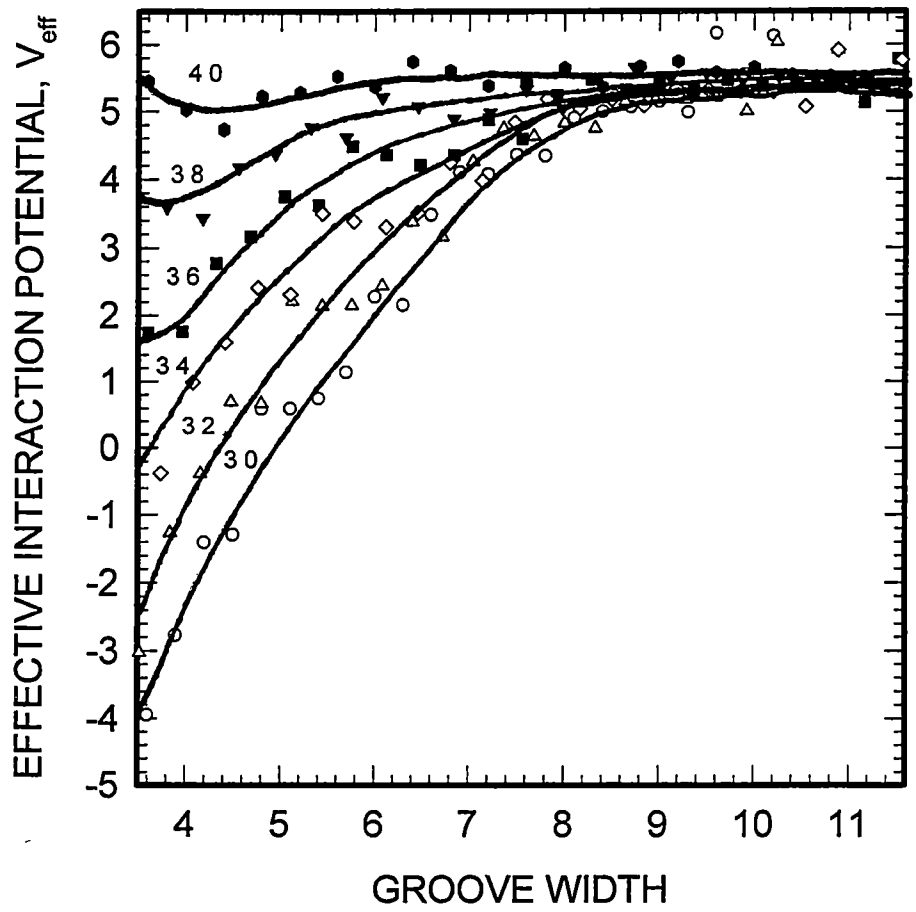


Figure 61
A plot of the effective interaction potential $V_{eff} = V_{coul} + V_{pol}$ as a function of groove width for different even nearest neighbor values β as indicated on the curves

$$\chi^2 = \Sigma |f(x_j) - y_j|^2$$

and taking the derivative of χ^2, yields

$$\frac{1}{2}\frac{\partial \chi^2}{\partial c_j} = \Sigma (f(x_j) - y_j)$$

Upon expanding, this becomes

$$\frac{1}{2}\frac{\partial \chi^2}{\partial c_1} = \Sigma c_1 x_j^{\,0} + \Sigma c_2 x_j^{\,1} + \Sigma c_3 x_j^{\,2} - \Sigma y_j x_j^{\,0} = 0$$

$$\frac{1}{2}\frac{\partial \chi^2}{\partial c_2} = \Sigma c_1 x_j^{\,1} + \Sigma c_2 x_j^{\,2} + \Sigma c_3 x_j^{\,3} - \Sigma y_j x_j^{\,1} = 0$$

$$\frac{1}{2}\frac{\partial \chi^2}{\partial c_3} = \Sigma c_1 x_j^{\,2} + \Sigma c_2 x_j^{\,3} + \Sigma c_3 x_j^{\,4} - \Sigma y_j x_j^{\,2} = 0$$

Let

$$S_n = \Sigma x_j^{\,n}$$

and

$$T_n = \Sigma y_j x_j^{\,n}$$

Then, collecting alike terms, we have

$$c_1 + c_2 S_1 + c_3 S_2 = T_n$$

Therefore, if $f(x) = c_1 + c_2x + c_3x^2$, then $df/dx = c_2 + 2c_3x$, which can be solved readily using the above method.

As s is decreased, the slope is seen to be positive which implies a negative force F; consequently, the direction of the force coincides with the direction of the displacement, and so the force is attractive and drives the system toward smaller values of s. This analysis has therefore yielded the very important conclusion that any reduction in the minor groove width, *e.g* as a result of thermal fluctuations or interactions with proteins or drugs, would tend to drive the system further toward smaller groove widths. Conversely, as the width is increased, the direction of the force is opposite to that of the displacement and thus it tends to restore the system to its original width. Figure 62 shows a plot of F as a function of the groove width s for several β values. It is seen that for $\beta = 3.5$ Å and $s = 8$ Å, $F \approx -23$ pN, whereas for $s = 5$ Å, $F \approx -75$ pN. Furthermore, upon going from $s = 4.5$ Å to $s = 3.5$ Å, F increases from about -85 pN to about -140 pN; this represents an increase of 55 pN/Å. The changes in the force values per Å are seen to be much smaller for larger widths. The force values are seen to be smaller across the width range for $\beta = 3.7$ Å. On the other hand, for $\beta \geq 4.1$ Å, the plots exhibit an upward curvature for small widths, which is the result of a reduced polarization interaction In that case, the Coulomb interaction predominates and the force is positive, *i.e.* following a decrease in the width, the force tends to restore the system to its original width. For the case of $\beta = 5$ Å, $F \approx 250$ pN at $s = 4$ Å, as compared to the value of about -110 pN for

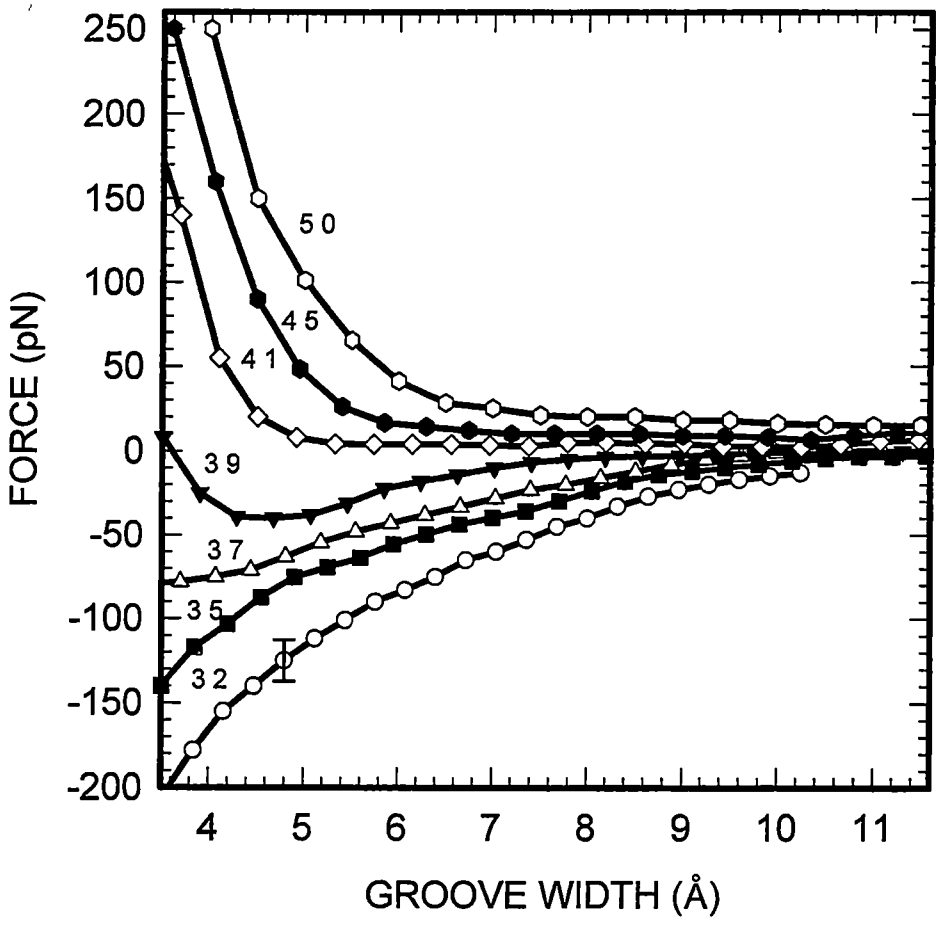


Figure 62
A plot of the effective electrostatic force F as a function of groove width for the following values of the nearest neighbor distance β: 3.2, 3.5, 3.7, 3.9, 4.1, 4.5, and 5.0 Å The force was calculated from the negative derivative of the V_{eff} with respect to the groove width s.
The error bar shown for β = 3.2 Å indicates the uncertainty in the calculation of the force.

$\beta = 3.5$ Å also at 4 Å . Furthermore, for s = 4 Å a value of $\beta = 3.9$ Å yields F ≈ -30 pN, whereas a value of $\beta = 4.1$ Å yields F ≈ 50 pN; *thus, within a 0 2 Å difference in β, the force changes from being attractive to being repulsive and its magnitude changes by 80 pN! These results emphasize the great importance of the structure of the medium in modulating the magnitude and the direction of the effective force in electrostatic interactions. This finding is contrary to the inference of the model that neglects completely the molecular structure of the medium and treats it as a continuum with a screening dielectric constant: in that case, the force is always positive, i.e. repulsive The present findings cast doubt on the validity of such a procedure.*

Regarding the value of 3.5 Å for the nearest neighbor distance β used in the present study, it is instructive to recall that this is very close to the axial rise in B-DNA; thus, the aromatic stack of the bases may provide a pathway for the propagation of the polarization interaction Of course, because of large-amplitude thermal fluctuations (Georghiou *et al* , 1996; Young *et al* , 1997; Shih and Georghiou, to be published) and interactions with proteins or drugs, β would be variable. In view of the large sensitivity of the electrostatic force to the value of β (Fig. 62), this variability may represent a way by which DNA exerts control in its function. With regard to the appropriate value of β, as was discussed above, 3 5 Å appears to be realistic. We should note that opposing these polarization-driven forces are repulsive forces at short interphosphate distances (typically below 3 Å) that stem from overlap of electronic clouds. Regarding the stacking interactions, as Manning (1983) pointed out, they are compressive and therefore they actually act constructively with the polarization-driven forces. Returning to the effective electrostatic forces, for comparison purposes we note that the forces which are holding

the AT and GC base pairs through intermolecular hydrogen bonds are about 10 pN and 15 pN, respectively (Essevaz-Roulet *et al.*, 1997), and those necessary for stretching DNA are about 70 pN (Cluzel *et al* , 1996). The implications of these findings regarding the wrapping of DNA around the histone octamer are discussed below.

It should be noted that the width of the minor groove is not constant but variable because of (a) static and (b) dynamic effects. In a series of seven dodecamers, crystallographic data show that the width varies from 2.6 Å in one dodecamer to 8.9 Å in another Also, within the same dodecamer it varies by as much as 5.2 Å, from 3.0 to 8 2 Å, over four base pairs (Heinemann *et al* , 1994). A large variation of the minor groove width with sequence was also reported for four dodecamers in a theoretical study (Stofer and Lavery, 1994). Thus, there is a strong sequence-dependence of the minor groove width. Moreover, a molecular dynamics simulation study (Young *et al* , 1997) for the Drew/Dickerson dodecamer has reported that the minor groove width undergoes a large variation (standard deviation equal to about 2 Å over a 5 ns time period). Thus, thermal fluctuations can induce large changes in the groove width. For relatively small widths and for the value of $\beta = 3.5$ Å that appears to be realistic for DNA (see above), these changes in the groove width would induce large changes in the attractive forces (Fig. 62). Consequently, a variable width of the minor groove would cause a local asymmetry in the overall forces exerted on the phosphates of minor grooves across the two strands; this would give rise to DNA bending toward the minor groove with the smaller width (for which the attractive force is larger). It is instructive to note that the minor groove has been reported to be very easily deformable (Akiyama and Hogan, 1996a; 1996b), requiring a very small energy. It takes only about 0.5 kcal/mol to bend a

dodecamer by 19° (Dickerson and Drew, 1981) and about 0.25 kcal/mol to bend a decamer by 20° (Jeltsch, 1998). The extent of bending would, of course, be expected to depend on the deformability of the base steps involved; *e g* , the TA step has been reported to be very deformable (McNamara *et al* , 1990; Dickerson *et al* , 1996).

These considerations suggest that base sequence variations in the width of the minor groove cause local bending of DNA toward the groove with the smaller width. In this regard, crystallographic studies find that the structures of a number of oligomers contain bends of 15-24° (Dickerson *et al.*, 1996). Furthermore, thermal fluctuations would cause instantaneous changes in the width of the minor groove with concomitant compression of the minor groove that would result in transient DNA bending toward the narrower minor groove. Bending is known to be coupled to the opening of the DNA base pairs (Manning, 1983; 1985; Ramstein and Lavery, 1988; 1990). Thus, the present findings suggest that base pair opening is a process that does not appear to be very infrequent and is driven by both sequence effects (of static origin) and by thermal fluctuations (of dynamic origin). This process may also lead to the formation of the intercalation cavity during drug-DNA interaction. In this regard, kinetic measurements find that it takes about 4 kcal/mol to form the intercalation cavity (Macgregor *et al.*, 1987; Chaires, 1998).

Regarding interactions between phosphates on the same DNA strand, the average distance involved is about 6.6 Å (Saenger, 1986; Neidle, 1994). For a series of four dodecamers, the distance varies from about 5.9 to 7.2 Å (Saenger, 1986). The polarization interaction would greatly reduce the effect of the repulsive Coulomb interaction (Fig. 59). The induced DNA distortion, however, would be much smaller

relative to that for interaction across a narrow minor groove [as narrow as 3 Å (Heinemann *et al.*, 1994)], because of the small change in V_{eff} (Fig. 59) and therefore in F. F is reduced by about 20 pN in the width range of 5.9 to 7.2 Å, whereas F would be reduced by about 40 pN for a groove width change from 4 Å to 5.3 Å (Fig 62).

DNA is generally considered to behave as a stiff rod because of the effects of the Coulomb repulsive interactions (Manning, 1983). Manning stated that "were it not for its polyelectrolyte aspect, DNA would be locally bent instead of locally rodlike." Because of the considerable magnitude of the polarization interaction found in the present analysis (Fig. 59), the effect of the repulsive Coulomb interaction is reduced and DNA exhibits a locally bent behavior rather than a rodlike behavior. These findings suggest that DNA has a pliable structure, which possesses considerable flexibility This inference is in agreement with the results of an intrinsic fluorescence anisotropy study (Georghiou *et al* , 1996) in which we reported that DNA undergoes large-amplitude motions in the picosecond range, as well as with the results of a molecular dynamics study (Young *et al.*, 1997) and of a harmonic dynamics analysis study (Shih and Georghiou, to be published).

Regarding bending by A-tracts, currently there is a dichotomy: measurements in solution suggest that these tracts are bent; the techniques employed include electrophoresis (Koo *et al* , 1988; Nadeau and Crothers, 1989; Crothers and Shakked, 1999), NMR (Nadeau and Crothers, 1989; Ulyanov *et al.*, 1993, Behling and Kearns, 1986), and hydroxyl radical footprinting (Burkhoff and Tullius, 1987; 1988; Price and Tullius, 1993). On the other hand, crystallographic studies (Dickerson, 1999; Young *et al* , 1995; DiGabrielle and Steitz, 1993; Nelson *et al.*, 1987; Shatzky-Schwartz *et al.*, 1997; Coll *et al.*, 1987) find that the A-tracts are straight. Based on the fact that these

base sequences have a very narrow minor groove, about 3.5 Å (Yoon *et al*, 1988, Fratini *et al.*, 1982; Lipanov and Chuprina, 1987; Neidle, 1994; Crothers and Shakked, 1999; Zurkhin *et al.* 1991, Young *et al*, 1997; Stofer and Lavery, 1994; Steitz, 1993), the present study suggests that they would tend to bend toward that groove. Electrophoretic studies by Crothers and co-workers (Koo *et al.*, 1988; Nadeau and Crothers, 1989, Crothers and Shakked, 1999) suggest that bending occurs in the direction of the minor groove relative to the center of the A-tracts. This inference is in agreement with the results of the present analysis. Of course, by how much these sequences bend would depend on how deformable they are. There is a debate in the literature as to how stiff these sequences are (Zhurkin *et al*, 1991; Dickerson *et al.*, 1996, Levene *et al*, 1986, Boutonnet *et al.*, 1993, Hagerman, 1990), if they are stiff, they may serve as a hinge around which the general-sequence segment would bend. The large reduction of the effect of the repulsive Coulomb interaction across the narrow minor groove of the A-tracts, which stems from a relatively large attractive polarization interaction, would reduce the tension between the phosphates; this would result in the formation of more stable intermolecular hydrogen bonds than those formed by general sequence base pairs. This prediction is born out by experiment: Leroy *et al* (1988) have reported that the lifetime of the hydrogen bonds formed by A-tracts is by one to two orders of magnitude greater than those for general sequence base pairs. This difference in lifetimes becomes less pronounced at higher temperatures, an observation which is consistent with the mechanism proposed here in terms of an increase of the width of the A-tracts minor groove as reflected in Fig. 62 (see below).

High temperature is known to greatly reduce the bending of A-tracts (Diekmann,

1987; Haran *et al.*, 1994). The spine of hydration is thought to stabilize the DNA structure (Chuprina, 1987). Thus, disruption of the spine at high temperatures would destabilize the structure and result in a wider minor groove. This is in agreement with the reported premelting behavior of A-tracts (Park *et al.*, 1991) and of poly(dA)•poly(dT) (Herrera and Chaires, 1989). A wider minor groove for the A-tracts would reduce the asymmetry in the helix and the concomitant bending.

In the nucleosome the A-tracts bind with their minor grooves facing in toward the histone octamer (Travers and Klug, 1987; Drew and Crothers and Shakked, 1985; Satchwell *et al.*, 1986) Because of the very small width of their minor grooves, about 3 5 Å (Yoon *et al* , 1998), DNA will be compressed as a result of a very large force, about -120 pN (Fig 62), and bent toward them. In this regard, the width of the minor groove of A-tracts decreases gradually as one goes from 5' to 3' (Katahira *et al.*, 1988, 1990, Ulyanov *et al.*, 1993). This observation was also made for the kinetoplast DNA (Burkhoff and Tullius 1987; 1988). Such a gradual decrease in the width would result in a relatively large force in the direction of that decrease for $\beta = 3.5$ Å (see Fig. 62) As a result, the minor groove of the A-tracts would be compressed, and the DNA would bend toward that groove This would cause the DNA to wrap around the histone octamer. The very large compaction of DNA in the nucleosome could result in a very dense DNA structure with a β value smaller than 3.5 Å, the resulting force would be quite large, see *e.g.* the curve for $\beta = 3.2$ Å in Fig. 62 that yields a value of about -200 pN for a groove width of 3.6 Å. Proposed models in the literature consider either smooth bending of DNA (Levitt, 1978; Sussman and Trifonov, 1978), bending into the minor groove through kink formation in DNA (Crick and Klug, 1975), or bending into the major

groove through DNA kinking (Sobell *et al* , 1976). Although smooth bending cannot be excluded, it appears that the known coupling between DNA bending and base pair opening (Manning, 1983; 1985; Ramstein and Lavery, 1988; 1990) would give rise to kink formation (a deformation which involves base pair opening); such a scenario is presented by the bending of A-tracts that was discussed above. This would support the model of Crick and Klug (1975). It was previously proposed that DNA wraps around the histone octamer because of charge neutralization accomplished through the interaction of phosphate groups with histone basic amino acid groups (Mirzabekov and Rich, 1979, Arents and Moudrianakis, 1993). Such interactions may be operating in the DNA folding to some extent. However, their contribution would be greatly reduced as a result of repulsive polarization interactions that are known to operate between charges of opposite sign (Jarque and Buckingham, 1992; 1989). As a consequence, the stabilization of the complex would be at a distance greater than the contact distance, and that would result in a relatively weak complex. Moreover, a large degree of charge neutralization is necessary for this mechanism to account for the wrapping of DNA around the histone octamer (Manning *et al.*, 1989).

It has long been puzzling as to how gene regulation at a distance is achieved Effects exerted at one DNA site affect the properties of another site which is removed by many base pairs (Bird *et al.*, 1975a; Bird *et al.*, 1975b; Hogan *et al.*, 1979; Sullivan *et al.*, 1988; Schurr *et al.*, 1997). A protein bound to one site influences the transcription of a gene that lies hundreds of thousands of base pairs away. The following mechanisms have been proposed for this communication between proteins at a distance (reviewed in Ptashne, 1986; Schleif, 1988): (i) looping, (ii) twisting, (iii) sliding, (iv) oozing The

results of the present analysis suggest an alternative mechanism. As was discussed above, the magnitude and direction of the electrostatic force depends strongly on the value on the structural parameter β: a change in β by only 0.2 Å results in the reversal in the direction of the force and in a change in its magnitude by almost two orders of magnitude! *Thus, many-body polarization interactions are extremely sensitive to structural changes and, being electrostatic in nature, can travel very fast over long distances and alter the dynamics of remote DNA sites*

The present analysis is also relevant to the B to A transition of DNA. In the region of 73 to 95% relative humidity there is a coexistence between A- and B-DNA. B-DNA exists for relative humidities ≥ 95% (Saenger, 1984). Particularly, for AT base pairs it is known that there is a hydration pattern in the minor groove which is called the spine of hydration (Fratini *et al* , 1982). Therefore, at a low relative humidity that induces the B to A transition, the spine would be disrupted. That would reduce the local polarization interaction and increase the width of the minor groove because of repulsive Coulomb interactions. By contrast, the width of the major groove would not be significantly affected (Figs. 60 and 61). Thus, DNA would become stiffer in the minor groove, and to a much smaller extent stiffer in the major groove. Consequently, the minor groove would tend to expand to a much greater extent than the major groove, resulting in a major groove compression. This mechanism is compatible with the wide minor groove and the narrow major groove of A-DNA, 11.1 Å and 2 7 Å, respectively (Saenger, 1984).

Regarding the heterogeneous polarizability of DNA and its environment, the large difference between the polarizability of DNA (11.8 $Å^3$) and that of water (1.45 $Å^3$) would

actually be reduced because of the highly cooperative nature of the polarization interaction in water (Frank and Wen, 1957; Bene and Pople, 1970; 1973; Hinkins, 1970; Stone, 1989). Thus, the effective polarizability of DNA and of its environment would be larger than the value of 7.6 $Å^3$ used in the present study, and so would the calculated forces.

PROTEIN-DNA COMPLEXES

The average value of the polarizability of the amino acid residues in proteins is about 13 $Å^3$ (McMeekin *et al* , 1964; Miller and Savichik, 1979). The average value of the nearest neighbor distance in a protein is about 4 Å. Therefore, by averaging as was done above for DNA in the absence of a protein, the overall nearest neighbor distance in the presence of the protein is found to be about 3 6 Å. Thus, $\alpha^* = \alpha/\beta^3 \approx 8.9/3.6^3 \approx 0\ 21$ Figure 63 shows a plot of V_{eff} as a function of the groove width both in the presence and in the absence of protein. It is seen that V_{eff} is somewhat lower in the presence of the protein; however, the two curves have very similar slopes and therefore the difference in the forces is within the uncertainty of the present calculations (data not shown) Consequently, no clear trend can be discerned for the direction of the induced DNA bending. This inference is in agreement (i) with the experimental observations that there is no unique direction toward which proteins bend DNA (Dickerson, 1998), and (ii) with the results of theoretical calculations (Dickerson, 1981; Jeltsch, 1998) that a very small energy is necessitated for DNA bending, less than ~ 1 kcal/mol. Other factors, such as the deformability of the sequences involved and contributions from other interactions , such as stacking, would then determine the direction and the extent of bending. Previous studies (Travers, 1995; Elcock and McCammon, 1996) used the continuum dielectric

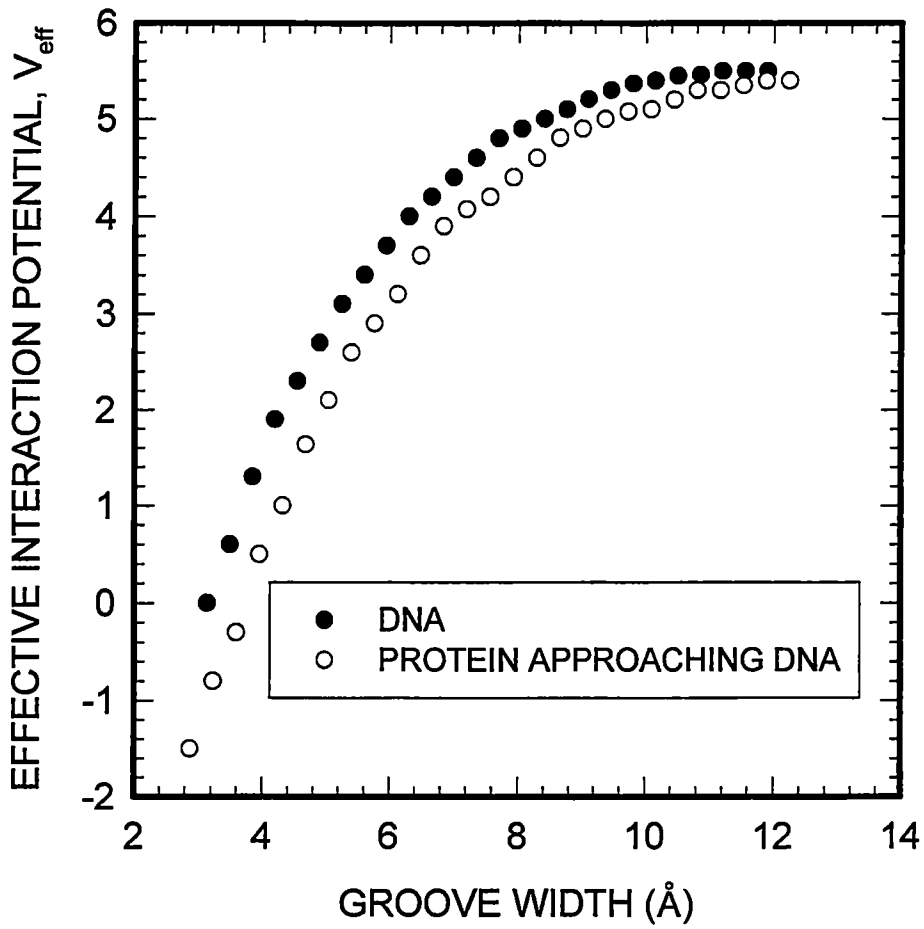


Figure 63
A comparison of the effective polarization potentials for electrostatic interactions across the grooves of DNA in the absence and in the presence of protein.

screening model and concluded that the interacting protein causes a large Coulomb repulsion between the phosphates that bends the DNA away from the protein. As was discussed above, this model is of doubtful validity, and therefore this inference is questionable and cannot be used as a basis for a general mechanism of protein-DNA interaction [see also (1) above].

If the protein approaches the DNA from the major groove, for which s = 11.6 Å, as can be inferred from Fig. 63 there would be no significant change in the magnitude of the force which in the absence of the protein is virtually zero (Fig. 62). Again, this does not allow an unambiguous prediction of the direction of the induced DNA bending.

REFERENCES

Akiyama, T. and M.E. Hogan, Proc. Natl. Acad. Sci., **93**, 12122, 1996a.

Akiyama, T. and M.E Hogan, J. Biol. Chem., **271**, 29126, 1996b.

Arents, G. and E.N. Moudrianakis, Proc. Natl. Acad. Sci., **90**, 10489, 1993

Behling, R.W and D.R. Kearns, Biochemistry, **25**, 3335, 1986.

Bene, J.D and J.A. Pople, J. Chem. Phys., **52**, 4858, 1970.

Bene, J.E.D. and J.A. Pople, J. Chem. Phys., **58**, 3605, 1973.

Bird, J.F., R.M. Wartell, J.B. Dodgson, and R.D. Wells, J. Biol. Chem, **250**, 5109, 1975b.

Bird, J.F., J.E. Larson, and R.D. Wells, J Biol. Chem., **250**, 6002, 1975b.

Boutonnet, N., X. Hui, and K Zakreskwa, Biopolymers, **33**, 479, 1993.

Buckingham, A.D. and J A. Pople, Faraday Society Trans, **51**, 1173, 1955

Burkhoff, A.M. and T.D. Tullius, Cell, 48, **935**, 1987.

Burkhoff, A.M and T.D. Tullius, Nature, **331**, 455, 1988.

Chaires, J.B., Biopolymers, **44**, 201, 1998.

Chuprina, V.P., N. A. Res., **15**, 293, 1987.

Cluzel, P., A. Lebrun, C. Heller, R. Lavery, J.L. Viovy, D. Chatenay, and F. Caron, Science, **271**, 792, 1996.

Coll, M., C.A. Frederick, A.H.J. Wang, and A Rich, Proc. Natl. Acad. Sci, **84**, 8385, 1987.

Crick, F.H.C. and A. Klug, Nature, **255**, 530, 1975.

Crothers and Shakked, D.M. and Z. Shakked in Oxford Handbook of Nucleic Acid Structure, 1999, ed. S. Neidle, Oxford University Press, New York.

Dickerson, R.E. and H.R. Drew, J. Mol. Biol., **149**, 761, 1981.

Dickerson, R.E , N. A Res., **26**, 1906, 1998

Dickerson, R. E. in Oxford Handbook of Nucleic Acid Structure, 1999, ed. S. Neidle, Oxford University Press, New York.

Dickerson, R.E., P. Goodsell, and M.L. Kopka, J. Molec. Biol, **256**, 108, 1996

Diekmann, S., N. A. Res, **15**, 247, 1987.

DiGabrielle, A.D. and T.A. Steitz, J. Molec. Biol., **231**, 1024, 1993.

Drew, H. and A.A. Travers, J. Molec. Biol., **186**, 773, 1985.

Elcock, A H. and J.A McCammon, J Am. Chem. Soc., **118**, 3787, 1996

Essevaz-Roulet, B., U. Bockelmann, and F. Heslot, Proc. Natl. Acad. Sci., **94**, 11935, 1997.

Frank, H.S. and W.I. Wen, Faraday Society Dis., **24**, 133, 1957.

Fratini, A.V., M.L Kopka, H.R Drew, and R.E. Dickerson, J. Biol. Chem. , **257**, 14695, 1982.

Georghiou S., Bradrick, T.D., A. Philippetis, and J.M. Beechem, Biophys. J., **70**, 1909, 1996.

Gurlie, R. and K. Zakreskwa, J. Biomol. Struct Dyn , **16**, 605, 1998.

Hagerman, P.J., Annual Reviews of Biochem, **59**, 755, 1990.

Haran, T.E., J.D. Kahn, and D.M. Crothers and Shakked, J. Molec. Biol., **244**, 135, 1994.

Heinemann, U., C. Alings, and M. Hahn, Biophys. Chem., **50**, 157, 1994

Herrera, J.E., and J.B Chaires, Biochemistry, **28**, 1993, 1989.

Hinkins, J Chem. Phys., **53**, 4544, 1970.

Hogan, M., N. Dattagupta, and D M Crothers, Nature, **278**, 521, 1979.

Jarque, C. and A.D. Buckingham, Chem. Phys. Lett., **164**, 485, 1989.

Jarque, C. and A. D. Buckingham, Molecular Liquids: New Perspectives in Physics and Chemistry, 1992, p. 253, Kluwer Academic Publishers, J.J.C. Teixeira-Dias, ed., Boston.

Jayaram, B., S. Swaminathan, and D.L. Beveridge, Macromolecules, **23**, 3156, 1990.

Jeffrey, G.A., An Introduction to Hydrogen Bonding, 1997, Oxford University Press, New York.

Jeltsch, A., Biophysical Chemistry, **74**, 53, 1998.

Katahira, M., H. Sugeta, Y. Kyogoku, N.A. Res, **18**, 613, 1990.

Katahira, M., H. Sugeta, Y. Kyogoku, S. Fujii, R Fujisawa, and K. Tomita, N. A. Res., **16**, 8619, 1988.

Koo, H.S., H.M Wu, and D.M. Crothers and Shakked, Nature, **320**, 501, 1986.

Leroy, J.L., E. Charretier, M. Kochoyan, and M. Gueron, Biochemistry, **27**, 8894, 1988.

Levene, S.D., H.M. Wu, and D.M. Crothers and Shakked, Biochemistry, **25**, 3988, 1986.

Levitt, M., Proc. Natl. Acad Sci., **75**, 640, 1978.

Lide, D R., CRC Handbook of Chemistry and Physics, 1992-1993, Chemical Rubber Co., Cleveland, Ohio.

Lipanov, A.A., and V. Chuprina, N. A. Res., **15**, 5833, 1987.

Lymann, W.J., W.F. Reehl, D.H. Rosenblatt, in Handbook of Chemical Property Estimation Methods, 1982, McGraw-Hill, New York.

Macgregor, R.B., R.M. Clegg, and T.M. Jovin, Biochemistry, **26**, 4008, 1987.

Manning, G.S., Biopolymers, **22**, 689, 1983.

Manning, G.S., Cell Biophysics, **7**, 57, 1985.

Manning, G.S , K.K. Ebralidse, A.D. Mirzabekov, and A Rich, J. Biomol Struc. Dyn., **5**, 877, 1989.

McMeekin, T.L., M.L. Groves, and N.J. Hipp, in Advances in Chemical Series,1964, **44**, 54.

McNamara, P.T., A. Bolshoy, E.N Trifonov, and R.E. Harrington, J. Biol Struc Dyn , **8**, 529, 1990.

Miller, K. J. And J.A. Sachik, J. Am. Chem Soc., **101**, 7206, 1979.

Mirzabekov, A.D. and A. Rich, Proc Natl. Acad. Sci., **76**, 1118, 1979.

Nadeau, J.G. and D.M. Crothers and Shakked, Proc. Natl. Acad. Sci, **86**, 2622, 1989.

Neidle, S., DNA Structure and Recognition, 1994, IRL Press, New York

Nelson, H. C. M., J.T. Finch, B.L. Luisi, and A. Klug, Nature, **330**, 221, 1987

Padmanabhan, S., B. Richey, C.F Anderson, and M.T. Record, Biochemistry, **27**, 4367, 1988.

Park, V.W., and K.J. Breslauer, Proc. Natl. Acad. Sci., **88**, 1551, 1991.

Price, A.M. and T.D. Tullins, Biochemistry, **32**, 127, 1993.

Ptashne, M., Nature, **322**, 697, 1986.

Ramstein, J. and R. Lavery, J. Biomol. Struct. Dyn., **7**, 915, 1990.

Ramstein, J. and R. Lavery, Proc. Natl. Acad. Sci., **85**, 7231, 1988.

Saenger, W., Nature, **324**, 385, 1986.

Saenger, W., Principles of Nucleic Acid Structure, 1984, Springer-Verlag, New York.

Satchwell, S. H.R. Drew, and A.A. Travers, J. Molec. Biol., **191**, 659, 1986.

Schleif, R., Science, **240**, 127, 1988.

Schurr, J.M., J.J Delrow, B.S. Fujimoto, and A.S. Benight, Biopolymers, **44**, 283, 1997.

Shatzky-Schwartz, M., N.D. Arbuckle, M. Eisenstein, D. Robinovich, A. Bareket-Samish, T.E. Haran, B.F. Luisi, and Z. Shakked, J. Molec. Biol., **267**, 595, 1997.

Shih, C.C. and S Georghiou, Dynamics of Double-Helical DNA in a Viscous Medium; to be published

Sobell, H.M , C C Tsai, S G. Gilbert, S.C Jain, and T.D. Sakore, Proc. Natl. Acad Sci., **73**, 3068, 1976.

Steitz, T.A., Structural Studies of Protein-Nucleic Acid Interaction, 1993, Cambridge University Press, Cambridge.

Stofer, E., and R Lavery, Biopolymers, **34**, 337, 1994.

Stone, A.J., in Hydrogen-Bonded Liquids, 1989, eds. John C. Dore and J. Teixeira, Kluwer Academic Publishers, Boston.

Stone, A.J., The Theory of Intermolecular Forces, 1996, Clarendon Press, Oxford.

Sullivan, K.M., A.I.H. Murchie, and D M.J. Lilley, J. Biol. Chem., **263**, 13074, 1988

Sussman, J.L. and E.N. Trifonov, Proc Natl Acad. Sci., **75**, 103, 1978.

Travers, A., Natl. Struc. Biol., **2**, 615, 1995.

Travers, A. and A. Klug, Nature, **327**, 1987.

Ulyanov, N.B., M.H. Sarma, V.B. Zhurkin, and R.H. Sarma, Biochemistry, **32**, 6875, 1993.

Warshel, A., Proc. Natl. Acad. Sci. USA, **75**, 5250, 1978

Yoon, C., G G. Prive, D.S. Goodsell, and R.E. Dickerson, Proc Natl. Acad. Sci., **85**, 6333, 1998.

Young, M.A., G. Ravishanker, and D.L. Beveridge, Biophys. J., **73**, 2313, 1997

Young, M.A., G. Ravishanker, D.L. Beveridge, and H.M. Berman, Biophys. J., **68**, 2454, 1995.

Zhurkin, V.B., N.B. Ulyanov, A.A Gorin, and R.L. Jernigan, Proc Natl. Acad. Sci, **88**, 7046, 1991

VITA

Catherine C. Large was born in Illinois in 1966. She attended Emory and Henry College in Emory, Va. where she received a Bachelors of Science in Physics with a minor in Mathematics in 1993 She subsequently entered the University of Tennessee and in May, 2000 received a Masters of Science degree in Physics with a minor in Mathematics.